Charged hydrogels for post-loading, release, and molecular imprinting of proteins

The printing of this thesis was financially supported by:
Utrecht Institute for Pharmaceutical Sciences

ISBN: 978-90-393-5461-2

Cover design: Studio Riesenkind, 's-Hertogenbosch
Printed by: Vandenberg, Maarn

Charged hydrogels for post-loading, release, and molecular imprinting of proteins

Electrostatisch geladen hydrogelen voor het beladen met eiwitten, eiwitafgifte, en het maken van eiwitafdrukken

(met een samenvatting in het Nederlands)

Proefschrift

ter verkrijging van de graad van doctor aan de Universiteit Utrecht op gezag van de rector magnificus, prof.dr. J.C. Stoof, ingevolge het besluit van het college voor promoties in het openbaar te verdedigen op maandag 29 november 2010 des middags te 12.45 uur

door

Joris Pieter Schillemans

geboren op 2 april 1978
te Enschede

Promotor: Prof.dr.ir W.E. Hennink

Co-promotor: Dr. C.F. van Nostrum

Table of contents

Chapter I

General introduction

Hydrogels

A hydrogel consists of a three dimensional polymer network that is able to retain large amounts of water with conservation of the network structure. As a result of the high water content, hydrogels are generally considered as biocompatible materials [1, 2], which makes them particularly interesting for biomedical and pharmaceutical applications. In the past few decades hydrogels have been studied extensively as materials for tissue engineering and the controlled release of therapeutic proteins [3-7]. Many hydrogel systems are described in literature, based both on synthetic polymers (for example poly(ethylene glycol) [8-10], and poly(hydroxyethyl methacrylate) [11-14]), and on polymers from natural origin, such as chitosan (derived from the natural polymer chitin) [15-17], alginate [18-21], and dextran [22-24].

The structure of hydrogels is preserved due to the presence of crosslinks between polymer chains, which can be either of chemical (covalent) or physical nature. Chemical crosslinks can be introduced by several reaction mechanisms, e.g. radical polymerization [25], click chemistry [26-28] or Michael addition [29, 30]. Physically crosslinked hydrogels are held together by non-covalent bonds, such as hydrophobic interactions [31, 32], stereocomplex formation [33, 34] or ionic interactions [35]. Both crosslinking methods have their advantages and drawbacks. In general, chemical crosslinking technologies provide excellent control over the crosslink density and lead to mechanically strong hydrogels [3, 36], while physical crosslinked networks tend to be weaker. On the other hand, physical crosslinks generally are reversible, for example by high shear forces [37-39] or external stimuli such as temperature [32, 40, 41], which allows administration by injection (*in situ* gel formation). Additionally, physical crosslinks are formed under mild reaction conditions, whereas chemical crosslinking usually occurs under harsh reaction conditions, or requires toxic reagents. Exposure to chemical crosslinking agents may cause unwanted chemical modification and/or grafting of the therapeutic to the network [42-44].

Hydrogels for controlled release of proteins

At present, most therapeutic proteins are administered parenterally. In order to relieve the burden to patients receiving treatment with therapeutic proteins and to reduce costs, controlled release formulations are being developed. Release of proteins from a hydrogel can occur by one or a combination of three different mechanisms; diffusion controlled, swelling controlled and degradation controlled release [1]. Diffusion controlled release occurs when the size of the protein is smaller than the mesh size of the polymer network, enabling the protein to move

through the free space between the polymer chains. The release is described by Fick's law of diffusion [45], which implies that it is dependent on the concentration gradient of the protein between the polymer matrix and the surrounding medium.. The release rate decreases with time, the fractional release being proportional to the square root of time [1]. The release kinetics of a protein from a hydrogel depends on the gel geometry, the protein loading and on the mesh size of the hydrogel network, i.e. the space available for diffusion. Therefore, the release can be modulated by adapting the crosslink density or the polymer volume fraction.

Both for swelling controlled and degradation controlled release systems, the initial mesh size of the network is smaller than the size of the protein. As a result, the protein is immobile in the matrix and no diffusion of protein can occur. For swelling controlled systems, the mesh size of the hydrogel increases with time through swelling of the hydrogel caused by influx of water. When upon swelling the mesh size of the networks exceeds that of the protein, release starts to occur. For degradation controlled systems increase of the mesh size is a result of degradation of the polymer/crosslinks, which can occur either by surface or by bulk erosion. In early stages, hydrogel degradation is often accompanied with an increase in swelling. For both swelling and degradation controlled systems increase of the mesh size beyond the size of the protein leads to diffusion and release of the protein. The release rate can vary between zero-order and first-order [46], depending on the swelling/degradation mechanism and its kinetics.

Protein release from dextran hydrogels

Dextran is a bacterial polysaccharide mainly consisting of α-1,6-linked D-glucopyranose units, with some degree of 1,3-branching. Dextran has been used clinically for over 60 years as plasma expander and antithrombolytic agent [47]. Dextran is stable under mild acidic and basic conditions and contains three hydroxyl groups per monomer unit available for chemical derivatization and conjugation. Hydrogels based on dextran derivatives can be formed by both chemical and physical crosslinking methods [48]. Physically crosslinked hydrogels can for example be obtained by crystallization of dextran (Mw 6000 Da) [49] or stereocomplex formation between L and D-lactate oligomers that are conjugated to dextran [33]. Dextran can be modified in several ways to obtain a chemically crosslinkable polymer [48]. Examples include crosslinking of dextrans bearing negatively charged groups using sodium trimetaphosphate [50, 51] and crosslinking of oxidized dextrans with hydrazide [52] or bisfunctional amines [53, 54]. Edman *et al.* were the first to report on hydrogels based on acrylate-derivatized dextrans [55], but their method suffered from poor control over the degree of acrylate-derivatization, and

methylene-bisacrylamide was needed as additional crosslinker to obtain stable hydrogels. Van Dijk-Wolthuis *et al.* developed a method for methacrylate-derivatization that allowed excellent control over the number of introduced methacrylate moieties per dextran chain. It was shown that release of proteins from hydrogels based on methacrylated dextran (Dex-MA) could be tailored by varying the initial water content of the gel and the degree of methacrylate substitution [56]. Additionally, Dex-MA hydrogels showed good biocompatibility in vitro [57] and in vivo [58]. However, no degradation of Dex-MA hydrogels occurred in vitro after 5 months under physiological conditions. Further, in vivo studies demonstrated that subcutaneously implanted Dex-MA hydrogels showed no sign of degradation after 21 days. Introduction of hydrolysable esters in the crosslinks by methacrylation with hydroxyethyl methacrylate (HEMA) led to the formation of Dex-HEMA hydrogels, which are biodegradable both in vivo and in vitro. The fate of the dextran chains that remain after degradation of the hydrogel depends on their molecular weight. Dextran with a molecular weight of <40 kDa is excreted by the kidneys ($t_{1/2}$ = 8 h), while higher molecular weight chains are degraded by the reticuloendothelial system [59].

Hydrogels as matrices for molecular imprinting of proteins

Molecular imprinting is a technique to create template-shaped cavities in polymer matrices with memory of the template molecules to be used in molecular recognition [60]. The concept of the formation of these cavities is shown in Figure 1.

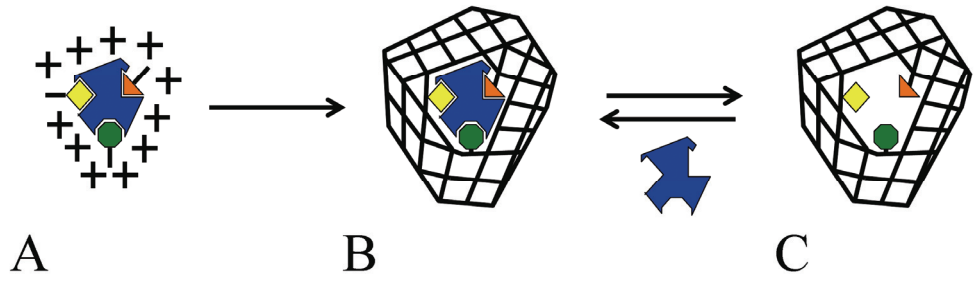

Figure 1. (A) The template (shown in blue), (functional) monomers (shown in yellow, green, and orange) and crosslinker (+) form a prepolymerization complex. (B) Polymerization of monomers and crosslinker fixes the complex. (C) Removal of the template leaves rebinding cavities.

The template and one or more monomers and crosslinker are mixed in a suitable solvent. Several interactions (e.g. hydrogen bonds, hydrophobic interactions, Van der Waals forces and dipole-dipole interactions) determine the organization of monomers around the template (A). Polymerization of monomers and crosslinker fixes the monomers in their spatial arrangement

around the template (B). Finally, removal of the template leaves cavities that are complementary to the target molecule with respect to size, shape, and polarity (C). Nowadays, molecular imprinting of low molecular weight compounds is a well established technique used to create high affinity materials with applications in analytical separation, enzyme-like catalysis, chemical sensors, drug discovery and delivery [60-64]. On the other hand, molecular imprinting of high molecular weight compounds such as proteins is not nearly as successful for various reasons. Firstly, due to the solubility properties and sensitive nature of proteins, imprinting can generally be performed in aqueous environment only. Hydrogen bonding interactions strongly contribute to the affinity of molecular imprinted polymers (MIPs) for low molecular weight compounds in organic, aprotic solvents, but are seriously hampered in water. Nevertheless, the use of hydrogels has led to some encouraging protein imprinting results. The most commonly used matrices are crosslinked polyacrylamide hydrogels, as introduced by Hjertén and co-workers [65, 66]. They suggested that the formation of multiple weak interactions between the hydrogel network and the protein template are responsible for creation of recognition sites within the generally inert polyacrylamide matrix [67].

The high molecular weight of protein templates is another factor complicating molecular imprinting. For low molecular weight compounds, highly crosslinked polymer networks can be used to ensure preservation of the imprint cavity after removal of the template. However, for large template molecules, high crosslink densities seriously hinder mass transfer of the template, leading to slow template removal and rebinding kinetics or, in the worst case, permanent entrapment of the template in the polymer network. A possibility to facilitate mass transfer is the creation of imprints exclusively on the polymer surface (surface imprinting) [68]. In surface imprinting the template is immobilized on a supporting surface or the interface between the monomer solution and a second immiscible phase. Examples of protein immobilization include covalent attachment [69], metal-ion coordination [68], and immobilization in lipid monolayers [70]. For successful surface imprinting of proteins it is essential that the immobilization method does not lead to conformational change or even denaturation of the template protein. Due to incompatibility with proteins, methods used to prepare polymer particles with surface imprints of low molecular weight compounds such as emulsion polymerization can not be applied for proteins.

Protein imprinted nanoparticles

In this thesis, an innovative method to prepare polymer nanoparticles with protein imprints on their surface is proposed. The concept of the preparation of these protein imprinted nanoparticles (PINAPLES) is shown in Figure 2. The hydrophilic part of membrane associated proteins is used as template. The membrane protein is immobilized in the lipid bilayer of a lipid vesicle (liposome), of which the internal aqueous compartment is filled with water-soluble monomers and crosslinker (Figure 2A). The monomers and crosslinker are polymerized forming a hydrogel around the template protein (Figure 2B). Finally, the PINAPLES are obtained by removal of the template and the lipid bilayer (C).

The proposed method has the advantage that the imprints are exclusively formed on the surface of nanoparticles. Moreover, the liposomal bilayer forms the natural environment for membrane proteins, which is essential for the imprinting of the template molecule in its native state.

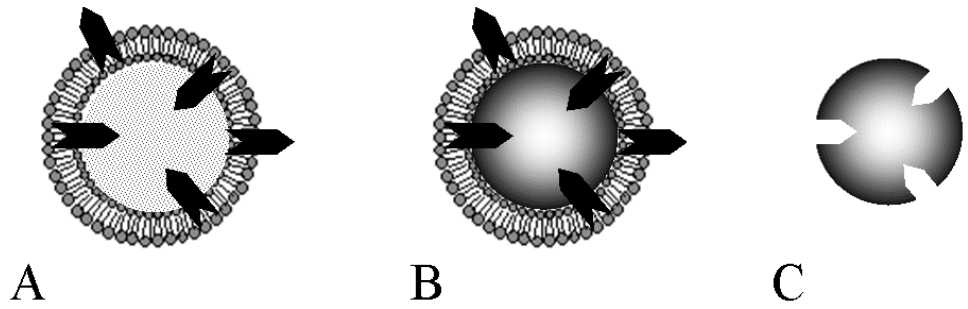

Figure 2. Concept of the preparation of protein imprinted nanoparticles. A membrane protein (shown in black) is immobilized in the lipid bilayer of a liposome containing monomers in the internal aqueous compartment (A). Polymerization of the monomers leads to the formation of a bilayer coated polymer particle, with the membrane protein inserted into the surface (B). The protein imprinted particle (PINAPLE) is obtained by removal of the lipid bilayer and the template protein (C).

For the successful development of PINAPLES four critical steps can be identified:

1. The template needs to be immobilized in a liposomal membrane with the proper orientation (available in the inner liposomal compartment).
2. Hydrogels need to be formed inside the liposomal reactor and polymerization of monomers and crosslinker present in the continuous external phase should be inhibited.
3. The liposomal membrane and template molecules need to be removed to obtain the bare nanogels.
4. The PINAPLES need to rebind the template preferably with high affinity and selectivity.

It is anticipated that PINAPLES can be used as targeted drug carriers. By choosing a template membrane protein that is overexpressed by certain cell types (e.g. tumor cells), PINAPLES will adhere and deliver an entrapped drug specifically to these cells. Alternatively, binding of the PINAPLES may block the target protein in exerting its biological function, and thus PINAPLES may serve as polymeric drugs. The foreseen advantages of PINAPLES as fully synthetic targeted drug (carrier) are their low immunogenicity and the high stability, which are common drawbacks of active drug targeting using e.g. monoclonal antibodies [62, 71].

Outline

This thesis focuses on hydrogel-protein interactions in two different ways. Firstly, the possibility to develop nanoparticles with specific protein recognition properties ('PINAPLES') as described in the previous section is investigated. Secondly, electrostatic interactions between proteins and hydrogel network as tool for the controlled release of proteins are explored.

Chapter 2 gives an overview of the methods currently used to prepare molecularly imprinted particles. It discusses how the hurdles related to the commonly used bulk imprinting method are challenged by the synthesis of polymer micro- and nanoparticles.

In **chapter 3** a method for the preparation of lipid coated nanoparticles suitable for the functional incorporation of membrane proteins is described. Liposomes are prepared by removal of detergent from mixed micelles in an aqueous solution of monomers. Subsequently it is shown that addition of ascorbic acid to the external phase inhibits polymerization of monomers outside the liposome reactor, which allows crosslinking of monomers inside the liposomal aqueous compartment without replacement of the external solution. In the appendix of this chapter it is shown that the detergent removal method can be used to incorporate a membrane protein in the liposomal bilayer in such a way that the hydrophilic part is oriented towards the internal compartment of the liposome.

With the method for nanoparticle synthesis and proper membrane protein incorporation available, the development of PINAPLES should be within reach. Removal of membrane and proteins template was successful. However, despite many attempts, the proof of principle for the PINAPLES concept was not obtained. Many papers describing the successful formation of protein imprinted polymers have been published. Therefore, in **chapter 4**, the scientific proof provided by these papers is subjected to critical review. In this chapter it is described that electrostatic interactions can lead to very high aspecific binding to non-imprinted polymers.

Although such strong interactions may not be advantageous to molecular imprinting, they could be employed to control the release of proteins from hydrogels, or for post-loading of proteins into hydrogels. In **chapter 5** the effect of network charge and charge density on the immobilization and release of model proteins is described. Electrostatic charge is introduced to chemically crosslinked dextran hydrogels by copolymerization of methacrylated dextran with negatively charged methacrylic acid or positively charged dimethylaminoethyl methacrylate.

The effects observed in **chapter 5** are employed in **chapter 6**, which describes an efficient and versatile method for post-loading of proteins in chemically crosslinked dextran hydrogels based on reversible electrostatic interactions. Also, the release of proteins form these post-loaded gels is studied. Importantly, it is demonstrated that this method is more protein-friendly compared to the conventional loading where protein is added during preparation of the hydrogel.

In **Chapter 7** the perspectives of the work presented in this thesis are discussed. Preliminary data are reported to support the feasibility of post-loading of proteins in dextran nanogels, combined with layer-by-layer coating with polyelctrolytes to prevent burst release.

References

[1] N.A. Peppas, P. Bures, W. Leobandung, H. Ichikawa, Hydrogels in pharmaceutical formulations, Eur. J. Pharm. Biopharm., 50 (2000) 27-46.

[2] H. Park, K. Park, Biocompatibility issues of implantable drug delivery systems, Pharm. Res., 13 (1996) 1770-1776.

[3] A.S. Hoffman, Hydrogels for biomedical applications, Adv. Drug Del. Rev., 54 (2002) 3-12.

[4] K.Y. Lee, D.J. Mooney, Hydrogels for tissue engineering, Chem. Rev., 101 (2001) 1869-1879.

[5] W.R. Gombotz, D.K. Pettit, Biodegradable polymers for protein and peptide drug-delivery, Bioconjug. Chem., 6 (1995) 332-351.

[6] N. Morimoto, S.I.M. Nomura, N. Miyazawa, K. Akiyoshi, Nanogel engineered designs for polymeric drug delivery, in: S. Svenson (Ed.) Polymeric drug delivery II: polymeric matrices and drug particle engineering, American Chemical Society, Washington, 2006, pp. 88-101.

[7] S. Stolnik, K. Shakesheff, Formulations for delivery of therapeutic proteins, Biotechnol. Lett., 31 (2009) 1-11.

[8] P. van de Wetering, A.T. Metters, R.G. Schoenmakers, J.A. Hubbell, Poly(ethylene glycol) hydrogels formed by conjugate addition with controllable swelling, degradation, and release of pharmaceutically active proteins, J. Control. Release, 102 (2005) 619-627.

[9] M.J. Mahoney, K.S. Anseth, Three-dimensional growth and function of neural tissue in degradable polyethylene glycol hydrogels, Biomaterials, 27 (2006) 2265-2274.

[10] S.X. Lu, K.S. Anseth, Release behavior of high molecular weight solutes from poly(ethylene glycol)-based degradable networks, Macromolecules, 33 (2000) 2509-2515.

[11] S. Brahim, D. Narinesingh, A. Guiseppi-Elie, Release characteristics of novel pH-sensitive p(HEMA-DMAEMA) hydrogels containing 3-(trimethoxy-silyl) propyl methacrylate, Biomacromolecules, 4 (2003) 1224-1231.

[12] W.F. Lee, Y.H. Lin, pH-reversible hydrogels. IV. Swelling behavior of the 2-hydroxyethyl methacrylate-co-acrylic acid-co-sodium acrylate copolymeric hydrogels, J. Appl. Pol. Sci., 81 (2001) 1360-1371.

[13] Y.Y. Liu, J. Lu, Y.H. Shao, Preparation and characterization of poly(N-isopropylacrylamide)-modified poly(2-hydroxyethyl acrylate) hydrogels by interpenetrating polymer networks for sustained drug release, Macromol. Biosci., 6 (2006) 452-458.

[14] R.M. Trigo, M.D. Blanco, P. Huerta, R. Olmo, J.M. Teijon, L-Ascorbic-Acid Release from Phema Hydrogels, Polymer Bulletin, 31 (1993) 577-584.

[15] J. Berger, M. Reist, J.M. Mayer, O. Felt, N.A. Peppas, R. Gurny, Structure and interactions in covalently and ionically crosslinked chitosan hydrogels for biomedical applications, Eur. J. Pharm. Biopharm., 57 (2004) 19-34.

[16] E.B. Denkbas, R.M. Ottenbrite, Perspectives on: Chitosan drug delivery systems based on their geometries, Journal of Bioactive and Compatible Polymers, 21 (2006) 351-368.

[17] N. Hagenaars, R.J. Verheul, I. Mooren, P.H.J.L.F. de Jong, E. Mastrobattista, H.L. Glansbeek, J.G.M. Heldens, H. van den Bosch, W.E. Hennink, W. Jiskoot, Relationship between structure and adjuvanticity of N,N,N-trimethyl chitosan (TMC) structural variants in a nasal influenza vaccine, J. Control. Release, 140 (2009) 126-133.

[18] W.R. Gombotz, S.F. Wee, Protein release from alginate matrices, Adv. Drug Del. Rev., 31 (1998) 267-285.

[19] M.A. Lawson, J.E. Barralet, L. Wang, R.M. Shelton, J.T. Triffitt, Adhesion and growth of bone marrow stromal cells on modified alginate hydrogels, Tissue Eng., 10 (2004) 1480-1491.

[20] S.Y. Rabbany, J. Pastore, M. Yamamoto, T. Miller, S. Rafii, R. Aras, M. Penn, Continuous delivery of stromal cell-derived factor-1 from alginate scaffolds accelerates wound healing, Cell Transplant., 19 (2010) 399-408.

[21] S.M. Jay, W.M. Saltzman, Controlled delivery of VEGF via modulation of alginate microparticle ionic crosslinking, J. Control. Release, 134 (2009) 26-34.

[22] S.R. Van Tomme, W.E. Hennink, Biodegradable dextran hydrogels for protein delivery applications, Expert Rev. Med. Devices, 4 (2007) 147-164.

[23] S.G. Levesque, R.M. Lim, M.S. Shoichet, Macroporous interconnected dextran scaffolds of controlled porosity for tissue-engineering applications, Biomaterials, 26 (2005) 7436-7446.

[24] R.S. Zhang, M.G. Tang, A. Bowyer, R. Eisenthal, J. Hubble, A novel pH- and ionic-strength-sensitive carboxy methyl dextran hydrogel, Biomaterials, 26 (2005) 4677-4683.
[25] J.T. Chung, K.D.F. Vlugt-Wensink, W.E. Hennink, Z. Zhang, Effect of polymerization conditions on the network properties of dex-HEMA microspheres and macro-hydrogels, Int. J. Pharm., 288 (2005) 51-61.
[26] M. van Dijk, C.F. van Nostrum, W.E. Hennink, D.T.S. Rijkers, R.M.J. Liskamp, Synthesis and Characterization of Enzymatically Biodegradable PEG and Peptide-Based Hydrogels Prepared by Click Chemistry, Biomacromolecules, 11 (2010) 1608-1614.
[27] M. Malkoch, R. Vestberg, N. Gupta, L. Mespouille, P. Dubois, A.F. Mason, J.L. Hedrick, Q. Liao, C.W. Frank, K. Kingsbury, C.J. Hawker, Synthesis of well-defined hydrogel networks using Click chemistry, Chemical Communications, (2006) 2774-2776.
[28] D.A. Ossipov, J. Hilborn, Poly(vinyl alcohol)-based hydrogels formed by "click chemistry", Macromolecules, 39 (2006) 1709-1718.
[29] R. Censi, P.J. Fieten, P. di Martino, W.E. Hennink, T. Vermonden, In situ forming hydrogels by tandem thermal gelling and Michael addition reaction between thermosensitive triblock copolymers and thiolated hyaluronan, Macromolecules, 43 (2010) 5771-5778.
[30] C. Hiemstra, Z.Y. Zhong, M.J. van Steenbergen, W.E. Hennink, J. Feijen, Release of model proteins and basic fibroblast growth factor from in situ forming degradable dextran hydrogels, J. Control. Release, 122 (2007) 71-78.
[31] B. Jeong, Y.H. Bae, D.S. Lee, S.W. Kim, Biodegradable block copolymers as injectable drug-delivery systems, Nature, 388 (1997) 860-862.
[32] T. Vermonden, N.A.M. Besseling, M.J. van Steenbergen, W.E. Hennink, Rheological studies of thermosensitive triblock copolymer hydrogels, Langmuir, 22 (2006) 10180-10184.
[33] S.J. de Jong, S.C. De Smedt, M.W.C. Wahls, J. Demeester, J.J. Kettenes-van den Bosch, W.E. Hennink, Novel self-assembled hydrogels by stereocomplex formation in aqueous solution of enantiomeric lactic acid oligomers grafted to dextran, Macromolecules, 33 (2000) 3680-3686.
[34] C. Hiemstra, Z.Y. Zhong, L.B. Li, P.J. Dijkstra, J. Feijen, In-situ formation of biodegradable hydrogels by stereocomplexation of PEG-(PLLA)(8) and PEG-(PDLA)(8) star block copolymers, Biomacromolecules, 7 (2006) 2790-2795.
[35] K.Y. Lee, J.A. Rowley, P. Eiselt, E.M. Moy, K.H. Bouhadir, D.J. Mooney, Controlling mechanical and swelling properties of alginate hydrogels independently by cross-linker type and cross-linking density, Macromolecules, 33 (2000) 4291-4294.
[36] W.E. Hennink, C.F. van Nostrum, Novel crosslinking methods to design hydrogels, Adv. Drug Del. Rev., 54 (2002) 13-36.
[37] X.P. Ni, A. Cheng, J. Li, Supramolecular hydrogels based on self-assembly between PEO-PPO-PEO triblock copolymers and alpha-cyclodextrin, J. Biomed. Mater. Res. A, 88A (2009) 1031-1036.
[38] S. Ramachandran, Y. Tseng, Y.B. Yu, Repeated rapid shear-responsiveness of peptide hydrogels with tunable shear modulus, Biomacromolecules, 6 (2005) 1316-1321.
[39] S.R. Van Tomme, M.J. van Steenbergen, S.C. De Smedt, C.F. van Nostrum, W.E. Hennink, Self-gelling hydrogels based on oppositely charged dextran microspheres, Biomaterials, 26 (2005) 2129-2135.
[40] B. Jeong, Y.H. Bae, S.W. Kim, Thermoreversible gelation of PEG-PLGA-PEG triblock copolymer aqueous solutions, Macromolecules, 32 (1999) 7064-7069.
[41] S. Kim, K.E. Healy, Synthesis and characterization of injectable poly(N-isopropylacrylamide-co-acrylic acid) hydrogels with proteolytically degradable cross-links, Biomacromolecules, 4 (2003) 1214-1223.
[42] A. Valdebenito, P. Espinoza, E.A. Lissi, M.V. Encinas, Bovine serum albumin as chain transfer agent in the acrylamide polymerization. Protein-polymer conjugates, Polymer, 51 (2010) 2503-2507.
[43] J.A. Cadee, M.J. van Steenbergen, C. Versluis, A.J.R. Heck, W.J.M. Underberg, W. den Otter, W. Jiskoot, W.E. Hennink, Oxidation of recombinant human interleukin-2 by potassium peroxodisulfate, Pharm. Res., 18 (2001) 1461-1467.
[44] C.-C. Lin, A.T. Metters, Hydrogels in controlled release formulations: Network design and mathematical modeling, Adv. Drug Del. Rev., 58 (2006) 1379-1408.

[45] P.L. Ritger, N.A. Peppas, A simple equation for description of solute release I. Fickian and non-fickian release from non-swellable devices in the form of slabs, spheres, cylinders or discs, J. Control. Release, 5 (1987) 23-36.
[46] S.W. Kim, Y.H. Bae, T. Okano, Hydrogels - swelling, drug loading, and release, Pharm. Res., 9 (1992) 283-290.
[47] R. Mehvar, Dextrans for targeted and sustained delivery of therapeutic and imaging agents, J. Control. Release, 69 (2000) 1-25.
[48] S.R. Van Tomme, W.E. Hennink, Biodegradable dextran hydrogels for protein delivery applications, Expert Rev. Med. Devices, 4 (2007) 147-164.
[49] R.J.H. Stenekes, H. Talsma, W.E. Hennink, Formation of dextran hydrogels by crystallization, Biomaterials, 22 (2001) 1891-1898.
[50] S.G. Levesque, M.S. Shoichet, Synthesis of cell-adhesive dextran hydrogels and macroporous scaffolds, Biomaterials, 27 (2006) 5277-5285.
[51] M. Maire, D. Logeart-Avramoglou, M.C. Degat, F. Chaubet, Retention of transforming growth factor beta 1 using functionalized dextran-based hydrogels, Biomaterials, 26 (2005) 1771-1780.
[52] J. Maia, L. Ferreira, R. Carvalho, M.A. Ramos, M.H. Gil, Synthesis and characterization of new injectable and degradable dextran-based hydrogels, Polymer, 46 (2005) 9604-9614.
[53] E. Schacht, B. Bogdanov, A. VandenBulcke, N. DeRooze, Hydrogels prepared by crosslinking of gelatin with dextran dialdehyde, React. Funct. Pol., 33 (1997) 109-116.
[54] L.H. Weng, X.M. Chen, W.L. Chen, Rheological characterization of in situ crosslinkable hydrogels formulated from oxidized dextran and N-carboxyethyl chitosan, Biomacromolecules, 8 (2007) 1109-1115.
[55] P. Edman, B. Ekman, I. Sjoholm, Immobilization of proteins in microspheres of biodegradable polyacryldextran, J. Pharm. Sci., 69 (1980) 838-842.
[56] W.E. Hennink, H. Talsma, J.C.H. Borchert, S.C. DeSmedt, J. Demeester, Controlled release of proteins from dextran hydrogels, J. Control. Release, 39 (1996) 47-55.
[57] C.J. De Groot, M.J.A. Van Luyn, W.N.E. Van Dijk-Wolthuis, J.A. Cadee, J.A. Plantinga, W. Den Otter, W.E. Hennink, In vitro biocompatibility of biodegradable dextran-based hydrogels tested with human fibroblasts, Biomaterials, 22 (2001) 1197-1203.
[58] J.A. Cadee, M.J.A. van Luyn, L.A. Brouwer, J.A. Plantinga, P.B. van Wachem, C.J. de Groot, W. den Otter, W.E. Hennink, In vivo biocompatibility of dextran-based hydrogels, J. Biomed. Mater. Res., 50 (2000) 397-404.
[59] G. Arturson, G. Wallenius, The intravascular persistence of dextran of different molecular sizes in normal humans, Scand. J. Clin. Lab. Invest., 16 (1964) 76-80.
[60] C. Alexander, H.S. Andersson, L.I. Andersson, R.J. Ansell, N. Kirsch, I.A. Nicholls, J. O'Mahony, M.J. Whitcombe, Molecular imprinting science and technology: a survey of the literature for the years up to and including 2003, J. Mol. Recognit., 19 (2006) 106-180.
[61] B. Sellergren, C.J. Allender, Molecularly imprinted polymers: a bridge to advanced drug delivery, Adv. Drug Del. Rev., 57 (2005) 1733-1741.
[62] C.F. Van Nostrum, Molecular imprinting: A new tool for drug innovation, Drug Disc. Today: Tech., 2(1) (2005) 119-124.
[63] J.Z. Hilt, M.E. Byrne, Configurational biomimesis in drug delivery: molecular imprinting of biologically significant molecules, Adv. Drug Del. Rev., 56 (2004) 1599-1620.
[64] L. Ye, K. Mosbach, Molecular imprinting: Synthetic materials as substitutes for biological antibodies and receptors, Chemistry of Materials, 20 (2008) 859-868.
[65] S. Hjerten, J.L. Liao, K. Nakazato, Y. Wang, G. Zamaratskaia, H.X. Zhang, Gels mimicking antibodies in their selective recognition of proteins, Chromatographia, 44 (1997) 227-234.
[66] J. Liao, Y. Wang, S. Hjertén, A novel support with artificially created recognition for the selective removal of proteins and for affinity chromatography, Chromatographia, 42 (1996) 259-262.
[67] D. Tong, C. Heényi, Z. Bikádi, J. Gao, S. Hjertén, Some studies of the chromatographic properties of gels ('Artificial antibodies/receptors') for selective adsorption of proteins, Chromatographia, 54 (2001) 7-14.

[68] M. Kempe, M. Glad, K. Mosbach, An approach towards surface imprinting using the enzyme ribonuclease A, J. Mol. Recognit., 8 (1995) 35-39.
[69] T. Shiomi, M. Matsui, F. Mizukami, K. Sakaguchi, A method for the molecular imprinting of hemoglobin on silica surfaces using silanes, Biomaterials, 26 (2005) 5564-5571.
[70] X.Z. Du, V. Hlady, D. Britt, Langmuir monolayer approaches to protein recognition through molecular imprinting, Biosens. Bioelectron., 20 (2005) 2053-2060.
[71] P. Holliger, P.J. Hudson, Engineered antibody fragments and the rise of single domains, Nat. Biotechnol., 23 (2005) 1126-1136.

Chapter 2

Molecularly imprinted polymer particles: synthetic receptors for future medicine

Joris P. Schillemans

Cornelus F. van Nostrum

Nanomedicine 2006, 1 (4), 437-447

Abstract

Molecular Imprinting is a relatively new and rapidly evolving technique used to create synthetic receptors, and possesses great potential for a number of applications in life sciences. Traditionally, molecular imprinted polymers (MIPs) are prepared by bulk polymerization, followed by crushing and sieving to obtain polymer beads. However, several methods can be used to directly synthesize polymer micro- and nanoparticles, thereby avoiding the time and labor consuming process of crush sieving. Applications are foreseen in enhanced drug loading, controlled drug delivery, and drug targeting. This review describes the different methods of synthesis of molecularly imprinted micro- and nanoparticles and discusses how these methods challenge the outstanding issues that molecular imprinting are facing today, thereby facilitating biomedical application in the future.

Introduction

Molecular recognition plays a role of obvious importance in innumerable processes in life. This is exemplified by the selectivity and activity of enzymes, and the interaction of receptors and antibodies with specific ligands. Also the effect of the majority of drugs is fully governed by recognition at the molecular level. Receptors obtained from natural sources, like enzymes and antibodies, are nowadays used in a variety of applications, ranging from analytical and preparative chemistry to nanomedicine, including diagnostics, drug development, and drug delivery. However, the stability of such biomolecules is limited and they can generally not be used under harsh conditions. Therefore, the search for more stable synthetic systems mimicking highly selective and sensitive recognition processes occurring in nature is booming. Although thus far nature's selectivity and sensitivity have not yet been matched, steady progress is being made in creating synthetic systems for molecular recognition.

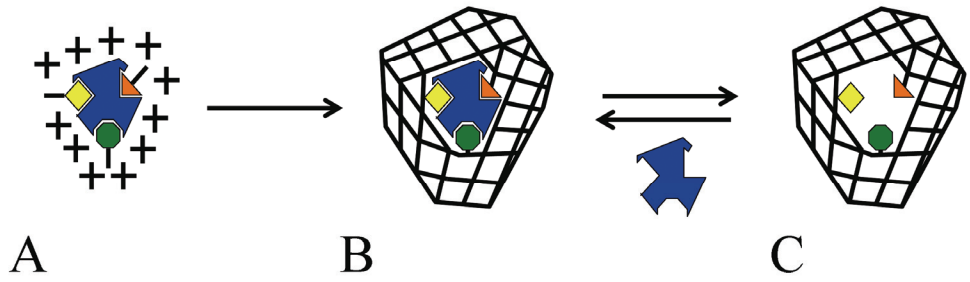

Figure 1. Schematic representation of the principle of molecular imprinting. (A) The template (shown in blue), (functional) monomers (shown in yellow green and orange) and crosslinker form prepolymerization complex. (B) Polymerization of monomers and crosslinker fixes the complex. (C) Removal of the template leaves rebinding cavities.

A relatively new and rapidly evolving technique in this field is molecular imprinting. This method involves the preparation of molecular-sized cavities in highly crosslinked polymer networks. The principle of molecular imprinting is surprisingly simple (Figure 1): The target molecule (template) and one or several monomers and crosslinkers are mixed in a suitable solvent. Molecular interactions determine the organization of monomers around the template (A), which are subsequently fixed by polymerization (B). Finally, removal of the template leaves cavities that are complementary to the target molecule with respect to size, shape, and polarity (C). These cavities can rebind the template with high selectivity and sensitivity. In general, the

methods used for MIP synthesis can be subdivided in three different approaches: covalent, semi-covalent, and non-covalent [1, 2]. In covalent imprinting the template is covalently attached to one or more polymerizable units. Both removal and rebinding of the template involve a chemical reaction. Also for semi-covalent imprinting a covalently attached template is used, but the rebinding step is non-covalent. A common feature in semi-covalent imprinting is a sacrificial spacer [3]. Incorporation of the template in non-covalent imprinting depends solely on attractive forces between monomers and template (hydrogen bonds, Van der Waals forces, ionic and dipole-dipole interactions). The interaction is often promoted using functional monomers with high affinity for the template.

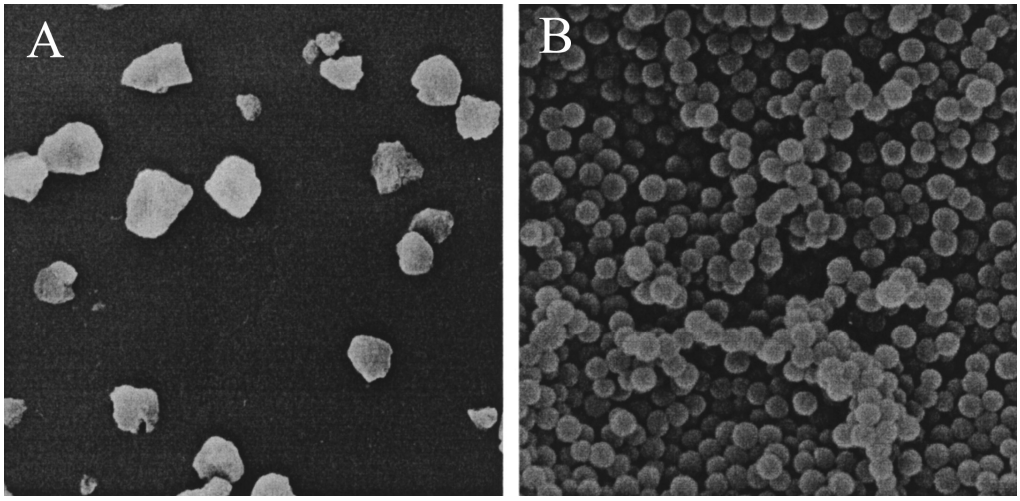

Figure 2. Scanning electron microscopy pictures of molecularly imprinted MAA/EDMA particles (reprinted with permission from reference [13]). (A) Irregularly shaped particles prepared by crush sieving (525x magnification) and (B) spherical particles prepared by precipitation polymerization (15000 x magnification).

The main advantages of molecular imprinted polymers (MIPs) are their robustness, versatility, and ease of preparation. At present, MIPs have already proven to be useful for several purposes, such as analytical separations, enzyme-like catalysis, chemical sensors, drug discovery and drug delivery [4-6]. Traditionally, MIPs are synthesized as monoliths by bulk polymerization, subsequently downsized by crush sieving, resulting in large, irregularly shaped particles (Figure 2). This method is simple, can be scaled up easily, and has shown to be useful for imprinting of small molecules. However, it also faces some serious problems. Poor rebinding in aqueous environments, heterogeneity of binding sites, slow mass transfer, and incomplete removal of template are some of the challenges that stood in the way of MIPs making biological antibodies

redundant until recently. One solution that can overcome some of the challenges is direct synthesis of MIP micro and nanoparticles (Figure 2). Several methods to synthesize MIPs as micro- or nanobeads have been described. This review gives an overview of the different methods of direct MIP particle synthesis and discusses how these methods challenge the outstanding issues that molecular imprinting is facing today, thereby facilitating biomedical application now and in the future.

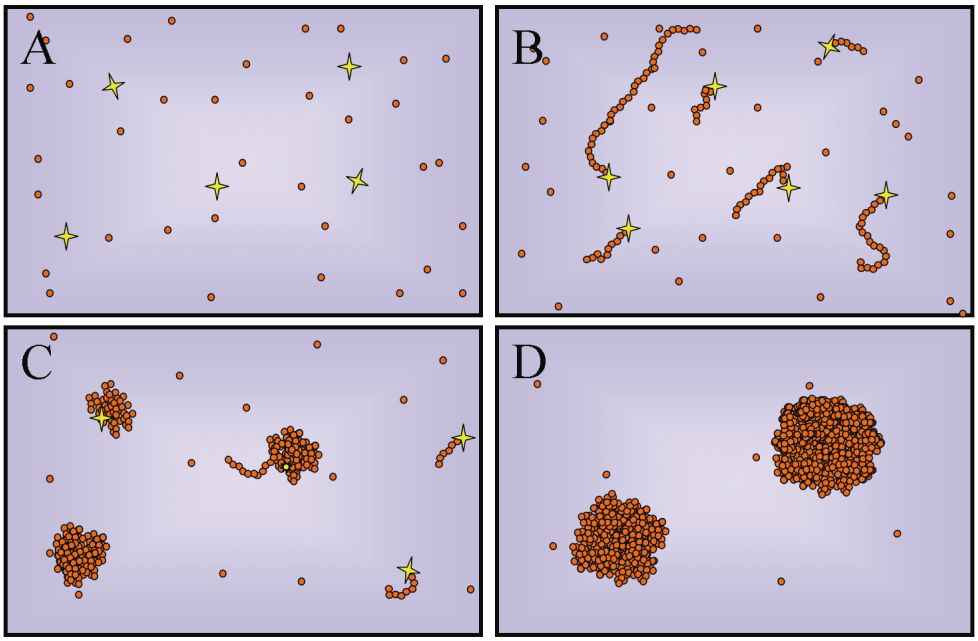

Figure 3. Schematic representation of dispersion polymerization. (A) Dilute mixture of monomers (●) and initiator (✦). (B) Propagation of soluble polymer chains. (C) Primary particles due to collapse of polymer at critical length. (D) Growth of primary particles.

Dispersion and precipitation polymerization

Dispersion polymerization was introduced as a simple means to synthesize monodisperse colloid polymer particles [7]. Using dilute solutions of monomers, crosslinker and initiator and certain temperatures, polymerization leads to the formation of colloidal stable particles in the micro/nano-range (Figure 3) [8, 9]. The polymerization begins with initiation by a soluble initiator, followed by propagation of the soluble monomers. At a critical length the growing polymer chain becomes insoluble in the polymerization medium, causing it to collapse. In

dispersion polymerization the collapsed primary particles are swollen in the medium and the polymerization proceeds largely within the particles, eventually leading to spherical particles in the range of 100 nm – 10 μm. In precipitation polymerization the primary particles do not swell in the medium. Therefore, precipitation polymerization produces more irregularly shaped and polydisperse particles. It must be noted that although polymer swelling is a useful guideline, a sharp distinction between dispersion and precipitation polymerization does not exist [9].

Sellergren was the first to use dispersion polymerization of methacrylic acid (MAA, monomer) and ethyleneglycoldimethacrylate (EDMA, crosslinker) for molecular imprinting of pentamidine (PAM), a drug used for treatment of AIDS-related disorders [10, 11]. The MIP particles were used for solid phase extraction to selectively enrich PAM from dilute solutions of PAM and related substances, enabling direct PAM quantification. Since then, dispersion and precipitation polymerization have been used by several groups [12-20]. Some interesting applications have been reported: Puoci *et al.* used sulfasalazine imprinted MIPs prepared by precipitation polymerization to allow pH-controlled release of sulfasalazine, a prodrug used in the treatment of Irritable Bowel Syndrome and Crohn's disease. After particle formation, the template was removed by soxhlet extraction, followed by prodrug (re)loading of imprinted and non-imprinted particles by soaking in a sulfasalazine solution. In a release experiment according to the drug release test of the United States Pharmacopoeia XXII, non-imprinted particles released 20% at pH 1.0 and showed dump release at pH 6.8 while imprinted particles showed no release at pH 1.0, and gradual release over several hours at pH 6.8 [21]. These differences are a result of the specific interaction between the MIP particles and sulfasalazine in the cavities created by the imprinting. Wulff *et al. s*ynthesized nanoparticles by dispersion polymerization of EDMA and methylmethacrylate (MMA) imprinted with a transition state analogue of carbonate hydrolysis and obtained MIPs with enzymatic activity showing Michaelis-Menten kinetics, increasing the rate of hydrolysis 2990 times as compared to the non-catalyzed hydrolysis [22].

In order to optimize the rebinding capacity and selectivity of the MIP particles, relative amounts of monomers, crosslinker and template can be varied [13, 16]. However, one should take into account that for dispersion and precipitation polymerization, the concentration of monomers should be kept low in order to prevent macroscopic polymerization. This could be a serious problem when using the non-covalent approach, because the excess of solvent will adversely shift the equilibrium binding between monomers and template. This results in low

imprinting efficiency, and therefore a low rebinding capacity of the template for the resulting MIP. For example, Ye *et al.* compared the template rebinding of a 17 β-estradiol imprinted polymer prepared by grinding and sieving of a monolith of MAA and EDMA or trimethylolpropane trimethacrylate (TRIM), to the rebinding of a MIP of similar composition prepared by dispersion polymerization. They showed that the imprinting factor, which is the difference in rebinding between imprinted and non-imprinted polymer, was higher for the microspheres than for the monolith, but the amount of template that was rebound per weight of polymer was less for the microspheres [13]. Therefore, it was anticipated that the covalent or semi-covalent imprinting approach should be more suited for precipitation polymerization, because linking the template to a monomer that participates in the polymerization would favor the incorporation of the template in the MIP. After particle formation, the link between polymer and template is cleaved, leaving the cavity for rebinding. Indeed, it was shown by Boonpangrak *et al.* that the semi-covalent approach in precipitation polymerization of MAA/EDMA mixtures led to higher template (cholesterol) incorporation during the formation of the MIP, compared to similar monolith MIP preparation [23]. Furthermore, the template was removed more efficiently, and the MIP showed higher template uptake.

For many biomedical applications, such as drug delivery or analysis in biological fluids, specific recognition and rebinding in aqueous environment is highly desirable. However, adaptation towards polar environment is an outstanding issue in molecular imprinting [4, 5, 24]. As shown by Silvestry *et al.*, precipitation polymerization in acetonitrile or isopropanol/water renders theophylline and caffeine imprinted MIPs with good rebinding characteristics in acetonitrile, but the template rebinding of these MIPs in aqueous solutions is poor [19]. This can be explained by the fact that template rebinding does not solely depend on the molecular interactions between template and MIP, but also on their respective interactions with the solvent. Hence, the affinity of MIPs is solvent dependent. Hydrogen bonding between monomers and template is a determining molecular interaction when organic solvents are used. In aqueous solutions however, competitive hydrogen bonding with the water molecules seriously reduces this specific interaction, while hydrophobic interactions become more important. In order to synthesize MIPs that show high rebinding in aqueous solutions, the polymerization should preferably take place in aqueous solution as well. Although dispersion polymerization in water is feasible [7, 25], to our knowledge there are no reports on MIPs synthesized by dispersion polymerization in water. However, adaptation towards aqueous

solutions was accomplished in a different way by Silvestri *et al.* They found that the recognition factor for theophylline and caffeine in physiological environment increased substantially when MIP nanospheres prepared by precipitation polymerization in acetonitrile and/or ethanol were immobilized in an acrylic membrane [19, 26]. It was suggested that the membrane created a microenvironment that enhanced the interaction between the template and the MIP.

Suspension and mini-emulsion polymerization

As mentioned above, an excess of solvent as is needed for dispersion polymerization could hamper the interaction of the formed particles with the template. Suspension polymerization provides a way to circumvent this problem. In suspension polymerization, the monomer and the initiator are insoluble in the dispersing medium (Figure 4). Prior to polymerization, both are dispersed in the medium forming an emulsion, if necessary by using a surfactant. Initiation and propagation occur exclusively inside the emulsion droplets and therefore the size of the resulting particles is controlled by the size of the droplets (20µm-2mm) [9]. In principle the imprinting efficiency of a template that is soluble in the polymerizing droplet is comparable to imprinting by bulk polymerization, the difference being the size of the reaction vessel. Indeed, using liquid perfluorcarbon as dispersing phase and a fluorinated stabilizer, Mayes and Mosbach reported that MIP beads prepared by suspension polymerization showed similar recognition properties for amino acid derivative Boc-L-phenylalanine as the traditional bulk polymerized MIP [27]. Kempe and Kempe recently introduced a simpler and less expensive protocol using mineral oil, and used it to perform an extensive systematic study to optimize the composition (MAA and TRIM) of propanolol imprinted particles, which clearly illustrates the advantage of the time and labor saving by direct particle synthesis [28]. Suspension polymerization leads to rather large particles in the micrometer range, which therefore exposes a relatively small surface area. This limits the accessibility of the imprinted sites, influencing template removal and rebinding kinetics. Sub-micron particles with larger relative surface area can be obtained using miniemulsion polymerization [29]. Miniemulsions are obtained by shearing a system containing oil, water, a surfactant, and a so-called cosurfactant, which is important for stabilizing the 50-500 nm sized droplets. Miniemulsion polymerization of MAA/EDMA has successfully been employed to synthesize MIP particles with strong rebinding of the imprinted molecule (Boc-L-phenylalanine-anilide) in water/methanol 75:25 [30-32]. Unfortunately, the authors did not report on the effect of the increased surface area on template removal and binding kinetics.

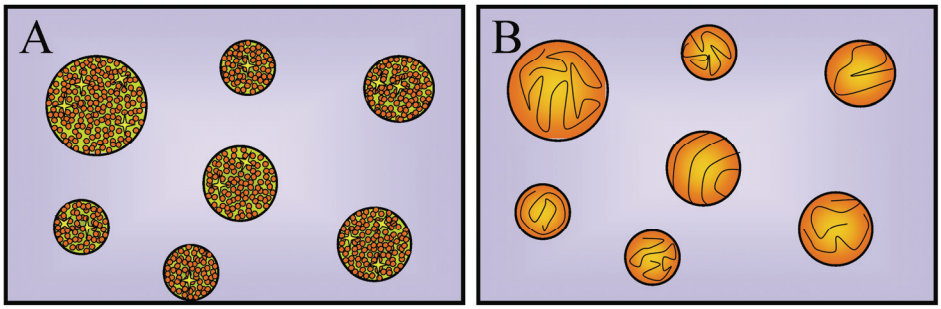

Figure 4. Schematic representation of suspension polymerization Monomers (●) and initiator (✦) dispersed in an emulsion (A). Polymerization leads to particles in the size of the emulsion droplet (B).

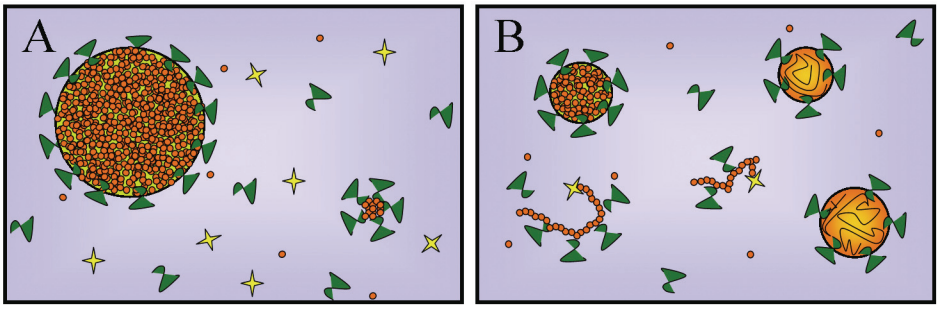

Figure 5. Schematic representation of emulsion polymerization. (A) Monomers (●) are dispersed using a surfactant ( ), while the initiator (✦) is dissolved in the continuous phase. (B) Polymer chains propagating in the continuous phase are stabilized by the surfactant, and continue to grow until all monomers are consumed.

Emulsion and seeded polymerization

The mechanism of particle formation and the control of particle size for emulsion polymerization are very different from suspension and miniemulsion polymerization (Figure 5). The main difference is the solubility of the initiator. The initiator used in suspension and miniemulsion polymerization, mostly 2,2'-azobis(isobutyronitrile) (AIBN), is only soluble in the dispersed phase, while in emulsion polymerization it is soluble only in the continuous phase (for example potassium peroxydisulfate). As a consequence, in emulsion polymerization, primary particle formation takes place in the continuous phase instead of in the emulsion droplet. The surfactant stabilizes not only the initial emulsion, but also the formed polymer particles, the eventual size of which (submicron range) is dependent on a number of factors, among others monomer solubility, surfactant and initiator concentration, and temperature [9]. In molecular imprinting, emulsion polymerization is most commonly used in combination with

preformed particles (seeded polymerization). These seed particles are added as an alternative for the initial nucleus formation, to serve as primary particles on which the polymer deposition can occur. The advantage of seeded polymerization is that particles with very narrow size distributions can be obtained over a wide range of sizes, depending on the size of the seed particles. However, the polymerization conditions have to be carefully chosen in order to avoid formation of secondary particles.

In some cases the monomer solution is absorbed by the seed particles, leading to swelling of the particles, which is followed by polymerization (seed swelling polymerization). A number of authors used particle formation by seed swelling in an attempt to prepare MIPs that show specific recognition properties in an aqueous environment. Haginaka and co-workers imprinted single enantiomers of a number of drugs using water as continuous phase, polystyrene seed particles, MAA or vinylpyridine (VPY) and EDMA as the functional monomer and crosslinker, respectively. The MIPs were used as the stationary phase in HPLC, which enabled chiral separation in aqueous environment for naproxen [33, 34], methylbenzamine [35], chlorpheniramine [36] and nilvidapine [37]. They also prepared MIPs that were modified with a hydrophilic external layer consisting of mixture of glycerol monomethacrylate and glycerol dimethacrylate to prevent adsorption of bovine serum albumin, making these MIPs applicable as stationary phase for direct serum HPLC-assays [38]. Chen *et al.* prepared particles imprinted with sulfamethazine (SMZ) using a modified seed swelling polymerization protocol that was less time-consuming, and showed that these particles were highly selective and could be used for chromatographic separation of SMZ from other sulfonamides, both in acetonitrile and in aqueous-rich media [39, 40].

When the monomers are not absorbed but form a separate layer on the surface of the seed particle upon polymerization, core-shell particles are formed (core-shell polymerization) [9]. An interesting feature of core-shell particles is the possibility to incorporate functional substances inside the core of the particle such as drug, fluorescent or magnetic compounds, which in principle do not interfere with the interaction of template and polymer in the shell. Pérez *et al.* incorporated a magnetic compound in the poly-MMA or polystyrene core of particles and imprinted a cholesterol derivative in the shell using the semi-covalent approach. This approach enabled efficient rebinding of cholesterol and subsequent particle sedimentation in a magnetic field within 30 seconds [41].

Although reducing the dimensions of MIPs to the nanoscale increases the relative surface area and therefore the accessibility of the imprinted cavities, poor diffusion of the template in the polymer matrix still hampers template removal and rebinding, especially when large molecules such as proteins are involved. Another approach to improve the accessibility is to create the imprints specifically on the surface of the MIP, a technique known as surface imprinting [42]. For example, Pérez *et al.* synthesized surface imprinted core-shell particles using a surfactant to which the template (cholesterol) was coupled via a cleavable linker. Thus the imprints were specifically located at the surface of the particles [43]. In order to create protein imprinted particles it could be interesting to combine this surface imprinting method with the so called epitope approach. The epitope approach was first described by Rachkov and Minoura in combination with the classical monolith imprinting approach (Figure 6). In the epitope approach, a short peptide template is used that represents a specific part (epitope) of a protein, enabling rebinding of the whole protein [44]. When these imprints are positioned on the relatively large surface area of nanoparticles, for example by coupling the epitope to the surfactant, diffusion will not be a limiting factor. In fact, this method is described in a patent owned by Aspira biosystems, inc. using suspension polymerization in an oil-in-water emulsion. Examples of proteins imprinted in particles consisting of acrylamide (AAM) and N,N'-methylene-bisacrylamide (MBA) as monomer and crosslinker, respectively, include bovine serum albumine, cytochrome C, estrogen receptor, alcohol dehydrogenase and creatine kinase [45].

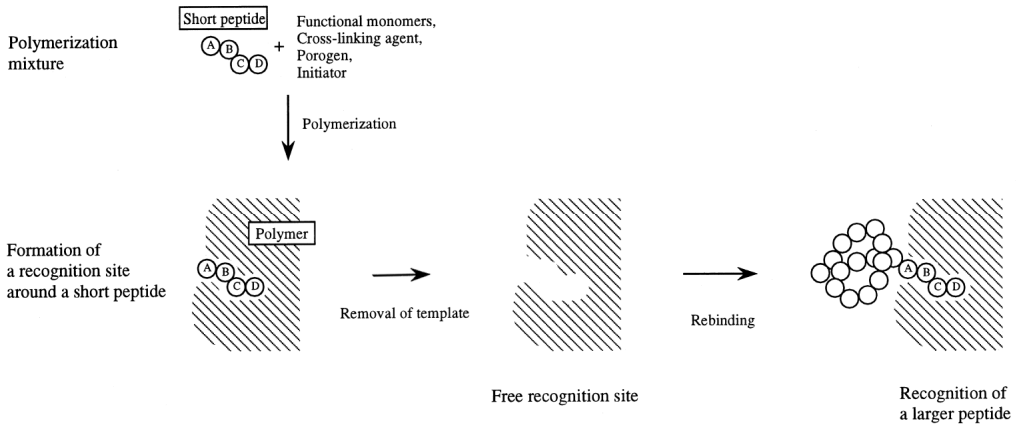

Figure 6. The epitope approach. Reprinted with permission from [44].

Other methods

Some authors have prepared molecular imprinted particles in ways that do not fall (exactly) into the above categories, but are worth mentioning, because they represent the current developments and potential future standards.

By introducing double bonds to the surface of a solid support, for example preformed silica particles, it is possible to graft a polymer to their surface [46]. The preparation protocol involves coating of the support with a thin film of monomers by solvent evaporation, followed by free radical polymerization. In this method the thickness of the deposited layer is hard to control. Additionally, capillary forces can cause irregular coating of the particles. Sulitzky *et al.* circumvented these problems by grafting the imprinted polymer *from* the preformed silica particles [47]. A free radical initiator was attached to the silica surface, either covalently or physically. Upon initiation in monomer solution, the polymerization occurred primarily at the particle surface, creating thin homogenous polymer films, of which thickness can be controlled by the reaction time. When using controlled radical polymerization (CRP) by adding a reversible addition-fragmentation chain transfer (RAFT) agent, solution gelation was undetectable. As stationary phase in HPLC, L-phenylalanine anilide imprinted particles showed baseline chiral separations within a few minutes [48].

Zimmerman *et al.* introduced a technique in which an imprinted cavity is created inside dendrimers [49]. A porphyrin was chosen as the template molecule, to which dendrons were covalently attached, creating a core-shell polydendritic molecule. Crosslinking of the dendritic end-groups, which occurred primarily intra-molecularly, and subsequent hydrolytic removal of the porphyrin core led to the formation of an imprinted "particle" consisting of a single dendritic molecule. Thus, this approach resulted in several desirable characteristics such as high imprinting efficiency and quantitative template removal.

A recent paper described the preparation of hollow polymeric nanocapsules, molecularly imprinted with estrone [50]. Preparation of these nanocapsules is very similar to miniemulsion polymerization; nanocapsule formation takes place in the droplets of a stable miniemulsion (oil in water). The oil phase (e.g. containing a water insoluble monomer), is made strongly hydrophobic due to the addition of a so-called hydrophobe, such as hexadecane or isooctane. The process of nanocapsule formation involves the polymerization of the monomers in the dispersed hydrophobe-monomer mixture, which phase separates due to incompatibility of the growing polymer chain and the hydrophobe. A hollow polymer capsule is formed when the

surface tension between the hydrophobe and the water phase is greater than the surface tension between the polymer and the water phase [51]. Ki and Chang imprinted estrone in polystyrene nanocapsules by the semi-covalent approach, and showed excellent rebinding and accessibility. Furthermore, the nanocapsules were loaded with a lipophilic compound using the imprinted cavities as 'gates', which could be blocked by the imprinting template, giving these nanocapsules a potential as controlled drug delivery vesicles [50].

In recent years a new approach to molecular imprinting has been introduced, in which a crosslinkable polymer instead of monomers is used to form the pre-polymerization complex with the template [52, 53]. One of the advantages of this approach is the possibility to incorporate several functionalities in the polymer in order to control the supramolecular structure. For example, Li *et al.* used a micelle-forming diblock copolymer for the synthesis of molecularly imprinted nanospheres (Figure 7) [54]. The core-forming part of the polymer was derivatized with hydrogen bond forming functional groups and crosslinkable moieties. After complex formation of the template (nucleotide bases uracil or thymine) with the functional units in the core, the micelles were crosslinked. The resulting nanospheres were stable, showed good dispersibility and rapid rebinding kinetics. When compared to the traditional monolith MIP the nanospheres showed higher rebinding capacity.

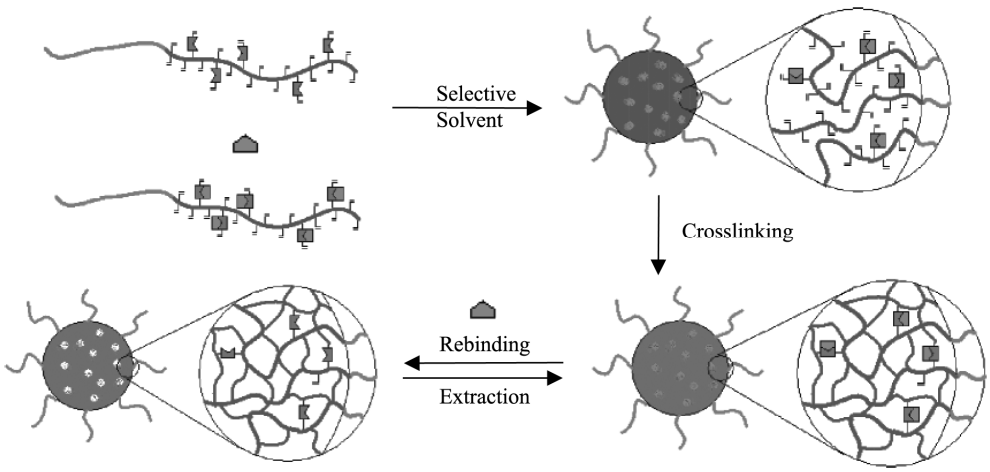

Figure 7. Preparation of imprinted micelles from a diblock copolymer. Diblock copolymer and template are dissolved in a selective solvent leading to the formation of micelles. Polymerization of the crosslinkable moieties of the polymer fixes the micellar structure, allowing extraction and rebinding of the template without disrupting the particle. Reprinted with permission from [54].

Instead of allowing the laws of physics determine the final size and shape of the imprinted particle, it can also be manipulated by the size and shape of the reaction vessel, as exemplified by creating nanofibrils inside the pores of a membrane [55] or nanoparticles inside lipid vesicles [56]. The preparation of nanofibrils was adapted using an immobilized template [57], to create surface-imprinted nanowires [58]; estrone was immobilized on the walls of the pores of a silane-treated nanoporous alumina membrane, and the pores were subsequently filled with the monomer mixture. After polymerization, the membrane and template were dissolved and washed away, leaving the surface imprinted nanowires with high binding capacity and good site accessibility. In a similar way, Li *et al.* successfully imprinted bovine hemoglobin using an all aqueous system of AAM and MBA (Figure 8) [59].

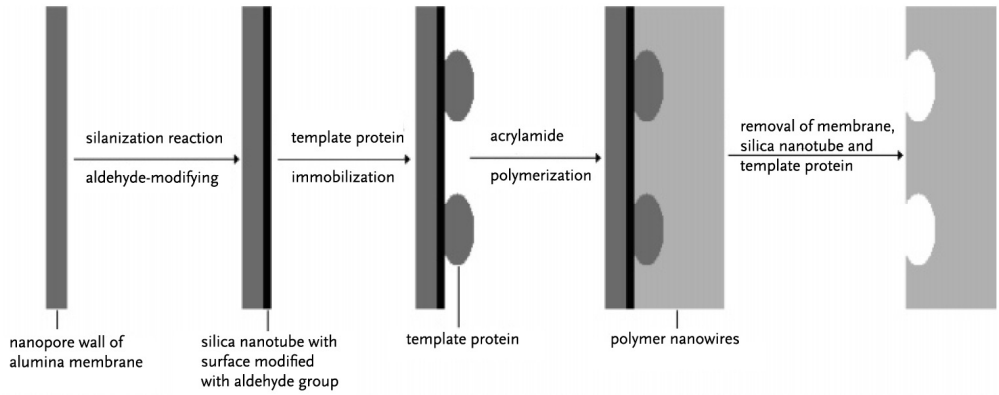

Figure 8. Preparation of protein imprinted nanowires. Reprinted with permission from [59].

Conclusion

The recent development of MIP micro- and nanoparticles, as outlined in this review, marks a big step forward to the applicability of molecular imprinting in nanomedicine. Direct synthesis of molecularly imprinted particles has been compared to the traditional bulk (monolith) polymerization and has proven to be more convenient and/or to display better performance. First of all it avoids the time and labor consuming process of crushing and sieving. Furthermore, direct MIP nanoparticle synthesis hands us some possibilities to overcome the outstanding issues in molecular imprinting, such as enhanced rebinding, improving rate of mass transfer, and production of regularly shaped imprinted particles with controlled particle size and a large surface area. Also progress towards the use in aqueous environments has been made. The

performances of the imprinted particles using different preparation methods have only occasionally been compared. Pérez-Moral and Mayes prepared MIPs non-covalently imprinted with propranolol by bulk, suspension, seed swelling, core-shell emulsion and precipitation polymerization [60]. The main finding was that the order of rebinding capacity of the different MIPs in organic solvent differs from the order in aqueous solution, which emphasizes the solvent dependency of MIP affinity. Zhang *et al.* directly compared MIPs prepared by either seed swelling or suspension polymerization and found similar adsorbing and separating properties. However, suspension polymerization was less time consuming and simpler, while seed swelling produced more regularly shaped and monodisperse particles [61]. The conclusion to be drawn from these data is that none of the compared methods is, in principle, universally superior. The choice of preparation method depends on the application and should be based on a careful consideration of the desired particle properties and rebinding conditions. Among the methods described here, seeded emulsion polymerization appears to be an interesting approach as it allows the preparation of, for example, core-shell particles and surface imprinting along with a good control of particle size. Besides, some advanced methods are recently described, including the preparation of imprinted nanocapsules, polymeric micelles and nanowires, which afford fascinating prospects in the nanomedical field.

In the biomedical field, MIP particles are presently used for the analysis of bioactive substances, as illustrated by the highly selective solid phase extraction and chromographic separation of enantiomers or structural analogues of drugs. Furthermore, MIP particles are applied for drug delivery as illustrated by the controlled release of sulfasalazine from imprinted particles obtained by precipitation polymerization. The imprinting of proteins in nanoparticles can be considered as an important starting point for further developments in the biomedical area.

Future perspective

The most important step towards the use of imprinted nanoparticles in medical or pharmaceutical applications would be the proof-of-principle for selective binding *in vivo*. For example, it has been shown that cholesterol imprinted polymers are able to absorb cholesterol from gastrointestinal fluids *in vitro* [56]. Therefore, it would be interesting to show its efficacy *in vivo* as well. Additionally, nanoscaled MIPs could offer interesting new possibilities in drug targeting and delivery, since it opens up the possibility of direct injection to the blood circulation. As discussed, it is possible to synthesize imprinted magnetic core-shell nanoparticles. Such

particles could prove to be useful carriers of therapeutic compounds, combining the targeting possibilities of magnetic particles [62] with the enhanced loading and controlled release properties of MIPs. Also, the large surface to volume ratio of nanoparticles makes surface imprinting, *i.e.* the preparation of uniform imprints only at the surface of the particles, a feasible approach. Surface imprinting of proteins, for example by the epitope approach, may make these techniques applicable to target (drug loaded) nanoparticles to specific cells or tissues that expose the imprinted protein. Other biological templates such DNA or viruses may also be interesting targets.

Recent developments in the MIP field that are expected to push the technology within reach of biomedical applications include the synthesis of new 'universal' and/or high affinity functional monomers, the use of macromolecular and/or multifunctional monomers, new polymerization and crosslinking methods, the use of polymers responsive to external stimuli (temperature, pH, redox potential, molecular stimuli), and the development of array technologies for high throughput MIP screening and biosensor applications.

The future of MIP particles lies wide open. Without doubt, new and advanced methods for nanoparticle synthesis will occur and will be applied to make imprints of new (bio)molecular targets, as is already seen for nanowires, nanocapsules and polymeric micelles. Combined with the continuously growing insights in the basic mechanisms of molecular imprinting, the broad application of MIP particles as synthetic receptors is only a matter of time.

Acknowledgement

This work was financially supported by the Innovational Research Incentives Scheme of the Netherlands Organization for Scientific Research (grant nr 700.53.422).

References

[1] A.G. Mayes, M.J. Whitcombe, Synthetic strategies for the generation of molecularly imprinted organic polymers, Adv. Drug Del. Rev., 57 (2005) 1742-1778.

[2] C. Alexander, H.S. Andersson, L.I. Andersson, R.J. Ansell, N. Kirsch, J. O'Mahony, M.J. Whitcombe, Molecular imprinting science and technology: a survey of the litterature for the years up to and including 2003, J. Mol. Recognit., 19 (2006) 106-180.

[3] M.J. Whitcombe, M.E. Rodriguez, P. Villar, E.N. Vulfson, A new method for the introduction of recognition site functionality into polymers prepared by molecular imprinting: synthesis and characterization of polymeric receptors for cholesterol, J. Am. Chem. Soc., 117 (1995) 7105-7111.

[4] B. Sellergren, C.J. Allender, Molecularly imprinted polymers: a bridge to advanced drug delivery, Adv. Drug Del. Rev., 57 (2005) 1733-1741.

[5] C.F. Van Nostrum, Molecular imprinting: A new tool for drug innovation, Drug Disc. Today: Tech., 2(1) (2005) 119-124.

[6] J.Z. Hilt, M.E. Byrne, Configurational biomimesis in drug delivery: molecular imprinting of biologically significant molecules, Adv. Drug Del. Rev., 56 (2004) 1599-1620.

[7] R.H. Pelton, P. Chibante, Preparation of aqueous latices with N-isopropylacrylamide, Colloids Surf., 20 (1986) 247-256.

[8] R. Pelton, Temperature-sensitive aqueous microgels, Adv. Colloid Interface Sci., 85 (2000) 1-33.

[9] R. Arshady, Suspension, emulsion, and dispersion polymerization: A methodological survey, Colloid Polym. Sci., 270 (1992) 717-732.

[10] B. Sellergren, Imprinted dispersion polymers: a new class of easily accessible affinity stationary phases, J. Chromatogr. A, 673 (1994) 133-141.

[11] B. Sellergren, Direct drug determination by selective sample enrichment on an imprinted polymer, Anal. Chem., 66 (1994) 1578-1582.

[12] L. Ye, P. Cormack, K. Mosbach, Molecularly imprinted monodisperse microspheres for competitive radioassay, Anal. Commun., 36 (1999) 35-38.

[13] L. Ye, R. Weis, K. Mosbach, Synthesis and characterization of molecularly imprinted microspheres, Macromolecules, 33 (2000) 8239-8245.

[14] A. Biffis, N.B. Graham, G. Siedlaczek, S. Stalberg, G. Wulff, The synthesis, characterization and molecular recognition properties of imprinted microgels, Macromol. Chem. Phys., 202 (2001) 163-171.

[15] J. Wang, P. Cormack, D.C. Sherrington, E. Khoshdel, Monodisperse, molecularly imprinted polymer microspheres prepared by precipitation polymerization for affinity separation applications, Ang. Chem. Int. Ed., 42 (2003) 5336-5338.

[16] G. Ciardelli, B. Cioni, C. Cristallini, N. Barbani, D. Silvestri, P.G. a, Acrylic polymeric nanospheres for the release and recognition of molecules of clinical interest, Biosens. Bioelectron., 20 (2004) 1083-1090.

[17] S.C. Maddock, P. Pasetto, M. Resmini, Novel imprinted soluble microgels with hydrolytic catalytic activity, Chem. Commun., 9 (2004) 536-537.

[18] Z. Meng, K. Sode, The molecular reaction vessel for a transesterification process created by molecular imprinting technique, J. Mol. Recognit., 18 (2005) 262-266.

[19] D. Silvestri, C. Borrelli, P. Giusti, C. C., G. Ciardelli, Polymeric devices containing imprinted nanospheres: a novel approach to improve recognition in water for clinical uses, Anal. Chim. Acta, 542 (2005) 3-13.

[20] O. Kotrotsiou, K. Kotti, E. Dini, O. Kammona, C. Kiparissides, Nanostructured materials for selective recognition and targeted drug delivery, J. Phys. Conf. Ser., 10 (2005) 281-284.

[21] F. Puoci, F. Iemma, R. Muzzalupo, U. Spizzirri, S. Trombino, R. Cassano, N. Picci, Spherical molecularly imprinted polymers (SMIPS) via a noval precipitiation polymerization in the controlled delivery of sulfasalazine, Macromol. Biosci., 4 (2004) 22-26.

[22] G. Wulff, B.-O. Chong, U. Kolb, Soluble single-molecule nanogels of controlled structure as matrix for efficient artificial enzymes, Ang. Chem. Int. Ed., 45 (2006) 2955-2958.

[23] S. Boonpangrak, V. Prachayasittikul, L. Bülow, L. Ye, Molecularly imprinted polymer microspheres prepared by precipitation polymerization using a sacrificial covalent bond, J. Appl. Pol. Sci., 99 (2006) 1390-1398.
[24] E.V. Piletska, M. Romero-Guerra, Antonio R. Guerreiro, K. Karim, A.P.F. Turner, S.A. Piletsky, Adaptation of the molecular imprinted polymers towards polar environment, Anal. Chim. Acta, 542 (2005) 47-51.
[25] M.S. Cho, K.J. Yoon, B.K. Song, Dispersion polymerization of acrylamide in aqueous solution of ammonium sulfate: Synthesis and characterization, J. Appl. Pol. Sci., 83 (2002) 1397-1405.
[26] G. Ciardelli, C. Borrelli, D. Silvestri, C. Cristallini, N. Barbani, P. Giusti, Supported imprinted nanospheres for the selective recognition of cholesterol, Biosens. Bioelectron., 21 (2006) 2329-2338.
[27] A.G. Mayes, K. Mosbach, Molecularly imprinted polymer beads: suspension polymerization using a liquid perfluorocarbon as the dispersing phase, Anal. Chem., 68 (1996) 3769-3774.
[28] H. Kempe, M. Kempe, Novel method for the synthesis of molecularly imprinted polymer bead libraries, Macromol. Rapid Commun., 25 (2004) 315-320.
[29] K. Landfester, N. Bechtold, F. Tiarks, M. Antonietti, Formulation and stability mechanisms of polymerizable miniemulsions, Macromolecules, 32 (1999) 5222-5228.
[30] D. Vaihinger, K. Landfester, I. Kräuter, H. Brunner, G.E.M. Tovar, Molecularly imprinted polymer nanospheres as synthetic affinity receptors obtained by miniemulsion polymerisation, Macromol. Chem. Phys., 203 (2002) 1965-1973.
[31] A. Weber, M. Dettling, H. Brunner, G.E.M. Tovar, Isothermal titration calorimetry of molecularly imprinted polymer nanospheres, Macromol. Rapid Commun., 23 (2002) 824-828.
[32] M. Lehmann, M. Dettling, H. Brunner, G.E.M. Tovar, Affinity parameters of amino acid derivative binding to molecularly imprinted nanospheres consisting of poly[(ethylene glycol dimethacrylate)-co-(methacrylic acid)], J. Chromatogr. B, 808 (2004) 43-50.
[33] J. Haginaka, H. Takehira, K. Hosoya, N. Tanaka, Molecularly imprinted uniform-sized polymer-based stationary phase for naproxen, Chem. Lett., 26 (1997) 555-556.
[34] J. Haginaka, H. Sanbe, Uniformly sized molecularly imprinted polymer for (S)-naproxen retention and molecular recognition properties in aqueous mobile phase, J. Chromatogr. A, 913 (2001) 141-146.
[35] K. Hosoya, K. Yoshizako, Y. Shirasu, K. Kimata, T. Araki, N. Tanaka, J. Haginaka, Molecularly imprinted uniform-size polymer-based stationary phase for high-perfomance liquid chromatography structural contribution of cross-linked polymer network on specific molecular recognition, J. Chromatogr. A, 728 (1996) 139-147.
[36] J. Haginaka, C. Kagawa, Uniformly sized molecularly imprinted polymer for *d*-chlorpheniramine. Evaluation of retention and molecular recognition properties in an aqueous mobile phase, J. Chromatogr. A, 948 (2002) 77-84.
[37] Q. Fu, H. Sanbe, C. Kagawa, K.-K. Kunimoto, J. Haginaka, Uniformly sized moleclarly imprinted polymer for (S)-nilvadipine. Comparison if chiral recognition ability with HPLC chiral stationary phases based on a protein, Anal. Chem., 75 (2003) 191-198.
[38] J. Haginaka, H. Takehira, K. Hosoya, N. Tanaka, Uniform-sized molecularly imprinted polymer for (S)-naproxen selectively modified with hydorphilic external layer, J. Chromatogr. A, 849 (1999) 331-339.
[39] Z. Chen, R. Zhao, D. Shangguan, G. Liu, Preparation and evaluation of uniform-sized molecularly imprinted polymer beads used for the separation of sulfamethazine, Biomed. Chromatogr., 19 (2005) 533-538.
[40] L. Zhang, G. Cheng, C. FU, Molecular selctivity of tyrosine-imprinted polymers prepared by seed swelling and suspension polymerization, Polym. Int., 51 (2002) 687-692.
[41] N. Pérez, M.J. Whitcombe, E.N. Vulfson, Molecularly imprinted nanoparticles prepared by core-shell emulsion polymerization, J. Appl. Pol. Sci., 77 (2000) 1851-1859.
[42] M. Kempe, M. Glad, K. Mosbach, An approach towards surface imprinting using the enzyme ribonuclease A, J. Mol. Recognit., 8 (1995) 35-39.
[43] N. Pérez, M.J. Whitcombe, E.N. Vulfson, Surface imprinting of cholesterol on submicrometer core-shell emulsion particles, Macromolecules, 34 (2001) 830-836.

[44] A. Rachkov, N. Minoura, Towards molecularly imprinted polymers selective to peptides and proteins. The epitope approach, Biochim. Biophys. Acta, 1544 (2001) 255-266.
[45] C.-S. Huang, C.C. Lynch, A. Strikovsky, Inverse emulsion methods of making polymeric imprint beads, in, Aspira Biosystems, inc., United States of America, 2002.
[46] G. Wulff, D. Oberkobusch, M. Minarik, Enzyme-analogue built polymers, 18 chiral cavities in polymer layers coated on wide-pore silica, React. Polym., Ion Exch., Sorb., 3 (1985) 261-275.
[47] C. Sulitzky, B. Rückert, A.J. Hall, F. Lanza, K. Unger, B. Sellergren, Grafting of molecularly imprinted polymer films on silica supports containing surface-bound free radical initiators, Macromolecules, 35 (2002) 79-91.
[48] M.-M. Titirici, B. Sellergren, Thin molecularly imprinted polymer films via reversible addition-fragmentation chain transfer polymerization, Chem. Mater., 18 (2006) 1773-1779.
[49] S.C. Zimmerman, M.S. Wendland, N.A. Rakow, I. Zharov, K.S. Suslick, Synthetic hosts by monomolecular imprinting inside dendrimers, Nature, 418 (2002) 399-403.
[50] C.D. Ki, J.Y. Chang, Preparation of a molecularly imprinted nanocapsule with potential use in delivery applications, Macromolecules, 39 (2006) 3415-3419.
[51] F. Tiarks, K. Landfester, M. Antonietti, Preparation of polymeric nanocapsules by miniemulsion polymerization, Langmuir, 17 (2001) 908-918.
[52] J. Matsui, N. Minamimura, K. Nishimoto, K. Tamaki, N. Sugimoto, Synthetic cinchonidine receptors obtained by cross-linking linear poly(methacrylic acid) derivatives as an alternative molecular imprinting technique, J. Chromatogr. B, 804 (2004) 223-229.
[53] Z. Li, M. Day, J. Ding, K. Faid, Synthesis and characterization of functional methacrylate copolymers and their application in molecular imprinting, Macromolecules, 38 (2005) 2620-2625.
[54] Z. Li, J. Ding, M. Day, Y. Tao, Molecularly imprinted polymeric nanospheres by diblock copolymer self-assembly, Macromolecules, 39 (2006) 2629-2636.
[55] C.R. Martin, Nanomaterials: A membrane-based synthetic approach, Science, 266 (1994) 1961-1966.
[56] J.P. Schillemans, F.M. Flesch, W.E. Hennink, C.F. Nostrum van, Synthesis of bilayer-coated nanogels by selective crosslinking of monomers inside liposomes, Macromolecules, 39 (2006) 5885-5890.
[57] E. Yilmaz, K. Haupt, K. Mosbach, The use of immobilized templates - A new approach in molecular imprinting, Ang. Chem. Int. Ed., 39 (2000) 2115-2118.
[58] H.-H. Yang, S.-Q. Zhang, F. Tan, Z.-X. Zhuang, X.-R. Wang, Surface molecularly imprinted nanowires for biorecognition, J. Am. Chem. Soc., 127 (2005) 1378-1379.
[59] Y. Li, H.-H. Yang, Q.-H. You, Z.-X. Zhuang, X.-R. Wang, Protein recognition via surface molecularly imprinted polymer nanowires, Anal. Chem., 78 (2006) 317-320.
[60] N. Pérez Moral, A.G. Mayes, Comparative study of imprinted polymer particles prepared by different polymerisation methods, Anal. Chim. Acta, 504 (2004) 15-21.
[61] L. Zhang, G. Cheng, C. Fu, Synthesis and characteristics of tyrosine imprinted beads via suspension polymerization, React. Funct. Pol., 56 (2003) 167-173.
[62] J. Dobson, Magnetic micro- and nano-particle-based targeting for drug and gene delivery, Nanomed., 1 (2006) 31-37.

Chapter 3

Synthesis of bilayer-coated nanogels by selective crosslinking of monomers inside liposomes

Joris P. Schillemans

Frits M. Flesch

Wim E. Hennink

Cornelus F. van Nostrum

Macromolecules 2006, 39 (17), 5885-5890

Abstract

Bilayer-coated polyacrylamide hydrogel nanoparticles were prepared by photoinitiated polymerization of acrylamide (AAm) and N,N'-methylene-bisacrylamide (MBA) in the inner compartment of liposomes. The liposomes were formed in AAm/MBA-solutions from lipid/Triton X-100 (TX100) mixed micelles by adsorption of TX100 to Bio-Beads SM2, and were studied by dynamic light scattering and transmission electron microscopy. The hydrodynamic diameters of the liposomes were approximately 100 nm with low polydispersity. Addition of ascorbic acid before photopolymerization prevented macroscopic hydrogel formation by inhibition of free-radical polymerization of non-encapsulated monomers. Bare nanogel particles were obtained by removal of the lipid bilayer. As opposed to the commonly used dilution method, this convenient and versatile method of nanogel synthesis will allow incorporation of membrane proteins in the bilayer and the use of monomers that readily pass the lipid membrane.

Introduction

In recent years hydrogel micro- and nanoparticles have been identified as valuable materials for a number of applications, including drug delivery and targeting, chromatography, etc [1-5]. Synthesis of these hydrogel particles can be accomplished in several ways, each with their own advantages and drawbacks. Emulsion polymerization is often used for the synthesis of both micro- and nanoparticles. Using this method, the size of the particles can be controlled by the size of the droplets in the w/o emulsions [6, 7]. However, such systems are generally incompatible with biological macromolecules like proteins. To ensure compatibility with proteins, water-in-water emulsions can be used for synthesis of microparticles, but control of the particle size down to the nanosize has not been accomplished thus far [8, 9]. Another method that is commonly used for both micro- and nanoparticle synthesis is dispersion polymerization [10, 11]. Upon initiation by a suitable initiator, dilute systems of monomer and crosslinker form polymer chains in solution, which collapse to form a precursor particle when reaching a critical chain length. Precursor particles continue to increase in size by additional chain growth and aggregation until a colloidally stable particle is formed [12]. The major drawback of this method is that it does not provide straightforward control over particle size, since the colloidal stability is dependent on monomer composition, initiator and temperature [13]. An alternative, less commonly used approach is available for hydrogel particle synthesis. Monshipouri *et al.* reported on a method that used the internal compartment of lipid vesicles (liposomes) for the preparation of hydrogel particles, which allows good control over particle size and size-distribution, and is compatible with biological macromolecules [14]. Using this method, Kazakov *et al.* [15, 16] described the synthesis of thermo- and pH-sensitive hydrogel nanoparticles, Van Thienen *et al.* [17] synthesized biodegradable dextran nanogels, and Patton and Palmer synthesized hemoglobin entrapped nanogels [18-20].

In addition to providing an alternative method for hydrogel nanoparticle synthesis, bilayer-coated nanogels as such could also have numerous applications. Combining the properties of both hydrogels and liposomes they could be used as, for example, controlled release devices, artificial cell analogues and biomimetic sensory systems [15]. Especially for the latter two, the incorporation of functional membrane proteins will be important. The method most commonly used for functional incorporation of membrane proteins in liposomes is detergent dilution [21, 22]. The liposomal reactors used for nanoparticle synthesis described thus far, however, were prepared by freeze-thawing, sonication and extrusion, which are less suitable for functional

protein incorporation. Using the detergent dilution method, a dispersion of lipid-containing mixed micelles is diluted below the critical micelle concentration (CMC) of the detergent, which leads to the formation of liposomes. Several detergents can be used for this purpose, e.g. octylglucoside, sodiumcholate, C8E12 and Triton X-100 (TX100). Additionally, several methods of detergent dilution are available such as dialysis, rapid addition of solvent and adsorption by Bio-Beads SM-2 [23-25]. Removal of TX100 by Bio-Beads has been described in literature extensively [26-29]. It has been proven to be an effective, simple and inexpensive way of incorporating functionally active membrane proteins in liposomes. Nevertheless, up until now this method has not been used to form liposomes in solutions of hydrogel forming monomers.

Liposomes formed in monomer solutions have monomers both on the inside and on the outside. Therefore, prevention of polymerization on the outside of the liposomes is required for controlled nanoparticle synthesis. This was accomplished previously by dilution of the exterior compartment to a concentration of monomers too low for hydrogel formation [15-20]. However, dilution causes a steep concentration gradient across the lipid membrane and is only applicable when the monomers can not diffuse through the liposomal bilayer. When relatively lipophilic monomers are used, diffusion could occur. Additionally, incorporation of membrane proteins can lead to increased permeability of the bilayer [30]. Therefore, in the current study we developed a method for nanoparticles synthesis that will be suitable for the functional incorporation of membrane proteins. First, the liposomes are prepared by detergent removal in order to allow incorporation of functional membrane proteins in the lipid bilayer. Second, for situations where selective removal or dilution of the monomers from the exterior is not feasible, we propose exterior polymerization inhibition using ascorbic acid.

Materials and methods

Preparation of macroscopic hydrogels.

Hydrogels were prepared by UV-initiated polymerization of aqueous solutions of acrylamide (AAm; MP Biomedicals) and N,N'-methylene-bisacrylamide (MBA; MP Biomedicals) as crosslinker. AAm and MBA were dissolved in HEPES buffered saline (HBS) pH 7.4. The nomenclature used to describe the composition of AAm/MBA-solutions is as follows: a (5/10)-solution contains 5% (w/v) total monomer (AAm+MBA) of which 10% (w/w) is MBA. Irgacure 2959 (Ciba Specialty Chemicals) was added as photoinitiator at a concentration of 0.006% (w/v). Crosslinking was performed in the absence or presence of varying amounts of the free-radical

inhibitor L-ascorbic acid (MP Biomedicals) dissolved in HBS (130 mg/mL, pH adjusted to 6.5 to retard degradation of ascorbic acid). All solutions were filtered before use through a 0.2 μm filter. Samples were purged with N_2 for 5 minutes and illuminated for 90 seconds under a N_2 atmosphere using a Bluepoint 4 UVC mercury lamp (150W, λ-range 230-600 nm, Honle UV Technology).

Dynamic mechanical analysis (DMA)

DMA measurements were performed on a DMA 2980 Dynamic Mechanical Analyzer (TA Instruments, Inc.) in 'controlled force' mode as described by Meyvis *et al.* [31]. Macroscopic hydrogels were prepared by free-radical polymerization in a cylinder-shaped reaction reservoir as described above. The resulting hydrogels (height 5 mm, diameter 4.5 mm) were placed between a parallel-plate compression clamp, and a force ramp was applied. Young's modulus (E') of the hydrogels was calculated using a plot of the compressional force versus the observed deformation, in which the value of the slope equals E'.

Liposome preparation

Liposomes were prepared either from mixed micelles by removal of TX100 by Bio-Beads or by extrusion. Appropriate amounts of dioleoylphosphatidylcholine (DOPC) (Lipoid GmbH), egg phosphatidylglycerol (EPG) (Lipoid GmbH) and cholesterol (Sigma), in a molar ratio of 4:1:1, were dissolved in chloroform in a round-bottom flask. A lipid film was prepared under reduced pressure using a rotary evaporator and dried further under a stream of nitrogen. An aqueous solution (20% w/v) of Triton X-100 (TX100) (BDH Laboratory Supplies) was added at a molar ratio of 3:1 (TX100 to total phospholipid (PL)), which is needed to form micelles [28]. Next, either HBS or monomer solution (in HBS) was added to yield a final PL concentration of 2.5 mM. Irgacure was added to a concentration of 0.006% (w/v). Controls consisted of mixed micelles without Irgacure in AAm/MBA solutions, AAm/MBA solutions with Irgacure, and AAm/MBA solutions without Irgacure.

Bio-Beads SM-2 (Bio-Rad) were extensively washed with methanol, and subsequently incubated in HBS or AAm/MBA solution [26]. Washed Bio-Beads (60 mg/mL, moist weight) were added to the micelle solutions, which were subsequently left for 3 h at room temperature (RT) under gentle shaking. Additional (120 mg/mL) Bio-Beads were added and samples were left for an additional 3 h at RT under gentle shaking. Bio-Beads were allowed to settle, and the supernatant was collected. Microparticles (aggregates) were removed by centrifugation at

18.000 g for 5 minutes. The PL content of the liposome preparations was determined by phosphate analysis according to Rouser [32] after destruction with perchloric acid.

Liposomes were prepared by extrusion as well. Lipid films prepared as described above were hydrated in HBS or AAm/MBA solution (without TX100), containing 0.006% (w/v) Irgacure. As a control, liposomes with encapsulated ascorbic acid were prepared by hydration of a lipid film in monomer solution containing ascorbic acid at a molar ratio of 600 relative to Irgacure. Subsequently, the formed multilamellar liposomes were extruded using a hand extruder (Avanti Polar Lipids) through polycarbonate filters with a pore size of 0.4 µm.

Nanogel synthesis

To prevent polymerization outside the liposomes, ascorbic acid dissolved in HBS (130 mg/mL, pH adjusted to 6.5) was added to the liposome dispersion immediately before illumination, in a molar ratio of 200 relative to Irgacure. To compare the method of external inhibition of polymerization to external monomer dilution, [15-19] part of the liposomes prepared in AAm/MBA (5/10) containing Irgacure were diluted 20 times in HBS. Samples and controls were purged with N_2 for 5 minutes and illuminated for 90 seconds under a N_2 atmosphere. To obtain bare nanogels, the PL bilayer was dissolved by addition of TX100-solution (20%, w/v) to a molar ratio of 60 relative to total PL.

Dynamic light scattering (DLS)

The size and size distribution of particles were measured by dynamic light scattering (DLS) using a Malvern CGS-3 multiangle goniometer (Malvern Ltd.), consisting of a HeNe laser source (λ = 632.8 nm, 22 mW output power), temperature controller (Julabo water bath) and digital correlator ALV-5000/EPP. Time correlation functions were analyzed to obtain the hydrodynamic diameter of the particles (Z_h) and the particle size distribution (polydispersity index, PDI) using the ALV-60X0 software V.3.X provided by Malvern, The determination of Z_h by dynamic light scattering is based on the Stokes-Einstein equation (eq 1)

$$Z_h = (k_B T \mathbf{q}2)/(3\pi\eta\Gamma) \qquad (1)$$

k_B is the Boltzmann constant, η is the solvent viscosity, Γ is the decay rate and $\mathbf{q}$ is the scattering vector ($\mathbf{q}$=($4\pi n \sin(\theta/2)$)/λ), in which n is the refractive index of the solution, θ is the scattering angle, λ is the wavelength of the incident laser light. Scattering was measured in an optical

quality 4 mL borosilicate cell at a 90° angle. The samples were analyzed at 25°C. For measurements in AAm/MBA-solutions the hydrodynamic diameter was corrected for differences in solvent viscosity.

Electrophoretic mobility

The particle ζ-potential can be calculated from the electrophoretic mobility using the Smoluchowski equation. The ζ-potential of both bilayer-coated and bare nanoparticles in HBS was determined using a Zetasizer 3000 (Malvern Instruments), equipped with a flow-through cell and PCS software (version 1.43). Following solubilization of the bilayer with TX100, bare particles were separated from mixed micelles by ultracentrifugation at 210.000 g for 2 h, 3 subsequent times. The pellet was resuspended in HBS.

Transmission electron microscopy (TEM)

Negative stain: Lipid-coated and bare nanoparticles were adsorbed on glow discharged Formvar-carbon-coated copper grids, washed twice in HBS, and negatively stained with 2% (w/v) uranyl acetate. The ultrastructure was analyzed with a Tecnai 10 electron microscope (FEI Company) at a 100 kV acceleration voltage.

Cryogenic-TEM: Samples were prepared in a temperature- and humidity-controlled chamber with an automatic blotting/plunging system using a "Vitrobot". A thin aqueous film of particle dispersion was formed by blotting a glow-discharged 200 mesh copper grid covered with Quantifoil holey carbon foil (Micro Tools GmbH) at 25°C and 100% relative humidity. The thin film was rapidly vitrified by plunging the grid into liquid ethane. Subsequently, the grids were transferred into the microscope chamber using a GATAN 626 cryoholder system. Samples were analyzed at -180°C using a Tecnai12 transmission electron microscope (FEI Company) operating at 120 kV. Low-dose imaging conditions were used to avoid melting of the vitrified film.

Results and discussion

Table 1. Effect of hydration-medium on phospholipid recovery, hydrodynamic diameter and polydispersity index of PL vesicles formed by TX100 removal by Bio-Beads.[a]

Medium	*PL after Bio-Beads (%)[b]*	*PL after centrifugation (%)[b]*	*Hydrodynamic Diameter (nm)[c]*	*PDI[c]*
HBS	73 ± 2	33 ± 7	159 ± 3	0.04 ± 0.02
AAm/MBA 5/10	78 ± 2	65 ± 3	115 ± 7	0.10 ± 0.04
AAm/MBA 10/20	72 ± 4	60 ± 2	94 ± 6	0.07 ± 0.06

[a] n=4, values represent avg. ± sd. [b] Percentage of the amount of PL before addition of Bio-Beads. [c] Measured in the supernatant after centrifugation.

Liposome preparation

Liposomes composed of DOPC:EPG:Chol 4:1:1 were prepared from mixed micelles using TX100 removal by adsorption to Bio-Beads in HBS and in solutions of monomer (AAm) and crosslinker (MBA) in HBS. After subsequent removal of the Bio-Beads, the formed vesicles were studied by determination of PL content, DLS-measurements, and Cryo-TEM (Table 1, Figure 1 and 2). The Bio-Beads did not only adsorb TX100 but also approximately 25% of the PL (Table 1). This corresponds to 2.7 mg lipid/g Bio-Beads, which is in agreement with earlier reports [28]. DLS measurements showed that two populations of particles were present after TX100 removal, i.e. particles that are in the nanometer-range (liposomes), and particles in the micrometer-range (Figure 1A). The larger particles could be lipid aggregates or (small parts of) Bio-Beads, which were removed by centrifugation. All samples contained a pellet after centrifugation. DLS measurements of the supernatant (Figure 1B) showed only one population of particles in each sample, with hydrodynamic diameters as expected for liposomal vesicles (Table 1).

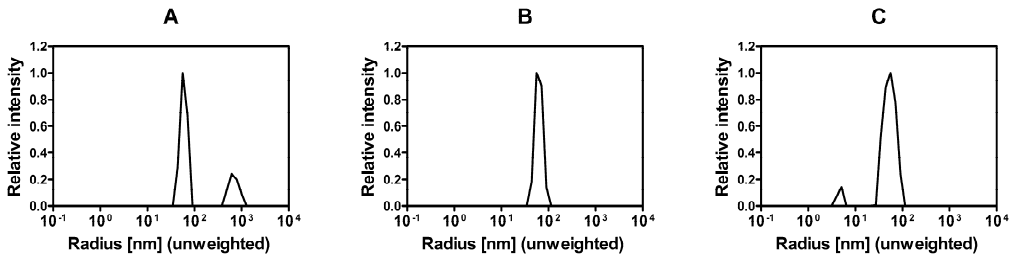

Figure 1. Particle size distribution (hydrodynamic radius (nm), unweighted regularized fit) for the different stages of nanogel preparation by TX100 removal by Bio-Beads. Bimodal distribution after TX100 removal (A), monomodal distribution in the supernatant after subsequent centrifugation (B), and bare nanogels and mixed micelles after re-solubilizing the lipid bilayer with TX100 (C).

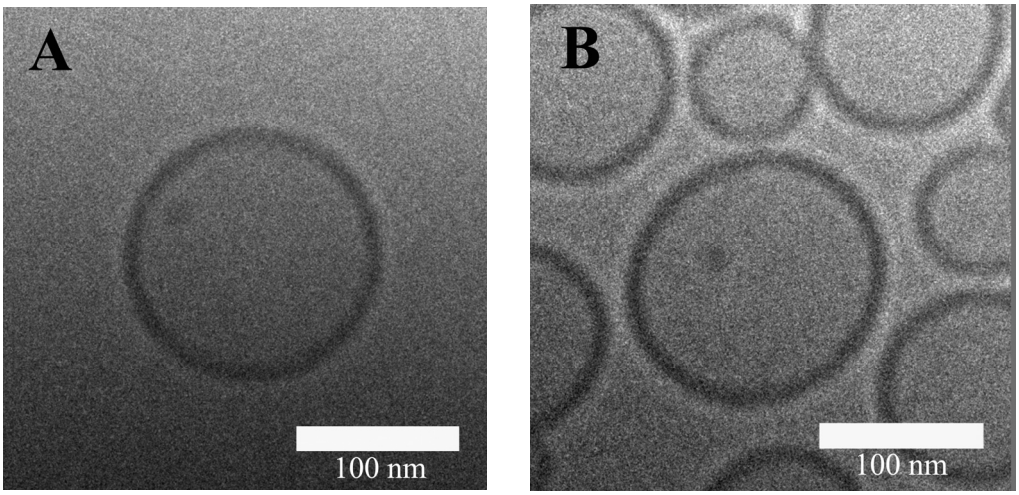

Figure 2. Cryogenic-temperature transmission electron microscope images of particles formed after TX100 removal by Bio-Beads in HBS (A) and AAm/MBA solution (B). Representative images are shown.

The presence of liposomes in the supernatant was confirmed with Cryo-TEM, showing spherical vesicles, homogenous in size, with no apparent morphological differences between vesicles formed in HBS or AAm/MBA solutions (Figure 2). Only 33% of the initial amount of PL was found in the supernatant in HBS, while in AAm/MBA solutions this percentage was significantly higher (65% for (5/10)-solution and 60% for (10/20)). Furthermore, the presence of AAm/MBA in the solution reduced the size of the liposomes: 159 nm in HBS, 115 nm in AAm/MBA (5/10) solution, and 94 nm in AAm/MBA (10/20) (Table 1). It has been shown before that the size of liposomes formed by detergent removal by Bio-Beads depends both on the detergent used [29, 33] and the rate of removal [23, 28, 34-36]. The smaller hydrodynamic diameter of the particles formed in AAm/MBA solutions could be caused by the higher viscosity of these solutions, which influences several processes determining particle size, such as micelle fusion [35], lipid exchange [36] and post vesiculation [34]. These processes are also the likely cause of the higher PL content of the supernatant after centrifugation.

Inhibition of free-radical polymerization

Liposomes that are formed in AAm/MBA solution contain monomer both in the inner compartment and in the outer liquid. In order to produce nanoparticles within the liposomal reactor, it is important to restrict the hydrogel formation of the monomers to the inner compartment of the liposomes. Therefore, polymerization outside the liposomes should be prevented, which can be accomplished in two ways: 1) dilution of the monomers to a

concentration too low for hydrogel formation, and 2) inhibition of free-radical polymerization. It is very likely that dilution leads to leaking of the monomer and particularly of the relatively hydrophobic crosslinker out of the liposomes, thereby also impairing hydrogel formation inside the liposome (as will be discussed below in the section Nanogel synthesis). Consequently, inhibition of polymerization is the preferred method to prevent hydrogel formation outside the liposome.

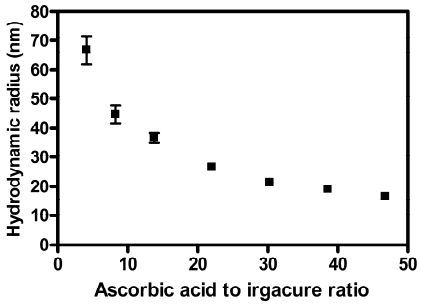

Figure 3. Particle size as a function of the ratio of ascorbic acid to Irgacure in the absence of liposomes. Samples containing AAm/MBA (5/10) solution, 0.006% (w/v) Irgacure and varying amounts of ascorbic acid were illuminated for 90 seconds. Particle size was measured by DLS. Error bars represent standard deviation (n=3).

Ascorbic acid is a well-known, water-soluble radical-scavenger. It is a bivalent acid, with respective pKa's of 4.17 and 11.57 [37], by which ascorbic acid carries one negative charge at pH 7.4. The lipid bilayer contains EPG, a lipid with a negatively charged headgroup at physiological pH, which prevents ascorbic acid from readily diffusing over the bilayer. These characteristics make ascorbic acid a suitable candidate for the inhibition of free-radical polymerization outside the liposomes. To assess to what extent ascorbic acid inhibits UV-induced free-radical polymerization, we tested its effect on macroscopic hydrogel formation. AAm/MBA (5/10) solutions containing ascorbic acid at a molar ratio of 4 and higher relative to Irgacure remained liquid upon UV illumination. However, DLS-measurements showed the presence of particles, whose size decreased from 66 to 15 nm with increasing ascorbic acid concentration (Figure 3). Using a (5/10) AAm/MBA solution containing 0.006% (w/v) Irgacure, and 90 seconds of illumination, the particle size leveled off at a ratio of approximately 40 while in a (10/20) AAm/MBA solution the same plateau value was reached at a ratio of approximately 150 (data not shown). Apparently, it is not possible to inhibit the polymerization completely. Upon UV-illumination some monomers will polymerize before ascorbic acid terminates the reaction by

radical scavenging. At higher concentrations the availability of monomers is higher, which explains the higher amount of ascorbic acid needed to reach the plateau using a (10/20) solution. It must be noted, however, that the scattering intensity at this plateau is just at the detection limit of the DLS-equipment.

Besides radical scavenging, ascorbic acid also absorbs UV-light (λ_{max} at neutral pH is 265 nm) [37]. To accomplish inhibition of polymerization outside liposomes while allowing polymerization inside, it is important to make sure that ascorbic acid does not inhibit polymerization inside by UV-absorption. Therefore, we determined the storage modulus of a macroscopic hydrogel when the initiating light first passed through a solution of ascorbic acid having a concentration equal to the highest concentration of the inhibition experiments (200 equivalents relative to Irgacure). The modulus of a 5/10 hydrogel as determined by DMA was not affected when the beam of UV light passed through a quartz cuvet before reaching the sample (1.9 ± 0.2 kPa), nor when this cuvet was filled with buffer, AAm/MBA (5/10) solution or ascorbic acid-containing AAm/MBA (5/10) solution.

Nanoparticle synthesis.

The monomer dilution method to prevent external polymerization failed in our hands. When liposomes in AAm/MBA-solution were diluted 20 times in HBS and illuminated, and subsequently the lipid bilayer was solubilized with TX100, DLS-measurements did not detect the presence of nanoparticles; only mixed micelles were observed (hydrodynamic diameter = 9 nm). It is most likely that dilution of the external compartment caused AAm and MBA to diffuse over the bilayer, leading to dilution of the monomers in the liposomal compartment to a concentration too low for hydrogel formation. This is in contradiction to earlier work by Kazakov *et al.*, who did observe nanoparticles by DLS using the same method [15]. This may be explained as follows. Kazakov *et al.* used dialysis in 25 kDa cut-off bags in an attempt to remove the lipids that were solubilized by TX100. However, dialysis of mixed micelles is also one of the methods to produce liposomes by detergent removal [24], which could mean that the remaining particles observed by Kazakov *et al.* were reformed (empty) liposomes instead of nanogels.

Because the dilution method results in the diffusion of monomers out of the liposomes, we used polymerization inhibition by radical scavenging. Ascorbic acid was added to the undiluted liposome preparations at an ascorbic acid/Irgacure ratio of 200, and the dispersions were UV-irradiated. The hydrodynamic diameter measured by DLS after illumination was unchanged, indicating that the polymerization of AAm/MBA did not affect the size of the liposomal reactor.

The small particles that may have been formed outside the liposomes in the presence of ascorbic acid (see above) could not be detected by DLS, because the corresponding signal was too low in presence of the liposomes. After solubilizing the lipid bilayer with TX100, particles of about 100 nm remained (Figure 1C). The particle size decreased by 13 ± 3 nm upon removal of the bilayer, whereas samples without monomers (HBS) or without photoinitiator decreased dramatically, showing only micelles after solubilization of the liposomes (Figure 4A). The decrease of 13 nm upon removal of the bilayer is slightly more than 2 times a DOPC bilayer, which is known to be approximately 4 nm thick [38, 39]. Macroscopic polyacrylamide gels of the same compositions were dimensionally stable in contact with buffer (results not shown). Therefore, the observed decrease in particle size may be due to the fact that liposomes are not always strictly unilamellar, but may have an average of more than 1 bilayer depending on their size [40].

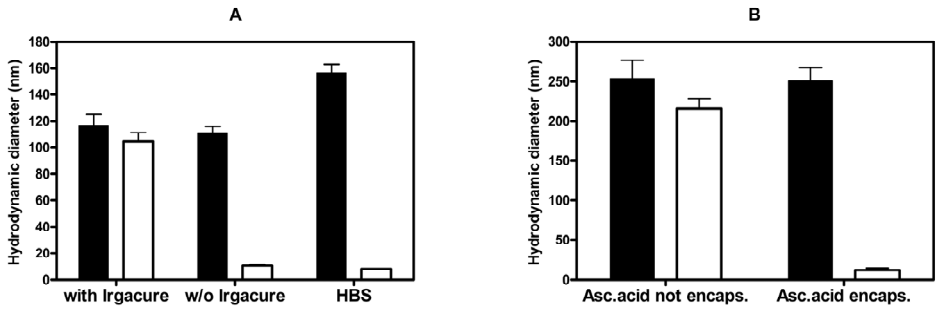

Figure 4. Hydrodynamic diameter as determined by DLS before (■) and after (□) lipid solubilization with TX100. Error bars represent the standard deviation (n=4). (A) Liposomes prepared by TX100-removal by Bio-Beads in either AAm/MBA-solution with or without Irgacure, or in HBS only (with Irgacure). (B) Liposomes prepared by extrusion in Irgacure-containing AAm/MBA-solution in the presence of ascorbic acid either only outside, or both outside and inside the liposomes.

To confirm that the polymerization indeed took place in the inner compartment of liposomes, larger liposomes were prepared by extrusion, which should result in larger nanoparticles accordingly. Besides, in one control sample ascorbic acid was also encapsulated in the inner compartment to prevent hydrogel formation inside the liposomes. As expected, extruded liposomes are larger than the liposomes prepared by TX-100 removal (115 nm and 250 nm, respectively), and consequently the formed bare nanoparticles are larger as well (compare Figures 4A and 4B). The difference between bilayer-coated and bare nanogels is 38 ± 13 nm, which is most likely due to increased oligolamellarity of the extruded liposomes. As expected, UV-polymerization of AAm and MBA inside liposomes could be completely inhibited by the

enclosure of ascorbic acid. After illumination and solubilization of the lipid bilayer of liposomes that contained both monomers and ascorbic acid, only micelles with a hydrodynamic diameter of 12 nm were detected. These results demonstrate that nanoparticles were indeed formed inside the liposomes. TEM-images acquired using negative staining with uranyl acetate confirmed the results presented above. After addition of ascorbic acid and illumination, samples of liposomes in Irgacure-containing AAm/MBA solutions showed lipid-coated nanoparticles, and bare nanoparticles when the lipid bilayer was solubilized with TX100 (Figure 5A and 5B).

The ζ-potential of the particles in HBS decreased after solubilization of the bilayer (–8.7 mV and –4.2 mV for bilayer-coated and bare particles, respectively) which is in agreement with what was reported earlier for acrylamide particles in PBS [20]. Particle size of both bilayer-coated and bare particles remained constant after storage during 2 months at 4°C, which suggests that particles are stable.

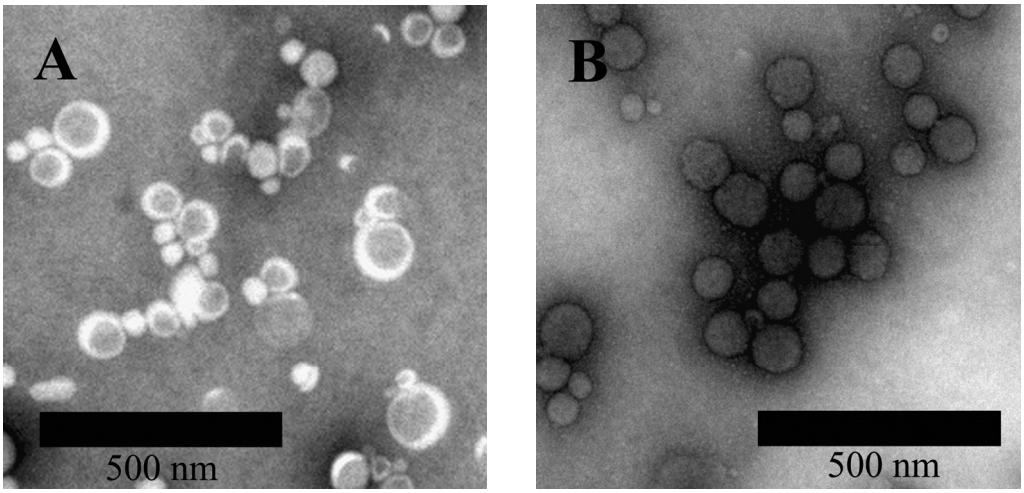

Figure 5. Transmission electron microscope images of lipid-coated (A) and bare (B) polyacrylamide (10/10) nanoparticles. Bare particles were obtained by treating lipid-coated particles with TX100. Samples were stained using 2% uranyl acetate. Lipid membranes appear light since uranyl acetate does not stain the hydrophobic core of membranes, whereas nanoparticles appear dark because uranyl acetate easily penetrates their hydrophilic environment.

Conclusion

Our experiments show that TX100 removal from mixed micelles by Bio-Beads can be used as a method of liposome preparation in monomer solutions. Phospholipid vesicles with a narrow particles size distribution were obtained. The size of these vesicles depends on the monomer concentration.

Formation of hydrogel nanoparticles can be accomplished when polymerization takes place in the inner compartment of the liposomes. In this paper we have shown that ascorbic acid is a good candidate to inhibit polymerization specifically outside the liposomes. The degree to which ascorbic acid inhibits free-radical polymerization depends both on the ascorbic acid and the monomer concentration.

In this paper we have broadened the possibilities for hydrogel nanoparticles synthesis in a liposome reactor using detergent removal and polymerization inhibition by ascorbic acid, which allows incorporation of membrane proteins and the use of monomers that easily diffuse through the lipid bilayer.

Acknowledgement

This work was financially supported by the Innovational Research Incentives Scheme of the Netherlands Organization for Scientific Research (grant nr 700.53.422). The Electron Microscope Facility of the Department of Biology Utrecht is thanked for the use of their microscopes and support. Hans Meeldijk is specially thanked for his comments and assistance with cryo-EM

References

[1] A. Prokop, E. Kozlov, G. Carlesso, J.M. Davidson, Hydrogel-based colloidal polymeric system for protein and drug delivery: physical and chemical characterization, permeability control and applications, Adv. Pol. Sci., 160 (2002) 119-173.

[2] M. Prabaharan, J.F. Mano, Chitosan-based particles as controlled drug delivery systems, Drug Deliv., 12 (2005) 41-57.

[3] J. Kim, S. Nayak, L.A. Lyon, Bioresponsive hydrogel microlenses, J. Am. Chem. Soc., 127 (2005) 9588-9592.

[4] N. Kayaman, D. Kazan, A. Erarslan, O. Okay, B.M. Baysal, Structure and protein separation efficiency of poly(N-isopropylacrylamide) gels: Effect of synthesis Conditions, J. Appl. Pol. Sci., 67 (1998) 805-814.

[5] B.J. Ficek, N.A. Peppas, Novel preparation of poly (vinyl alcohol) microparticles without crosslinking agent for controlled drug delivery of proteins, J. Control. Release, 27 (1993) 259-264.

[6] N. Munshi, T.K. De, A. Maitra, Size Modulation of Polymeric Nanoparticles under Controlled Dynamics of Microemulsion Droplets, J. Colloid Interface Sci., 190 (1997) 387-391.

[7] B. Kriwet, E. Walter, T. Kissel, Synthesis of bioadhesive poly(acrylic acid) nano- and microparticles using an inverse emulsion polymerization method for the entrapment of hydrophilic drug candidates, J Control Rel, 56 (1998) 149-158.

[8] R.J. Stenekes, O. Franssen, E.M. van Bommel, D.J. Crommelin, W.E. Hennink, The preparation of dextran microspheres in an all-aqueous system: effect of the formulation parameters on particle characteristics, Pharm. Res., 15 (1998) 557-561.

[9] O. Franssen, R.J. Stenekes, W.E. Hennink, Controlled release of a model protein from enzymatically degrading dextran microspheres, J. Control. Release, 59 (1999) 219-228.

[10] R.H. Pelton, P. Chibante, Preparation of aqueous latices with N-isopropylacrylamide, Colloids Surf., 20 (1986) 247-256.

[11] X.Y. Wu, P.I. Lee, Preparation and characterization of thermal- and pH-sensitive nanospheres, Pharm. Res., 10 (1993) 1544-1547.

[12] S. Nayak, L.A. Lyon, Soft nanotechnology with soft nanoparticles, Angew. Chem. Int. Ed. Engl., 44 (2005) 7686-7708.

[13] R. Pelton, Temperature-sensitive aqueous microgels, Adv. Colloid Interface Sci., 85 (2000) 1-33.

[14] M. Monshipouri, A.S. Rudolph, Method of forming hydrogel particles having a controlled size using liposomes, in, U.S. Patent 5626870, 1997.

[15] S. Kazakov, M. Kaholek, I. Teraoka, K. Levon, UV-Induced gelation on nanometer scale using liposome reactor, Macromolecules, 35 (2002) 1911-1920.

[16] S. Kazakov, M. Kaholek, D. Kudasheva, I. Teraoka, M.K. Cowman, K. Levon, Poly(N-isopropylacrylamide-co-1-vinylimidazole) hydrogel nanoparticles prepared and hydrophobically modified in liposome reactors: Atomic force microscopy and dynamic light scattering study, Langmuir, 19 (2003) 8086-8093.

[17] T.G. Van Thienen, B. Lucas, F.M. Flesch, C.F. Van Nostrum, J. Demeester, S.C. De Smedt, On the synthesis and characterization of biodegradable dextran nanogels with tunable degradation properties, Macromolecules, 38 (2005) 8503-8511.

[18] J.N. Patton, A.F. Palmer, Photopolymerization of bovine hemoglobin entrapped nanoscale hydrogel particles within liposomal reactors for use as an artificial blood substitute, Biomacromolecules, 6 (2005) 414-424.

[19] J.N. Patton, A.F. Palmer, Engineering temperature-sensitive hydrogel nanoparticles entrapping hemoglobin as a novel type of oxygen carrier, Biomacromolecules, 6 (2005) 2204-2212.

[20] J.N. Patton, A.F. Palmer, Physical properties of hemoglobin-poly(acrylamide) hydrogel-based oxygen carriers: effect of reaction pH, Langmuir, 22 (2006) 2212-2221.

[21] E. Racker, Reconstitution of membrane processes, Methods Enzymol., 55 (1979) 699-711.

[22] G.D. Eytan, Use of liposomes for reconstitution of biological functions, Biochim. Biophys. Acta, 694 (1982) 185-202.

[23] W. Jiskoot, T. Teerlink, E.C. Beuvery, D.J. Crommelin, Preparation of liposomes via detergent removal from mixed micelles by dilution. The effect of bilayer composition and process parameters on liposome characteristics, Pharm. Weekbl. Sci., 8 (1986) 259-265.
[24] M. Ollivon, S. Lesieur, C. Grabielle-Madelmont, M. Paternostre, Vesicle reconstitution from lipid-detergent mixed micelles, Biochim. Biophys. Acta, 1508 (2000) 34-50.
[25] P.J. Sizer, A. Miller, A. Watts, Functional reconstitution of the integral membrane proteins of influenza virus into phospholipid liposomes, Biochemistry, 26 (1987) 5106-5113.
[26] P.W. Holloway, A simple procedure for removal of Triton X-100 from protein samples, Anal. Biochem., 53 (1973) 304-308.
[27] O. Nussbaum, M. Lapidot, A. Loyter, Reconstitution of functional influenza virus envelopes and fusion with membranes and liposomes lacking virus receptors, J. Virol., 61 (1987) 2245-2252.
[28] D. Levy, A. Bluzat, M. Seigneuret, J.L. Rigaud, A systematic study of liposome and proteoliposome reconstitution involving Bio-Bead-mediated Triton X-100 removal, Biochim. Biophys. Acta, 1025 (1990) 179-190.
[29] J.-L. Rigaud, D. Levy, G. Mosser, O. Lambert, Detergent removal by non-polar polystyrene beads. Applications to membrane protein reconstitution and two-dimensional crystallization, Eur. Biophys. J., 27 (1998) 305-319.
[30] D. Papahadjopoulos, M. Cowden, H. Kimelberg, Role of cholesterol in membranes. Effects on phospholipid-protein interactions, membrane permeability and enzymatic activity, Biochim. Biophys. Acta, 330 (1973) 8-26.
[31] T.K. Meyvis, B.G. Stubbe, M.J. Van Steenbergen, W.E. Hennink, S.C. De Smedt, J. Demeester, A comparison between the use of dynamic mechanical analysis and oscillatory shear rheometry for the characterisation of hydrogels, Int. J. Pharm., 244 (2002) 163-168.
[32] G. Rouser, S. Fkeischer, A. Yamamoto, Two dimensional then layer chromatographic separation of polar lipids and determination of phospholipids by phosphorus analysis of spots, Lipids, 5 (1970) 494-496.
[33] S.A. Smith, J.H. Morrissey, Rapid and efficient incorporation of tissue factor into liposomes, J. Thromb. Haemost., 2 (2004) 1155-1162.
[34] M. Ueno, C. Tanford, J.A. Reynolds, Phospholipid vesicle formation using nonionic detergents with low monomer solubility. Kinetic factors determine vesicle size and permeability, Biochemistry, 23 (1984) 3070-3076.
[35] D.D. Lasic, The mechanism of vesicle formation, Biochem. J., 256 (1988) 1-11.
[36] S. Almog, T. Kushnir, S. Nir, D. Lichtenberg, Kinetic and structural aspects of reconstitution of phosphatidylcholine vesicles by dilution of phosphatidylcholine-sodium cholate mixed micelles, Biochemistry, 25 (1986) 2597-2605.
[37] Merck Index, Thirteenth ed., Merck & Co., Inc., Whitehouse Station, New Jersey, USA, 2001.
[38] B.A. Lewis, D.M. Engelman, Lipid bilayer thickness varies linearly with acyl chain length in fluid phosphatidylcholine vesicles, J. Mol. Biol., 166 (1983) 211-217.
[39] Y. Tahara, Y. Fujiyoshi, A new method to measure bilayer thickness: cryo-electron microscopy of frozen hydrated liposomes and image simulation, Micron, 25 (1994) 141-149.
[40] M. Frohlich, V. Brecht, R. Peschka-Suss, Parameters influencing the determination of liposome lamellarity by 31P-NMR, Chem. Phys. Lipids, 109 (2001) 103-112.

Appendix to chapter 3

Introduction

The method for the synthesis of nanoparticles described in this chapter is intended to be used for the preparation of protein imprinted nanoparticles (PINAPLES, see general introduction). For the formation of imprints it is essential that the template is available for interaction with the monomers. In the case of a membrane protein reconstituted in a liposomal bilayer, the protein region of interest needs to be positioned in the inner compartment of the liposome. Therefore, using the detergent removal method to prepare liposomal reactors described in chapter 3, we tested whether the hydrophilic part of an incorporated protein is evenly distributed over the inside and outside of the liposomal membrane. SN/GpA, a membrane protein construct containing the transmembrane region of glycophorin A fused to the C-terminus of staphylococcal nuclease, was used as a model protein [1]. The reasons this protein was chosen were that it can easily been produced and isolated in large quantities and the SN-moiety of the provides a 17 kD hydrophilic protein segment available for imprinting.

Expression, extraction and purification of SN/GpA

SN/GpA was expressed and purified as described elsewhere [1]. In short, pT7SN/GpA (kindly provided by I. Mingarro, university of Valencia) was transformed into E.coli BL-21(DE3) (Invitrogen). Bacteria were grown in terrific broth to an A_{600} of 2.5. Protein expression was induced by addition of isopropyl-β-D-thiogalactopyranoside (IPTG) (Fisher Emergo) to a final concentration of 0.8 mM. After lysation, the protein was purified using Ni-NTA superflow (Qiagen). SN/GpA was eluted with 100 mM imidazole containing 2% (w/v) 3-[(3-cholamidopropyl) dimethylammonio]-1-propanesulfonate (CHAPS) in HBS. Protein identity and purity were assessed by gel electrophoresis, and protein concentration was determined using A_{280}. Samples were stored in 50% glycerol at -20 °C until further use.

Preparation of SN/GpA proteoliposomes

SN/GpA was incorporated in unilamellar liposomes prepared from mixed micelles by removal of Triton X-100 (TX100) by Bio-Beads [2]. Appropriate amounts of dioleoylphosphatidylcholine (DOPC) (Lipoid GmbH), egg phosphatidylglycerol (EPG) (Lipoid GmbH) and cholesterol (Sigma), in a molar ratio of 4:1:1, were dissolved in chloroform in a round-bottom flask. A lipid film was obtained under reduced pressure using a rotary evaporator and dried further under a

stream of nitrogen. An aqueous solution (20% w/v) of TX100 (BDH Laboratory Supplies) was added at a molar ratio of 3:1 (TX100 to total phospholipid (PL)), which is needed to form micelles [3]. SN/GpA was added to a ratio of 14 µg/µmol lipid. Next, 10 mM HEPES pH 7.4 was added to yield a final total lipid concentration of 2.5 mM. Bio-Beads SM-2 (Bio-Rad) were extensively washed with methanol, and subsequently incubated in 10 mM HEPES [4]. Washed Bio-Beads (60 mg/mL, moist weight) were added to the micelle dispersions, which were subsequently left for 3 hours at room temperature (RT) under gentle shaking. Additional (120 mg/mL) Bio-Beads were added and samples were left for an additional 3 hours at RT under gentle shaking. Bio-Beads were allowed to settle, and the supernatant was collected. Samples were centrifuged at 18.000 g for 5 minutes to remove Bio-Bead remainders and possible lipid/protein aggregates. Samples were filtrated 3x using Vivaspin centrifugal filters with a molecular weight cut off of 300 kD to remove SN/GpA not incorporated in the liposomal bilayer. The size and size distribution of the particles were measured by dynamic light scattering (DLS) using a Malvern CGS-3 multiangle goniometer (Malvern Ltd.).

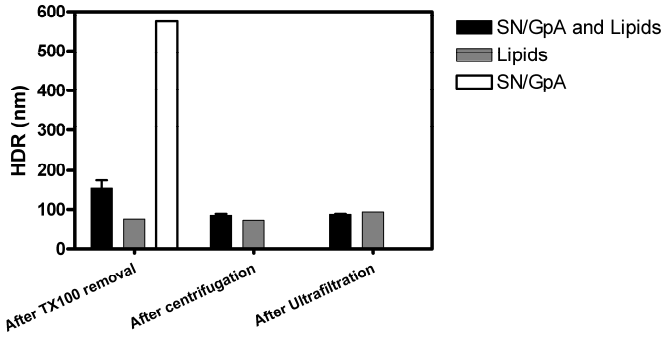

Figure 1. Hydrodynamic radius of SN/GpA proteoliposomes, control liposomes and SN/GpA control at the different stages of preparation.

Figure 1 shows the hydrodynamic radius of proteoliposomes at the different stages of preparation. It appears that the detergent removal method led to the formation of proteoliposomes with a radius of approximately 90 nm in the presence of SN/GpA, comparable to the size of particles formed when no SN/GpA was present. When SN/GpA was subjected to the same protocol in the absence of lipids, protein aggregates were formed after removal of TX100, which can be explained by the presence of the hydrophobic transmembrane domain of the protein. No particles were detected in these samples after centrifugation, which indicates that the aggregates were successfully removed. SDS-PAGE analysis showed that SN/GpA was

present in all stages of proteoliposome preparation, but was not detectable in the samples without lipid (Figure 2). These data show that SN/GpA was successfully incorporated into proteoliposomes.

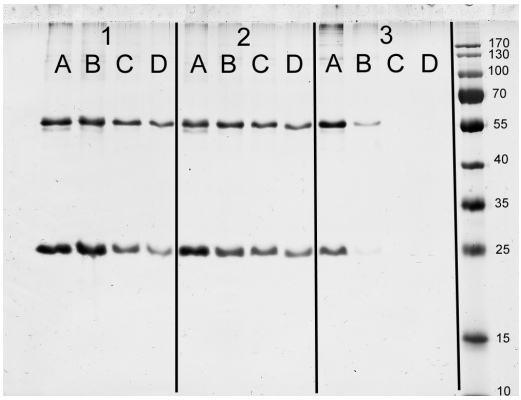

Figure 2. SDS-PAGE analysis (10% polyacrylamide) with silver staining of SN/GpA proteoliposomes at the different stages of preparation (A = mixed micelles, B = after TX100 removal, C = after centrifugation, and D = after ultrafiltration). Shown are proteoliposome duplicates (1 and 2), control SN/GpA without lipids (3), and the protein ladder (Pageruler, Fermentas) with molecular weight indication (kD). Bands represent SN/GpA monomer (22 kD) and dimer.

2.1.3 Determination of SN/GpA orientation in the liposomal membrane.

The SN/GpA oriented outward from the liposomal bilayer was biotinylated using the membrane impermeable biotin-sulfo-NHS (Fisher Emergo), according to the manufacturer's protocol. Proteoliposomes treated with TX100 were used as positive control. To determine the ratio of biotinylated to total SN/GpA, two SDS-PAGE gels (10%) were run under denaturing conditions. The total protein amount was determined by silver staining of the gel, while the level of biotinylation was determined by western blotting using streptavidin-HRP to detect the biotin label. A calibration series with a fixed amount of SN/GpA but increasing levels of biotinylation was prepared. Therefore, increasing amounts of liposomal SN/GpA treated with TX100 were biotinylated. Addition of TX100 leads to the formation of mixed micelles, in which the hydrophilic part of SN/GpA is directed towards the outer aqueous phase, and thus available for biotinylation. After inactivation of the biotin-sulfo-NHS with an excess of glycine, additional liposomal SN/GpA was added to an equal total amount of SN/GpA in all samples of the calibration series.

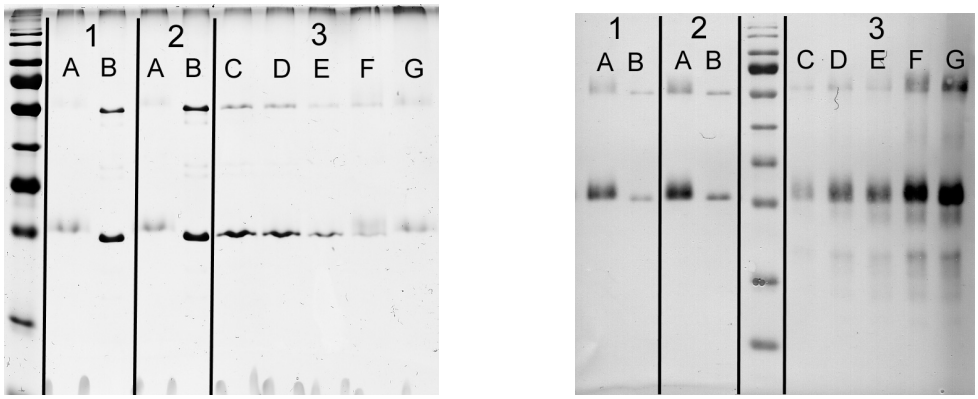

Figure 3. SDS-PAGE (10% polyacrylamide) with silver staining (fig 3A) and western blot (fig 3B) of intact biotinylated proteoliposomes (lanes B), positive control proteoliposomes treated with TX100 (lanes A), and calibration series with 20, 40, 60, 80, and 100% biotinylation (C, D, E, F, and G, respectively). Section 1 and 2 represent duplicates.

Silver staining of the SDS-PAGE analysis was used to confirm equal loading in all samples. From the decreasing intensity of the bands in the calibration series with increasing biotinylation in Figure 3A, it becomes clear that the biotin labeling interfered with the silver staining. Nevertheless, the clear bands in lanes B confirm the presence of SN/GpA in the proteoliposomes. This rules out that a decrease in intensity in Figure 3B is caused by lower SN/GpA loading. The band intensities of the calibration samples in Figure 3B confirm that increasing biotinylation levels were detectable. The relative intensity of the bands of intact proteoliposomes (lanes B) compared to the intensity of destructed proteoliposomes (lanes A, where all SN/GpA was available for biotinylation) show that SN/GpA in proteoliposomes was only partially available to the biotin labeling agent. Although it is not possible to accurately quantify this percentage, it can be concluded that a significant part of the SN/GpA in proteoliposomes is directed towards the inner compartment of the liposomes, and therefore would be available for the formation of imprints.

Nanoparticles were prepared in the inner compartment of the proteoliposomes as described in chapter 3. The affinity of these particles towards the template SN/GpA was determined by surface plasmon resonance (as described for LII-imprinted particles in chapter 4). Unfortunately, the imprinted particles did not show increased affinity as compared to non-imprinted particles. Various compositions of acrylamide, *N,N*-methylene bisacrylamide and acrylic acid were tested, but an imprint effect was not obtained.

References

[1] M.A. Lemmon, J.M. Flanagan, J.F. Hunt, B.D. Adair, B.J. Bormann, C.E. Dempsey, D.M. Engelman, Glycophorin A dimerization is driven by specific interactions between transmembrane alpha-helices, J. Biol. Chem., 267 (1992) 7683-7689.

[2] J.P. Schillemans, F.M. Flesch, W.E. Hennink, C.F. Nostrum van, Synthesis of bilayer-coated nanogels by selective crosslinking of monomers inside liposomes, Macromolecules, 39 (2006) 5885-5890.

[3] D. Levy, A. Bluzat, M. Seigneuret, J.L. Rigaud, A systematic study of liposome and proteoliposome reconstitution involving Bio-Bead-mediated Triton X-100 removal, Biochim. Biophys. Acta, 1025 (1990) 179-190.

[4] P.W. Holloway, A simple procedure for removal of Triton X-100 from protein samples, Anal. Biochem., 53 (1973) 304-308.

Chapter 4

Molecular imprinting of proteins: Fit for the future?

Joris P. Schillemans*

Ellen Verheyen*

Martin van Wijk

Marie-Astrid Demeniex

Wim E. Hennink

Cornelus F. van Nostrum

Manuscript in preparation

* equal contribution

Abstract

Molecular imprinting is a promising technique used to create artificial receptors by the formation of a polymer network around a template molecule. This technique has proven to be particularly effective for molecules with low molecular weight (< 1500 dalton), and during the past five years the number of research articles on the imprinting of larger (bio)templates is increasing considerably. However, expanding the methodology towards imprinted materials for selective recognition of proteins, DNA, viruses and bacteria appears to be extremely challenging. This paper presents a critical analysis of data presented by several authors and our own experiments, showing that the molecular imprinting of proteins still faces some fundamental challenges. The main topics of concern are proper monomer selection, washing method/template removal, quantification of the rebinding and reproducibility. Use of charged monomers can lead to strong electrostatic interactions between monomers and template but also to undesired high aspecific binding. Up till now, it has not been convincingly shown that electrostatic interactions lead to better imprinting results. The combination of a detergent (SDS) and AcOH, commonly used for template removal, can lead to experimental artifacts, and should ideally be avoided. In many cases template rebinding is unreliably quantified, results are not evaluated critically and lack statistical analysis. Therefore, it can be argued that presently, in numerous publications the scientific evidence of molecular imprinting of proteins is not convincing.

Introduction

Molecular imprinting is a technique used to create artificial receptors by the formation of a polymer network around a template molecule (Figure 1). In the pre-polymer mixture, several possible interactions, such as hydrophobic interactions, hydrogen bonds, Van der Waals forces and electrostatic interactions determine the spatial arrangement of monomers around the template. This spatial arrangement is then fixed by polymerization of monomers and crosslinker. Removal of the template leaves a chemically and sterically complementary void (imprint) in the polymer network, which is able to rebind the template.

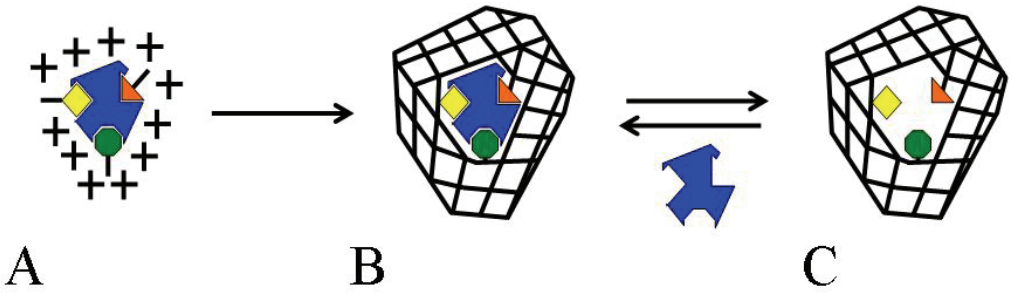

Figure 1. Schematic representation of the principle of molecular imprinting. (A) The template (shown in blue), (functional) monomers (shown in yellow, green and orange) and crosslinker (+) form a pre-polymerization complex. (B) Polymerization of monomers and crosslinker fixes the complex. (C) Removal of the template leaves rebinding cavities. Reprinted with permission from [1].

Although the first paper describing the formation of imprints was published in 1931 [2], research on molecular imprinting was scarce until the 1980's. In an excellent and extensive review, Whitcombe *et al.* illustrated the maturation of the field by the dramatic increase in publications seen over the past 20 years (Figure 2A) [3]. From this and many other reviews that describe the progress made over the years, it becomes clear that molecular imprinting is a very promising and rapidly evolving technology , with many possible applications such as analytical separations, enzyme-like catalysis, chemical sensors and drug delivery [3-7].

Molecular imprinting has proven to be particularly successful for low molecular weight compounds [8-11]. Although imprinting of larger, more complex molecules such as proteins, DNA, and even whole cells and viruses has also been reported [12-15], the number of research papers using such templates is relatively small (Figure 2B).

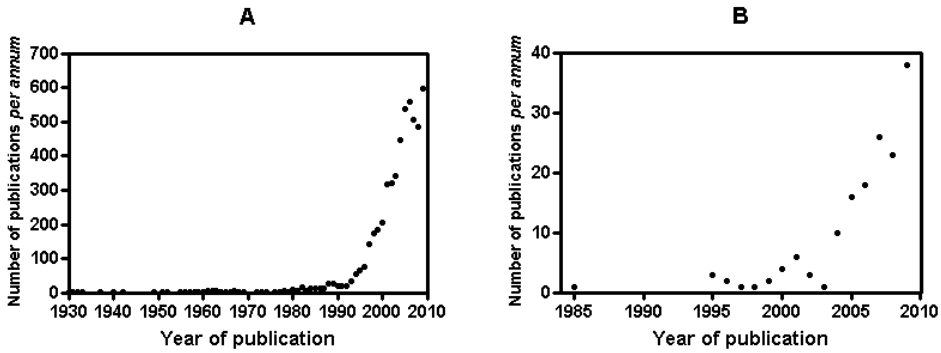

Figure 2. (A) The number of publications within the field of molecular imprinting science and technology per annum for the period 1931 – 2009 (adapted from [3] supplemented by data from [16]). (B) Number of research papers on biomacromolecular imprinting per annum for the period 1985 – 2009.

Till 2003, less than 10 research papers on imprinting of biomacromolecules were published per year, which reflects the difficulties faced when trying to imprint large and sensitive biomolecules [17, 18]. Firstly, for low molecular weight compounds, highly crosslinked gels are used to ensure preservation of the imprint cavity after removal of the template. However, for large template molecules, high crosslink densities seriously hinder mass transfer of the template, leading to slow template removal and rebinding kinetics or, in the worst case, permanent entrapment of the template in the polymer network due to physical immobilization. Additionally, crosslinking of the template to the network can also lead to chemical immobilization [19]. Secondly, due to the solubility properties and sensitive structural nature of biomacromolecules, imprinting can generally only be performed in aqueous environment, which limits the choice of monomers. Moreover, hydrogen bonding interactions strongly contribute to the affinity of molecularly imprinted polymers (MIPs) for low molecular weight compounds in organic, aprotic solvents, but are seriously hampered in water. Thirdly, biomacromolecules are highly complex. Physicochemical properties such as charge or hydrophobicity can strongly vary in different regions of e.g. the protein template, whereas similar regions may be present in other templates. This could lead to high aspecific binding and cross-reactivity of the imprinted polymer.

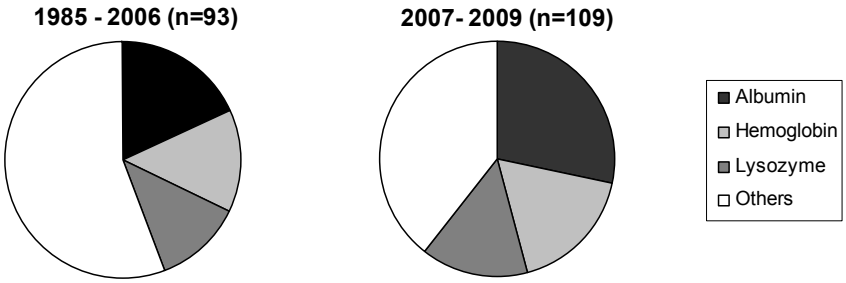

Figure 3. Relative frequency of the templates used in molecular imprinting of protein over the periods 1985 – 2006 and 2007 – 2009.

Despite the challenges, after an initial lag in biomacromolecule imprinting relative to the rest of the field (Figure 2), the number of papers has now begun to increase. Interestingly, Figure 3 shows that in recent years (2005-2009) the model proteins albumin, hemoglobin, and lysozyme are being used more frequently (54%) than in the period up to 2006 (44%). This is opposed to what can be expected from an emerging research field and illustrates that molecular imprinting of proteins is still in its initial phase of development, where research is mostly focused on proof of concept using well defined, relatively stable and inexpensive model proteins. We believe that especially in this time of increasing research intensity, proof of concept, and setting of standards for future research, it is important to subject the published data to a critical review. Therefore, the aim of this paper is to critically analyze published data and conclusions in relation to our own experimental data. The articles discussed are selected on the basis of an extensive literature study on papers published between 2001 and 2009. We focused on the publications that contained sufficient data to allow proper analysis and recalculations. We would like to emphasize that the points raised in this chapter are only meant to initiate debate and it is not our intention to discredit anyone.

Materials and methods

Materials

Acrylamide (AAm, ultra pure) and *N,N'*-methylene-bis-acrylamide (MBA, ultra pure) were purchased from MP Biomedicals, methacrylic acid (MA, 99%), *N,N'*-bis(acryloyl) cystamine, fluorescein isothiocyanate (FITC), lysozyme from hen egg white (96381 U/mg), cytochrome C

from bovine heart (purity >95%), hemoglobin from bovine blood (purity >90%), myoglobin from horse heart (purity >90%) and *N*-octyl β-D-glucopyranoside (OG) from Sigma-Aldrich. Acetic acid (AcOH), acrylic acid (AAc, synthesis grade) and *N,N*-dimethylformamide p.a. were obtained from Merck. *N,N,N',N'*-tetramethylethylenediamine (TEMED), ammonium peroxodisulfate (APS) and sodium dodecylsulfate (SDS) were obtained from Fluka. *N,N*-dimethylaminoethyl-methacrylamide (DMAEMA) was obtained from Polysciences Europe GmbH. The Bio-Rad *DC* protein assay was purchased from Bio-Rad Labs. Dioleoylphosphatidylcholine (DOPC) was purchased from Lipoid GmbH, Triton X-100 (TX100) from BDH Laboratory Supplies, and Irgacure 2959 from Ciba Specialty Chemicals. Lipid II, a bacterial membrane-associated peptidoglycan precursor [20], was kindly provided by Dr. E. Breukink (Utrecht University). FITC labeled lysozyme was synthesized as described before [21]. In detail: 300 mg lysozyme was dissolved in 50 ml borate buffer (100 mM, pH 9). While stirring, 0.28 mL FITC solution (10 mg/ml in DMF, FITC:lysine mol ratio 1:20) was added to the lysozyme solution drop-wise and the resulting mixture was stirred for 1h at room temperature. Next, the pH was adjusted to 7.2 by adding boric acid and the protein solution was filtered (0.2 µm). Finally, the solution was extensively dialyzed against water (1 week, at 4 °C) to remove unreacted FITC and the FITC-lysozyme was collected after freeze-drying.

Surfaces coated with a lysozyme imprinted polyacrylamide hydrogel layer

The method was adopted from Matsunaga *et al* [22]. First, the gold surface of surface plasmon resonance (SPR) chips (1 by 1 cm, Biacore,) was modified with vinylgroups by incubation for 30 min with 5 mM bisacryloylcystamine in methanol. Next, chips were washed 5 times with methanol and RO-water. The pre-polymer mixture was prepared by dissolving 72.2 mg AAm, 13.6 mg MBA, 12 µL AAc (10% w/w in 10 mM HEPES, pH adjusted to pH 7.4, molar ratio AAm:MBA:AAc = 11:1:0.2) and 50 mg lysozyme in a total volume of 1 mL 10 mM HEPES (pH 7.4). Neutral pre-polymer mixtures were prepared without adding AAc. After flushing with nitrogen for 5 min, 10 µL APS (10 % w/w) was added. The components were mixed and 50 µL of the mixture was pipetted onto the gold surface, and allowed to polymerize for 3 h at 37 °C. The surfaces were washed with 3 times 5 mL 1 M NaCl and 3 times 5 mL RO-water to remove the template. Non-imprinted polymers were prepared in the same way, without adding lysozyme. Rebinding was studied by adding 40 µL of a 30 mg/mL FITC-lysozyme solution in 10 mM HEPES pH 7.4 to the surfaces. After 1.5 h incubation at room temperature, the surfaces were rinsed 3 times with 10 mM HEPES (pH 7.4) to remove unbound protein. Bound FITC-

lysozyme was visualized using a Nikon TE-2000 inverted fluorescence microscope (Nikon Europe).

Preparation and analysis of cytochrome C imprinted hydrogels

The synthesis was done according to Kimhi and Bianco-Peled [23]. In detail, 0.86 g AAm, 0.2 g MBA, 1.025 mL MA and 2.05 mL DMAEMA (molar ratio AAm:MBA:MA:DMAEMA =10:1:10:10) and 0.2 g Cytochrome C were dissolved in 10 mM HEPES buffer (final volume 10 mL, pH was adjusted to 7.4). The pre-polymer mixture was flushed with nitrogen for 10 min to remove oxygen. Next, 0.70 mL APS (1.5% w/w in RO-water) and 0.56 mL TEMED (3.75% in 10 mM HEPES buffer, pH adjusted to 7.4) were added to initiate polymerization. The gels were allowed to polymerize overnight at room temperature and subsequently ground by using an IKA® Ultra-turrax tube drive, and wet-sieved through a 80 µm sieve. The template was removed from the granulated gel particles by successive washing with 100 mL RO-water, 100 mL 1 M NaCl, 100 mL 10% SDS:AcOH and 200 mL RO-water. The protein concentration in the wash fractions was determined with the Bio-Rad *DC* protein assay, using the microplate-assay procedure [24]. Next, the particles were freeze-dried and stored at room temperature. Non-imprinted polymers were prepared in the same way without adding cytochrome C.

The rebinding was done with 50 mg dry particles, which were hydrated with 1 mL TRIS-HCl buffer pH 8, prior to the addition of 4 mL cytochrome C or lysozyme solution (final concentration ranging from 0.5 to 4 mg/mL). After overnight incubation on a roller bench at room temperature, the particles were allowed to sediment (visually completely sedimented within 10 min) and the protein remaining in the supernatant was determined spectrophotometrically after filtration (0.2 µm), using a calibration curve (A_{410} cytochrome C, E^{1}_{1}= 86 [25], A_{280} lysozyme E^{1}_{1}= 2.7 [26]).

Myoglobin recovery after incubation and centrifugation

As a control experiment, the effect of experimental conditions on the protein concentration in solutions not containing any polymer was assessed. Eppendorf tubes containing 200 µL myoglobin solutions (0.05, 0.15, 0.25, 0.35 and 0.45 mg/mL) in 10 mM HEPES pH 7.4 were incubated on roller bench for 6 h at room temperature. Samples were centrifuged at 22.000 g for 15 min and the concentration of myoglobin in the supernatant was determined by measuring the absorbance at 410 nm, using a calibration curve (E^{1}_{1} = 157 [27]).

Preparation and analysis of hemoglobin imprinted hydrogels

Neutral protein imprinted polyacrylamide hydrogels were synthesized essentially as described previously [28, 29]. In detail, 270 mg AAm, 30 mg MBA (molar ratio 19:1) and 40 mg bovine hemoglobin were dissolved in 5 mL RO-water. The pre-polymer mixture was flushed with nitrogen for 10 min to remove oxygen. Next, 50 µL APS (20% w/w in RO-water, pH adjusted to 7.4) and 50 µL TEMED (10% v/v in RO-water, pH adjusted to 7.4) were added to initiate the polymerization. The gels were allowed to polymerize overnight at room temperature and subsequently ground by using an IKA® Ultra-turrax tube drive and wet-sieved through a 80 µm sieve. The template was removed from the granulated gel particles by successive washing with 100 mL RO-water, 100 mL 10% SDS and 300 mL RO-water. The hemoglobin concentration in the wash fractions was determined spectrophotometrically (A_{410}, hemoglobin calibration curves were made in RO-water and in 10% SDS). The removal of SDS was verified by adding potassium chloride to the wash fractions. Non-imprinted (control) polymers were prepared in the same manner without adding the template protein.

After template extraction, the gel particles were conditioned with phosphate buffer (PB, 10 mM) pH 6.8. The dry weight of the obtained particle suspension was determined by incubation in a vacuum oven for 2 h at 40°C. Subsequently, fixed amounts of the MIP and NIP suspension corresponding to 20 mg of dry polymer (~300 mg wet) were transferred to 2 mL tubes and PB buffer pH 6.8 was added to a total weight of 0.5 g. Subsequently, hemoglobin in PB pH 6.8 was added, the final concentration ranging from 0.125 mg/mL to 1.0 mg/mL, (total volume of 1.65 mL). Since the volume of wet particles was not exactly the same for MIP and NIP, the exact concentration of hemoglobin was determined immediately after addition (C_0). After overnight incubation, samples were centrifuged (15.000 g, 2 min), and filtered (0.2 µm) to remove remaining gel particles. The protein concentration in the filtered supernatant was then determined spectrophotometrically (A_{410}).

Lipid II surface-imprinted nanoparticles

Crosslinked polyacrylamide nanoparticles (10% w/v total monomer, AAm: MBA: AAc 32:8:1 w/w/w, molar ratio 9.6:1:0.27) were synthesized using a liposomal nanoreactor as reported earlier [30], except using extrusion to prepare DOPC liposomes. Lipid II (LII) was incorporated in the liposomal bilayer in a ratio of 1 mol LII per 1333 mol phospholipids. In short, DOPC (2 µmol) and LII (1.5 nmol) were dissolved in chloroform in a round-bottom flask. A lipid film was prepared under reduced pressure using a rotary evaporator and dried further under a stream of

nitrogen. Next, 0.8 mL monomer solution in 10 mM HEPES pH 7.4 was added to yield a final phospholipid concentration of 2.5 mM. Irgacure 2959 (photoinitiator) was added to a concentration of 0.01% (w/v). Subsequently, the formed multilamellar liposomes were extruded using a hand extruder (Avanti Polar Lipids) through polycarbonate filters with a pore size of 0.1 µm. To prevent polymerization of the monomers outside the liposomes, 200 µL ascorbic acid dissolved in HEPES (130 mg/mL, pH adjusted to 7.4) was added to the liposome dispersion immediately before illumination. Photopolymerization was initiated by illumination for 90 seconds under a N_2 atmosphere using a Bluepoint 4 UVC mercury lamp (150W, λ-range 230-600 nm, Honle UV Technology). After polymerization, the lipid bilayer and the LII-template molecules were removed from the particles by addition of Triton X100, followed by 4 ultracentrifugal cycles (250.000 g, 1 h) and removal of the supernatant. Removal of DOPC was confirmed by a phosphate determination according to Rouser after destruction with perchloric acid [31]. The size and size distribution of the obtained particles were measured by dynamic light scattering (DLS) using a Malvern CGS-3 multiangle goniometer (Malvern Ltd.).

Surface plasmon resonance

The rebinding of the imprinted nanoparticles (MIP) to the LII-template was determined by surface plasmon resonance (SPR) using a Biacore3000 (Biacore,). LII-containing DOPC monolayers were immobilized (flowcell 2) on a HPP chip (XanTec bioanalytics GmbH) according to the protocol provided by Biacore (for DMPC monolayers on a HPA chip). In short, LII-containing DOPC liposomes (2 mM phospholipids, molar ratio DOPC:LII = 333:1) in 10 mM HEPES pH 7.4 containing 2 mM CaCl were prepared by extrusion. After cleaning the HPP-chip surface by an injection (25 µL, flow 5 µL/min) of octyl-β-D-glucopyranoside (40 mM in H_2O), monolayers were formed by an injection (30 µL, flow 2 µL/min) of liposomes, followed by a pulse (30 µL, flow 50 µL/min) of 10 mM NaOH to remove loosely bound vesicles. DOPC monolayers without LII where used a reference surface (flowcell 1).

After the immobilization, sensorgrams were recorded in running buffer (10 mM HEPES, pH 7.4, filtered and degassed) until a stable baseline was reached. Different concentrations of MIP and control nanoparticles were injected at 10 µL/min during 6 min. Dissociation in running buffer was followed for 5 min, followed by regeneration of the surface with 10 mM NaOH.

Results and discussion

Polymer composition: The first critical parameter

After selecting a protein as target template for molecular imprinting, the next step is the selection of an appropriate polymer matrix, in which high affinity binding sites can be created, ideally without introducing aspecific interactions. Proteins are very complex and possess many potential recognition sites at their surface, such as charged amino acids and hydrophobic/hydrophilic regions. This makes the creation of molecular imprinted polymers with high selectivity challenging, due to possible cross-reactivity with proteins with similar charge or hydrophobic/hydrophilic structure as the imprinted template protein. It has been proposed, in contrast to small molecules in aprotic organic solvents, where a few strong bonds are responsible for the selective interaction between template and polymer, multiple weak interactions are necessary for the generation of a strong-protein binding polymer network in aqueous environment [32, 33]. Hjertén and co-workers, introduced acrylamide (AAm) and *N,N'*-methylene-bisacrylamide (MBA) for the design of imprinted hydrogels of several proteins, e.g. cytochrome C [34], hemoglobine [34], ribonuclease [32], human growth hormone [32] and human serum albumin [35]. They typically used hydrogels with a relatively low crosslink density, i.e. 3% (w/w) relative to the total monomer amount. The polyacrylamide matrix is non-charged and multiple weak interactions, like hydrogen bonds and dipole-dipole interactions are assumed to be responsible for the polymer-template interactions [36]. Additionally, the polymerization of monomers in the vicinity of a template protein leads to the formation of a cavity with the shape and size of the imprinted template, and with the sites of interaction in a pre-determined orientation [32, 35].

Theoretically, electrostatic interactions due to introduction of charged monomers in the polymer network can contribute to more specific and stronger template-imprint interactions. However, charged residues can also cause non-specific binding of the template, resulting in a decreased imprint effect. Hjertén en coworkers indeed observed that introducing acrylic acid (AAc) as negatively charged monomer at neutral pH in the polymer matrix, led to a decreased selectivity towards hemoglobin and they concluded that the use of functional (charged) monomers should be avoided. High aspecific interactions, due to the presence of charged monomers was also observed by our group. We prepared lysozyme imprinted and non-imprinted polyacrylamide gels without and with 1.5 mol% AAc (AAc:lysozyme molar ratio = 5:1), with a crosslink density of 15.5% (w/w), as described in the Materials and Methods section. The

rebinding of FITC-labeled lysozyme was evaluated with fluorescence microscopy. In order to make comparison possible between the different samples, the microscope settings (exposure time and gain) were kept constant for all the formulations. As can be seen in Figure 4, the (bright green) fluorescence intensity (FITC-lysozyme) of the AAc-containing MIP is substantially higher than that of the neutral MIP, where almost no fluorescence is observed(black to slightly green). However, this is also the case for the non-imprinted polymer (NIP), which indicates that this effect is mostly the result of aspecific binding. Although both charged and neutral MIPs seemed to bind more FITC-lysozyme than the non-imprinted counterparts, experiments with bulk imprinted hydrogels of the same composition where the rebinding was assessed by the depletion of protein from the supernatant did not confirm an imprint effect. Also in this experiment the negatively charged bulk imprinted hydrogels showed quantitative rebinding of lysozyme for both the MIP and NIP. These results clearly illustrate the non specific binding caused by electrostatic interaction between positively charged lysozyme and the negatively charged networks.

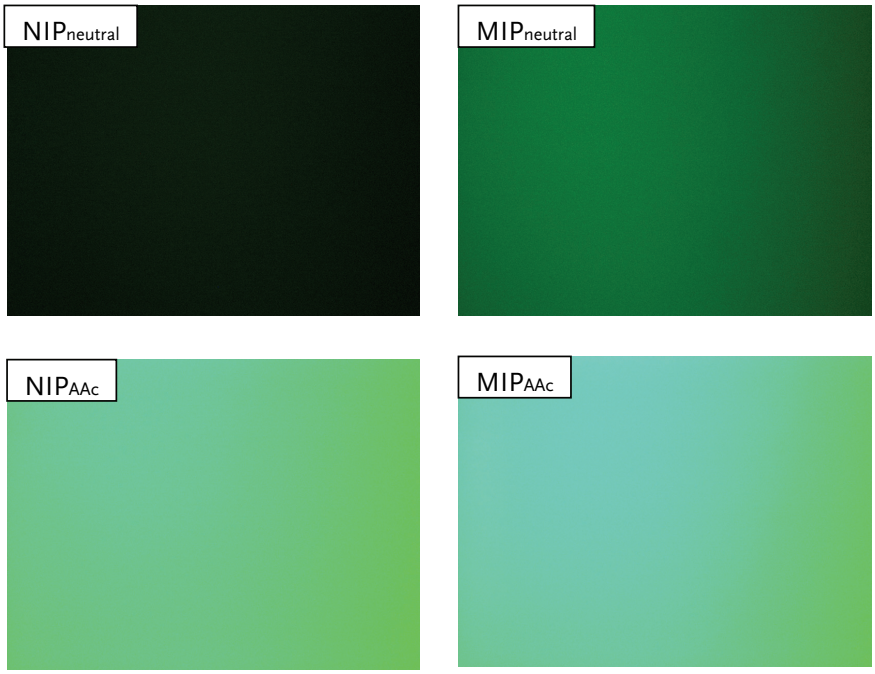

Figure 4. Fluorescent images of neutral (top) and negatively charged (bottom) MIP and NIP after rebinding with FITC-lysozyme (green) (50% of the initially imprinted amount) in 10 mM HEPES, pH 7.4. These figures clearly illustrate the non-specific binding of lysozyme to acrylic acid (AAc)-containing polyacrylamide hydrogels. The exposure time and gain were kept constant for all the samples.

3-Aminophenylboronic acid (APBA) has been frequently used as functional monomer for the preparation of protein imprinted polymers, with varying results [37-40]. APBA possesses several functional groups (hydroxyl, secondary amine and an aromatic ring), which can interact with different amino acids present in proteins [41, 42]. As observed by Bonini *et al.*, these multiple interaction points can sometimes result in high non-specific binding [38]. They used aminopropyl silica beads coated with APBA as functional monomer for imprinting of human serum albumin (HSA). The protein was first covalently bound to an aldehyde-modified aminopropyl silica surface (2 mg HSA/g beads). Thereafter, a thin film of pAPBA was deposited on the particle surface (15.2 mg/g beads, thickness of the layer not specified). The template was removed by washing the beads with RO-water and 1 M oxalic acid. The strong acidic solution breaks the covalent bond between the protein and the modified silica surface. From the release profile presented by the authors, it is clear that only ~50 µg was removed from the beads, whereas initially 2 mg HSA was added to derivatize the beads. This suggests that there is still a considerable amount of template present on the beads (97.5%, assuming quantitative immobilization of HSA on the beads), which could be due either to strong interaction between the aminopropyl silica and HSA [43], or to permanent entrapment of HSA between the silica surface and the deposited pABPA layer. Beads were conditioned with phosphate buffer (PB, 10 mM, pH 8) before rebinding. .We would like to point out that the pABPA is a linear polymer deposited on the silica surface. In our view, the absence of permanent (covalent) crosslinks makes the creation of stable imprint cavities very unlikely. Rebinding studies were performed with different protein amounts (0.02 up to 2.4 mg/g beads). Only at high rebinding protein concentrations (> 1.56 mg HSA/g beads), a significant difference in binding behavior was observed between the imprinted and non-imprinted beads (imprint factor = 1.4, Figure 5). At lower concentrations, both MIP and NIP adsorbed the loaded HSA quantitatively. This observation is contrary to what is expected for specific protein (re)binding, where one would expect a difference in adsorption at low protein concentrations until all specific binding sites on the MIP are occupied, whereas at higher concentrations aspecific protein binding to the surface of both MIP and NIP would occur. Additionally, the difference in binding between MIP and NIP (~500 µg/g) beads was 10 times higher than the removed amount of template (50 µg/g beads). Therefore it is likely that the difference in binding between the MIP and NIP observed at high concentrations is caused by a difference in exposed surface area per g particles, which could originate from the presence of the protein during the polymerization.

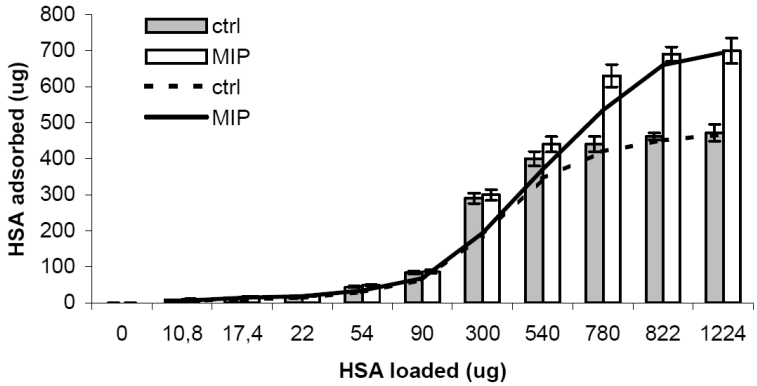

Figure 5. Binding capacity for control (solid) and MIP beads (open). The amount in micrograms bound to the beads is plotted as function of amount in micrograms added to 0.5 g particles for rebinding. Rebinding is done with different amounts of proteins in phosphate buffer (10 mM pH 8). *Reprinted with permission from* [38].

Even though it is clear that functional (charged) monomers can induce aspecific binding of the template to the polymers, it has been shown that the charge density of the network [44], as well as the pH [45] and ionic strength of the buffers used for imprinting and rebinding [22, 37] have an effect on the experimentally determined imprint specificity. Matsunaga *et al.* presented a detailed study on the effect of salt concentration on both the imprinting process and rebinding to negatively charged polyacrylamide hydrogels [22]. They synthesized lysozyme imprinted and non-imprinted polymers on SPR-chips with AAc as negatively charged monomer. The effect of ionic strength (0, 20 and 40 mM NaCl) of the buffer (HEPES, pH 7.4) during the polymerization and the rebinding assay was evaluated with SPR. AAc was added to provide negatively charged binding sites for the positively charged lysozyme. The template was removed by washing with 1 M NaCl (the amount of template removed was not quantified). When rebinding was conducted in absence of NaCl, high non specific binding of lysozyme was observed for both the MIP and NIP, likely caused by the electrostatic interaction between the template and the polymer (control experiments using polymers without AAc were not performed). Rebinding to the lysozyme-MIP and NIP was also done with other proteins (cytochrome C, RNAse, myoglobin, lactalbumin) to examine the selectivity of the imprints. Cytochrome C and RNAse (both positively charged at pH 7.4) bound to a high extent to both MIP and NIP, whereas no adsorption was observed for myoglobin (neutral) and lactalbumin (negatively charged). Interestingly, when the rebinding of lysozyme and the different control proteins was done in the presence of NaCl (20 or 40 mM), the aspecific binding to both MIP

and NIP decreased, but this did not result in an increased imprint factor for lysozyme. In case the preparation of the MIPs was done in absence of salt (50 mM HEPES, pH 7.4), no specific adsorption of lysozyme to the MIP was observed (imprinting factor = 1.0). On the other hand, when imprinting was done in presence of salt, 20 or 40 mM, the imprint factor for lysozyme in 20 mM NaCl increased to 1.2 and 3.4, respectively. However, when rebinding was done with these gels in presence of 40 mM instead of 20 mM NaCl the rebinding efficiency decreased. This can be attributed to the interference of the salt ions with the specific charged binding sites, thereby masking the charges and resulting again in loss of rebinding efficiency.

It is clear that the selection of proper monomers is critical for the performance of the imprinted polymer. One has to take into account that strong interactions, either electrostatic or hydrophobic, between monomers and template can lead to aspecific binding. Moreover, the imprinting and rebinding conditions (pH, salt concentration) have a clear effect on the experimental results, which makes it even more challenging to develop standardized protocols for the design and evaluation of protein imprinted polymers.

The essence of template removal

An important step in the process of creating imprints with high selectivity and absorption capacity is the removal of the imprinted template, especially because the imprint cavities of interest, i.e. those with the highest binding affinity, will most strongly retain the template molecules during template extraction. Moreover, removal of proteins from imprinted polymers is challenging due to their high molecular weights, which retards diffusion through the dense polymer network. In the past decade, several washing methods have been developed and optimized for protein/template extraction. The pioneering work by Hjertén and co-workers has been used as a starting point by other research groups [32, 34, 36]. In order to remove the template from (neutral) polyacrylamide hydrogels, they used several methods, depending on the protein properties (size, *pI*). For example, cytochrome C was removed by washing with a solution of high salt (0.5 M), whereas for hemoglobin, albumin and myoglobin 10% SDS/10% AcOH was needed and even then traces of both proteins were permanently entrapped (the gels remained slightly red colored after washing) [34]. Nowadays, these methods are still frequently used for template removal. For smaller proteins like cytochrome C and lysozyme, washing with RO-water and solutions with high salt concentrations is sufficient to remove 73 up to 92% of the template molecule, depending on the polymer composition [23, 46, 47]. At present, the combination of acetic acid (AcOH) with a detergent (SDS or Tween-20) is the most frequently

used washing procedure, however this harsh method does not guaranty complete template removal either; results varying from 50% up to 95% have been published [28, 37, 38, 48, 49]. In 2005, Hawkins *et al.* evaluated the use of a mixture of SDS/AcOH and trypsin as washing solutions for the removal of hemoglobin from polyacrylamide hydrogels [28]. They polymerized acrylamide and bisacrylamide in presence of hemoglobin (12 mg/g polymer). After polymerization, the hydrogels were granulated by sieving and washed with different solutions, and subsequently the rebinding efficiency was determined by incubating the imprinted and control particles with 6 mg hemoglobin/g. The best imprint effect was obtained with 10% SDS/10% AcOH (45% of the initially imprinted amount rebound), even though only approximately 50% of the template was removed. By increasing the SDS/AcOH concentration to 15%:15%, more template was removed (~70%), but the rebinding decreased to ~35%, which Hawkins *et al.* assigned to changes of the network structure, caused by the high SDS:AcOH concentrations. When trypsin was used, up to 87.4% of template was removed from the imprinted network; however, only 20% of the amount initially used for imprinting was rebound. This was explained by the blocking of imprinted sites with residual protein fragments. Although the results of Hawkins *et al.*[28] look promising, some issues need to be addressed. Firstly, the time used for template removal is not specified, nor do the authors state whether the last wash fraction still contained protein. Therefore it is not certain whether the template that was not removed (up to 50%) did not continue to leak out during rebinding studies. Second, the template rebinding was allowed for only 10 min, which is too short to reach equilibrium (vide infra). Third, a bias is observed in the data presented on the hemoglobin recovery after rebinding. According to the described method, 12 mg hemoglobin was used for the imprinting process, whereas the rebinding to the MIP and NIP was done with 6 mg hemoglobin (because only ~50% of the template was removed). However, based on the presented results, the amount of protein recovered in the different wash fractions after rebinding for the NIP, was 7.25-7.75 mg, which is 20-30% more than the initial amount used for rebinding (Figure 6). On the other hand, in case of the MIP, the total amount of protein recovered during the washing steps after rebinding (4.5-5.9 mg) is less than the amount used for rebinding, suggesting some irreversible rebinding of the protein to the MIP. These uneven mass balances were not addressed by the authors. Therefore, given the inaccuracy of the method used to assess rebinding, the author's conclusion that 10% SDS/10% AcOH would be the best template removal method is probably not justified.

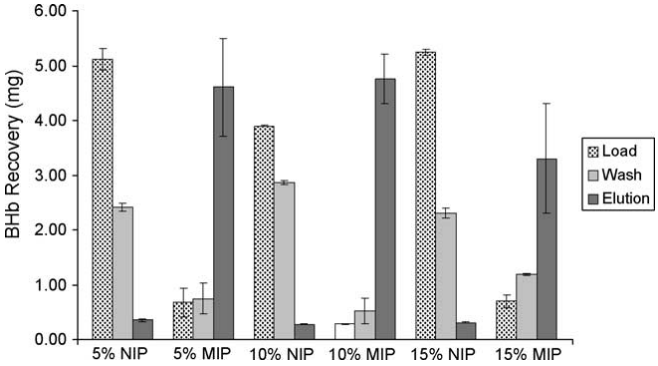

Figure 6. Effect of washing method (SDS/AcOH 5%:5%, 10%:10% and 15%:15%) on the rebinding to MIP and NIP. The figure shows the amount of hemoglobin present in the different wash fractions after rebinding. (load fraction = unbound protein remaining in the supernatant after rebinding, Wash: low affinity bound protein removed by washing with water, Elution: strong affinity bound protein eluted with SDS/AcOH). All values are means of duplicate experiments and the error bars represent the two "actual" results for each data set groups. In case of the NIPs, accumulation of the protein recovered in the different wash fractions, resulted in a higher amount of protein than originally added to the polymers. *Reprinted with permission from [28]*

In a second paper, the same authors evaluated the efficiency of the SDS/AcOH washing method with confocal microscopy [49]. Fluorescently labeled (FITC) albumin was imprinted in a polyacrylamide hydrogel and visualized by confocal microscopy. After addition of 50 µL 10% SDS/10% AcOH to the MIP an immediate and almost complete decrease in fluorescence signal was observed. This observation was ascribed to the structural denaturation of the FITC-labeled protein and subsequent extraction from the hydrogel network. However, fluorescein (and also FITC) is a pH-sensitive fluorescent probe and has been used e.g. as pH sensor to measure the intracellular pH [50, 51]. The fluorescence intensity of fluorescein has a maximum above pH 7 and a minimum below pH 5. Consequently, the observed instant loss of the fluorescence signal is more likely caused by the decrease of the pH after adding SDS/AcOH (pH ~2.8), rather than due to denaturation and removal of FITC-albumin form the gel network. Moreover, immediate release is highly unlikely because of the low diffusion rates of proteins in highly crosslinked hydrogel matrices. Despite the above mentioned concerns, many researchers adopted this method to remove protein templates from MIPs [29, 48, 52-55].

As demonstrated by Fu *et al.*, template removal by SDS and AcOH can be associated with another artifact. They synthesized BSA imprinted chitosan-polyacrylamide gels by graft copolymerization of acrylamide on chitosan in presence of bisacrylamide. The gels were sieved (70-mesh sieve) and the obtained granules were washed with 10% SDS/10% AcOH to remove

the template. When performing a rebinding experiment (acetate buffer pH 4.6 in which BSA has no net charge), they observed that the MIP had a binding capacity exceeding the theoretical capacity at least twice, whereas the template binding to NIP was very low [48]. In a later publication they verified that the mixture of SDS/AcOH, used to remove the imprinted template, was responsible for this extremely high absorption by the MIP [56]: when non-imprinted polymers were washed with the same solution (10% SDS/10% AcOH), a comparable amount of template (hemoglobin) was bound to the NIP as to the MIP (Figure 7). In a control experiment, using crosslinked chitosan beads, high non specific protein adsorption to the beads occurred when they were washed with a combination of SDS and AcOH, whereas after washing with only AcOH or SDS, a much lower protein sorption was observed (Figure 8). It is possible that anionic SDS binds electrostatically to the positively charged chitosan surface, which is more pronounced at the low pH (~2.8) of the SDS/AcOH solution. The SDS molecules may remain adsorbed to the surface after washing and can thereby cause aspecific hydrophobic interactions with BSA and hemoglobin (both neutral at pH 4.6 and pH 6.8, respectively). These results indicate that non-specific sorption induced by the washing step with SDS/AcOH, rather than the creation of imprinted sites, is responsible for the very high binding capacity. As suggested by the authors, it is very important to treat the MIP and NIP in exactly the same way during the whole imprinting process.

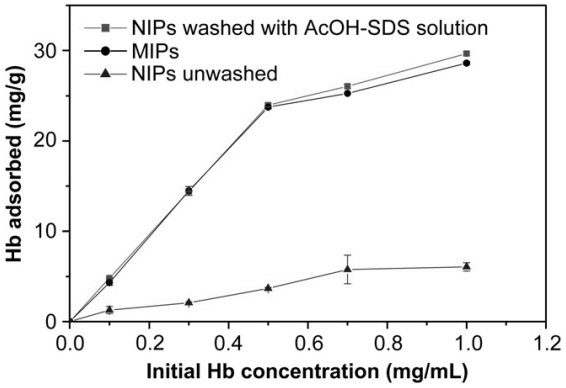

Figure 7. Hemoglobin binding isotherms for imprinted hydrogels based on polyacrylamide-chitosan semi-interpenetrating network, and for the NIP-washed or unwashed with the AcOH/SDS solution. Binding conditions: temperature 25°C, time 8 h, Particles 0.1 g, volume 5 mL, 20 mM phosphate buffer pH 6.8. All values are means of three measurements. *Reprinted with permission from* [56].

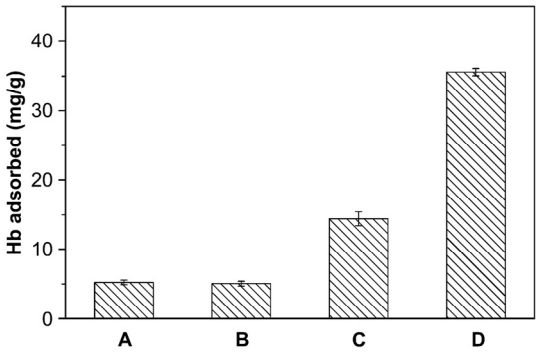

Figure 8. Hemoglobin binding to bare crosslinked chitosan beads treated differently. (A) Original crosslinked chitosan beads; (B) beads washed with 10% (v/v) AcOH; (C) washed with 10% (w/v) SDS solution; and (D) washed with the AcOH/SDS solution. Binding conditions: temperature 25 °C, time 18 h, polymer mass 0.1 g, rebinding volume 5 mL, Initial concentration (C_0) 1.0 mg/mL, and 20 mM phosphate buffer pH 6.8. All values are means of three measurements. *Reprinted with permission from* [56].

Tan and Tong also reported extremely high adsorption capacities for a protein imprinted methylmethacrylate polymer crosslinked with ethylene glycol dimethacrylate, up to 100-fold of the theoretical maximum binding capacity, however, this was not addressed in their discussion [54, 57, 58]. In a comment on one of their papers, the washing step with SDS/AcOH was proposed to be responsible for this exceptionally high rebinding capacity. Moreover it was suggested that the MIP and NIP were treated differently during the washing steps [59]. Tan and Tong replied and assured that both MIP and NIP were treated in a similar way and explained the unrealistic high adsorption capacity by means of the general mechanism of protein adsorption to hydrophobic surfaces [60]. The authors argued that the presence of binding sites in the imprinted polymer would create a stable layer of adsorbed proteins, onto which other proteins can be adsorbed, leading to multiple layers of proteins. In absence of these binding sites, the adsorbed layer is not stable and can be desorbed again. However, the explanation is based on hypothesises is not supported by experimental data. Moreover, multi-layer protein adsorption has only been observed with some protein-surface combinations, and there is still a lot of controversy on this topic [61, 62].

Recently, Janiak *et al.* also discussed the problems they encountered with the use of SDS/AcOH to remove imprinted protein molecules from charged polyacrylamide hydrogels [29, 63]. Like Fu *et al.*[56], they observed that the presence of SDS in the wash solution, in particular in combination with AcOH, led to an increased non-specific binding to the imprinted and non-imprinted polymers.

Also in our work we observed high non-specific rebinding due to insufficient washing after removal of the template with 10% SDS/10% AcOH. Cytochrome C imprinted and non-imprinted neutral polyacrylamide hydrogels (containing equal amounts of negatively (MA) and positively (DMAEMA) charged monomers) were prepared according to Kimhi and Bianco-Peled [23], as described in the Materials and Methods section. The template was removed (85 % ± 5 %) by washing of the granulated gels with 10% SDS/10% AcOH, comparable with results reported by Kimhi *et al.* [23]. After washing, the gels were equilibrated in TRIS buffer pH 8. To assess the selectivity of the imprinted polymers, rebinding was performed with cytochrome C and lysozyme, which are similar with respect to their size and isoelectric point (*pI*; lysozyme = 14.3 kDa, *pI* = 9; cytochrome C = 12.6 kDa, *pI* = 11). The rebinding was done by incubation of 50 mg MIP and NIP (dry weight) with different amounts of both proteins (2.5, 5, 10, 15 and 20 mg) for 14 h. Based on the initial template concentration, the maximum rebinding capacity of the MIP was 50 mg/g. After sedimentation of the particles, the unbound protein in the supernatant was determined spectrophotometrically. Surprisingly, for all initial rebinding concentrations used (0.5 mg/ml - 4 mg/mL), no protein was detected in the supernatant of solutions incubated with both MIP and NIP. The absence of a red color in the supernatant after rebinding with cytochrome C confirmed this finding. However, a closer examination of the MIP and NIP after rebinding revealed that the protein molecules had neither penetrated into nor adsorbed onto the polymers, but were precipitated on top of the polymers, as shown for lysozyme in Figure 9. The MIP was still slightly red colored, indicating the presence of cytochrome C that was permanently entrapped in the hydrogel network after imprinting (Figure 9A). For all lysozyme concentrations used, quantitative precipitation occurred for both MIP and NIP. Determination of the pH revealed that the solution was slightly acidic (pH 5), even though they were washed with H_2O, and TRIS-buffer (pH 8) was used during hydration of the polymer particles and during rebinding. This suggests that AcOH, and likely also SDS, used for template removal were not extracted quatitatively from the gels. Therefore, the stability of lysozyme and cytochrome C was tested in 10% SDS, 10% AcOH and a mixture of 10% SDS/10% AcOH. Only the combination of SDS and AcOH caused precipitation of the proteins, which confirms the hypothesis that traces SDS and AcOH were still present in the gels during the rebinding.

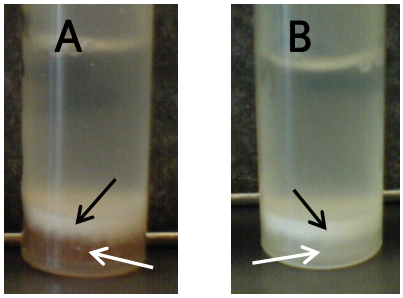

Figure 9. Precipitation of lysozyme after rebinding to cytochrome C imprinted particles (**A**) and non-imprinted particles (**B**). Lysozyme (3 mg/ml in TRIS pH 8) was added to 0.5 gram dry particles and incubated overnight. Black arrows: protein precipitate, white arrows: sedimented particles (slightly red colored in the case of the imprinted particles (A)).

Based on the examples mentioned above, it has become clear that a harsh washing method, like SDS/AcOH, may improve the removal of imprinted template proteins, but care must be taken to avoid non-specific interactions or protein precipitation by e.g. residual SDS molecules present in the polymer network. As shown, such artifacts might lead to false positive results. First of all, imprinted and non-imprinted polymers should be subjected to identical procedures used for the template removal and washing of the polymers. This way, non-specific interaction introduced by the washing procedure can be identified. Second, one should ensure that washing compounds are removed completely prior to the rebinding step. In case of SDS and AcOH, this can be done easily by measuring the pH of the supernatant (AcOH) and by adding potassium chloride to the supernatant which will cause precipitation of KDS. Nevertheless, SDS entrapped inside the gel matrix may still cause artifacts.

Assessment of template rebinding

Incubation time/equilibrium

Affinity is a parameter that describes the binding of substances (e.g. ligand and receptor) in equilibrium. Logically, in order to assess the affinity of a MIP for the template, it has to be made sure that equilibrium has been reached. It is well-known that the diffusivity of proteins in a highly crosslinked polymer matrix is rather slow. Polymer geometry, polymer hydration, crosslink density, protein size and temperature all play a role in the time needed for a protein to diffuse into the polymer matrix and to reach equilibrium. As a result, the required incubation time needs to be validated before affinity can be properly assessed. Surprisingly, in many

articles on protein imprinting the incubation time is not accounted for. For example, Ou *et al.* reported on lysozyme imprinted polyacrylamide beads (solid content up to 40% w/w) of 105 – 149 µm using an incubation time of 30 min [46]. Their formulation and incubation time were adopted by Kimhi and Bianco-Peled [23], but in a later paper by the same group it was stated that it took at least 2 h to reach equilibrium, and the incubation time was adjusted to 5 h [64]. Even more striking are the papers on hemoglobin imprinted polyacrylamide gels (6% w/w total monomers, 10% crosslinker), by Hawkins *et al.* [28] (sieved through a 75 µm sieve) and Janiak *et al.* [29] (granulated, dimensions not specified), where an incubation time of only 10 min was used. Judging from the time-dependent adsorption curves shown by others for similar hydrogel compositions [65-67], it can be stated with certainty that equilibrium was not reached.

Also when time needed to reach equilibrium is determined, the results should be analyzed critically. For example, Lu *et al.* showed that the concentration of BSA and lysozyme upon incubation with their corresponding polyacrylamide MIP beads (25% w/w total monomer, 10% crosslinker) decreased with the same kinetics. This is contradictive to what is expected, considering that the molecular weight of BSA is approximately 6 times higher than that of lysozyme. The difference in size leads to much slower movement of BSA in the crosslinked polyacrylamide matrix and therefore one would expect that more time is needed to reach equilibrium for BSA. The finding that equilibrium was reached within the same time interval raises the question whether the change in concentration was indeed caused by specific binding to imprint cavities in the polymer matrix, or that it was rather caused for example by protein aggregation or aspecific binding to the polymer surface or test tube.

Quantification of rebinding

In the majority of papers the indirect method of template depletion from solution is used to quantify template rebinding. MIP and template are mixed and the concentration of unbound protein in the solution is determined after a certain incubation period (when equilibrium is reached). A major shortcoming of the template depletion method is that it does not confirm that the template is in fact bound to the polymer. The drop in concentration of protein in the supernatant can have other causes, such as the SDS/AcOH combination (vide supra). Also other unexpected effects could lead to serious artifacts, as is illustrated with some of our own data shown in Figure 10.

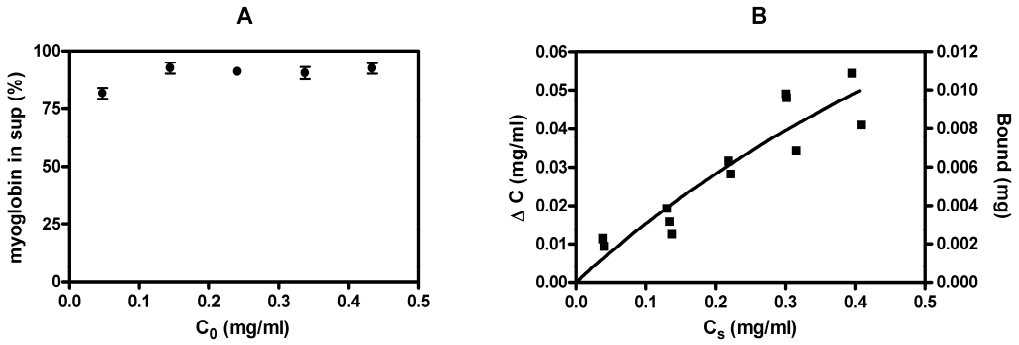

Figure 10. Depletion of myoglobin from solution after 6 h incubation (10 mM Hepes buffer pH 7.4) and subsequent centrifugation. The concentration was determined by A_{410} and expressed as % of the original amount (A, n = 3), and the resulting Langmuir isotherm expressed as both decrease in concentration (left y-axis) and amount bound (right y-axis) vs. equilibrium concentration (B). Individual triplicates are shown because the x-coordinate (equilibrium concentration) is a sample-dependent value. The line in Figure B represents the fit using a one site binding model.

Figure 10 A shows the relative amount of myoglobin measured in 10 mM Hepes buffer, pH 7.4, after incubation in eppendorf tubes without MIP/NIP for 6 h at room temperature followed by centrifugation. It becomes clear that ~90% of the myoglobin remained in the solution, independent of the original concentration. When this picture is converted into a Langmuir curve (Figure 10 B) it seems that significant "binding" occurred. This background binding could result from adsorption of protein to the test tube and loss of protein (aggregates) as a result of centrifugation. Solid surfaces can adsorb up to 1 µg protein/cm² (monolayer of globular protein) [68]. The surface of an eppendorf tube is ~10 cm², which means that it can adsorb approximately 10 µg of protein and could indeed explain the observed decrease of protein (ΔC = 0.05 µg/ml, V = 200 µl). If MIP/NIP would have been present, such phenomena could lead to false positive results. Therefore, when indirect measurements are used to show template rebinding, samples not containing MIP/NIP should be included as an extra control, additional to the normal non-imprinted polymer. It should be noted that in some papers protein rebinding is quantified by determining the bound protein directly, for example by ELISA [69] or using a quartz crystal microbalance (QCM) [70-72]. Also for these methods it is essential that they are validated, to be able to make the distinction between rebinding and for example change of the availability or conformation of epitopes in the case of ELISA, and polymer swelling and deswelling in the case of QCM. To our knowledge, no papers have been published in which the affinity of a MIP for the template protein is assessed using equilibrium dialysis, a method commonly used in pharmacology, immunology and biochemistry to assess the affinity of

ligand/protein complexes [73, 74]. In this method, the distribution of a radiolabeled ligand is determined over two compartments separated by a semipermeable membrane. Only one of the compartments contains the receptor (MIP), while the ligand (template) can freely diffuse over the membrane. Ligand binding to the receptor results in an increased amount of total radioactive ligand in the receptor compartment. This method has several advantages. First, there is no need to separate the unbound template from the MIP by centrifugation or filtration, which could lead to unwanted loss of ligand. Second, artifacts due to protein aggregation or adsorption to the compartment walls do not affect the outcome in such an experimental set-up, since those phenomena occur to the same extent in both compartments. Third, a proper mass balance of the ligand is obtained, which strengthens the power of the experiment. Therefore, adopting this method would be an improvement to the field of protein imprinting.

The most common method for determination of protein concentration in solution after rebinding to MIPs or NIPs is UV-VIS spectrometry, using either absorption of the aromatic amino acids (at 280 nm) [46, 53, 55, 66, 67, 75-79], the absorption maximum of the heme group at ~410 nm in the case of hemoglobin, cytochrome C or myoglobin [29], or a colorimetric protein assay such as Bradford [47, 80]. In most papers, results are converted to represent the amount of protein bound per weight of MIP/NIP Presented this way many results look quite convincing. However, the raw data should always be considered in order to judge whether the proposed imprinting effects are significant. For example, Bolisay *et al.* reported that mosaic virus imprinted polymers rebound 8.82 mg virus/g MIP while NIP bound 4.22 mg/g [13]. The binding was obtained by indirect measurement of virus concentration, using UV-VIS spectrometry after removal of the polymer with a 0.45 µm filter from samples containing a ratio of 1 mg polymer per 1 mg/mL virus. Using these data, it can be calculated that the ΔC measured for MIP and NIP were 0.00882 and 0.00422 mg/mL, respectively. In can be calculated that the concentration in the supernatant was 99.1% and 99.6% of the original, respectively, which is without doubt within the margin of error of the assay. Silvestri *et al.* reported that when α-amylase was passed through a poly(ethylene-co-vinyl alcohol)/dextran MIP/NIP membrane, the imprinted membrane retained 0.41 µmol/g more than the control (MIP 0.60 µmol/g, NIP 0.19 µmol/g) [77]. With a MW of 51 kDa and knowing that the imprinted membrane was prepared using a protein concentration of 2% w/w, (= 0.39 µmol/g), this translates into an imprint efficiency of 105%. However, the difference in non-adsorbed α-amylase was 8% of the original α-amylase concentration (0.15 mg/mL), which is 0.012 mg/mL. Using ε = 95925 $M^{-1}cm^{-1}$ [81,

82], it can be calculated that this results in a difference of A_{280} between MIP and NIP of only 0.022.

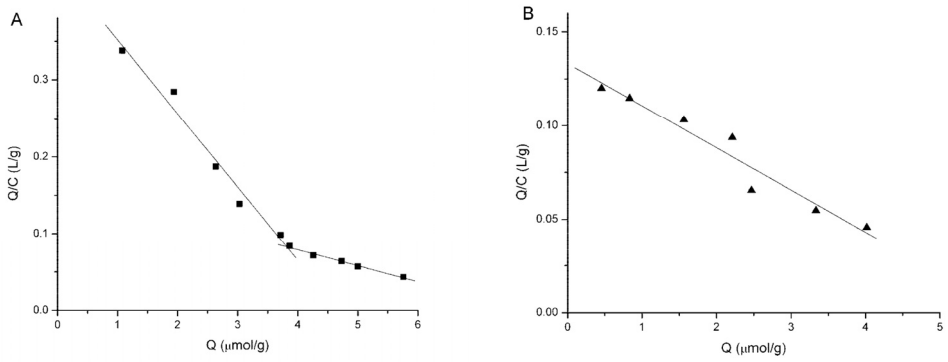

Figure 11. Scatchard plot of the BSA readsorption assay of MIP (A) and NIP (B) presented by Hua *et al.* [75]. 5 mg MIP and NIP composed of *N*-Isopropylacrylamide (3.5 mmol), *N*-[3-(dimethylamino)propyl]-methacrylamide (0.085 mmol), AAm (0.070 mmol) and MBA (0.117 mmol) were incubated in 8 mL BSA solutions in 10 mM TrisHCL pH 7.4 containing 1 mM NaCl for 24 h. *Reprinted with permission.*

Table 1. The original concentrations (C_0) (given in material and methods) and the equilibrium concentrations (C_{eq}) and corresponding A_{280} values recalculated from Figure 11. A_{280} values were calculated using $\varepsilon = 43800\ M^{-1}cm^{-1}$, assuming a path length of 1 cm, and not considering dilution of the samples.

C_0	*C_{eq} (mg/mL)*		*A_{280}*	
(mg/mL)	MIP	NIP	MIP	NIP
2.27				
4.55	3.25	3.76	0.14	0.17
7.58	6.82	7.28	0.30	0.32
15.2	14.3	15.3	0.63	0.67
22.7	21.6	23.6	0.94	1.03
30.3				
37.9	37.4	37.7	1.64	1.65
45.5	45.1		1.98	
60.6	58.0	61.1	2.54	2.68
75.8	75.2		3.29	
	89.2	86.9	3.91	3.81
	134		5.88	

Hua *et al.* showed Scatchard plots of BSA rebinding to MIP and NIP disks (Figures 11 A and B, respectively) [75]. Solutions of various concentrations of BSA were incubated for 24 h with 5 mg polymer and the concentration of BSA was determined using A_{280}. They found that the MIP exhibited two binding sites, one with high and one with low affinity, while the NIP only had one

binding site with low affinity. An interesting point not mentioned by the authors is that the maximum amount of bound protein to the high affinity site (Q_{max}), which can be deducted from the plot by extrapolation of the line to the x-axis, is ~4.5 µmol/g dry polymer. According to their Materials and Methods section, the MIPs were prepared with 229 mg BSA/g monomer, which leads to a theoretical maximum of 3.5 µmol/g dry polymer. Taking into account that template removal was 93.4% reduces Q_{max} to 3.2 µmol/g The equilibrium concentration C (µmol/L) can be calculated from the points in Figure 11 by C = x/y (Q/(Q/C). The approximate A_{280} can then be calculated using $\varepsilon = 43800\ M^{-1}cm^{-1}$ for BSA, and assuming a 1 cm path length. The results of this calculation are shown in Table 1. Considering the small differences in A_{280} between the MIPs and the NIPs, the likely error in weighing 5 mg polymer, the general error in absorbance measurements and the fact that no standard deviations are given, it is questionable whether these measurements show an imprinting effect.

When aspecific and error sensitive indirect measurements are used, especially when the amount of protein bound is just a fraction of the total amount of protein offered, standard deviations or duplicates/triplicates are essential to judge the significance of the presented data. However, standard deviations are often missing in papers on molecular imprinting of proteins. This is illustrated further by a paper by Guo *et al.* [78], in which rebinding of hemoglobin to polyacrylamide MIP beads was studied using A_{280} (Figure 12).

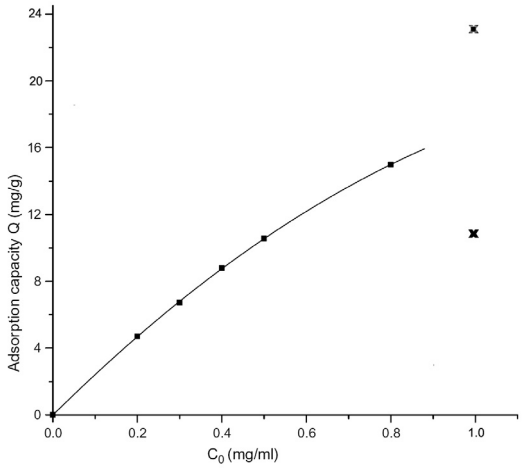

Figure 12. Adsorption isotherm of hemoglobin on MIP beads as presented by Guo *et al.* (*Reprinted with permission from* [78]), supplemented with data showing the calculated values for C_0 = 1.0 mg/mL (depicted as X).. Hemoglobin (600 mg) imprints were prepared using 1.9 g AAm and 0.1 g MBA graft polymerized to 16 g (wet) porous crosslinked chitosan beads. Template removal was not quantified. Rebinding studies were performed at 25°C for 16-17 h using 0.5 g wet beads and 10 mL (= max 10 mg) of hemoglobin solution.

When the adsorption isotherm was linearly converted according to the Langmuir equation they found a correlation coefficient of 0.9989, suggesting an excellent fit. However, it is interesting to note that in the same paper, from another experiment at the same conditions, the adsorption capacity (Q-value) at C_0 = 1.0 mg/mL was determined to be 20.4 mg/g, which deviates substantially from the curve presented in Figure 12. Yet another Q value at C_0 = 1.0 mg/mL can be calculated from the reported K_D value of 23.2. Given that $K_D = C_p/C_s$ (C_p = concentration of protein in the MIP in mg/g, C_s = concentration in the solution in mg/mL), C_0 =1.0 mg/mL, V = 10 mL and the amount of beads is 0.5 g, Q is 10.8 mg/g. Adding these two additional values for Q to Figure 12 (depicted in the figure as X) it becomes clear that there is an enormous deviation from the presented curve. Besides that, the authors did not show the adsorption isotherm to the NIP.

According to our own experience, reproducibility is a difficult issue in protein imprinting. Figure 13 A shows the A_{410} values of the supernatant after hemoglobin rebinding to MIP and NIP (crushed polyacrylamide gels with 6% (w/v) total monomer, AAm:MBA = 9:1, 40 mg hemoglobin/g dry polymer, template removal 55 ± 3%). The differences in absorption are minimal but significant (paired t-test, p = 0.0234), and when these data are converted to a Langmuir plot (Fig 13 B) there seems to be a clear imprinting effect. However, the imprints were prepared using 200 mg hemoglobin/g dry polymer, while the maximum amount of hemoglobin bound to MIP was only 17 mg/g dry polymer (= 8.5% of the imprinted amount). Moreover, the reproducibility of these data was poor: an imprint effect was observed in less than 50% of our repeated experiments.

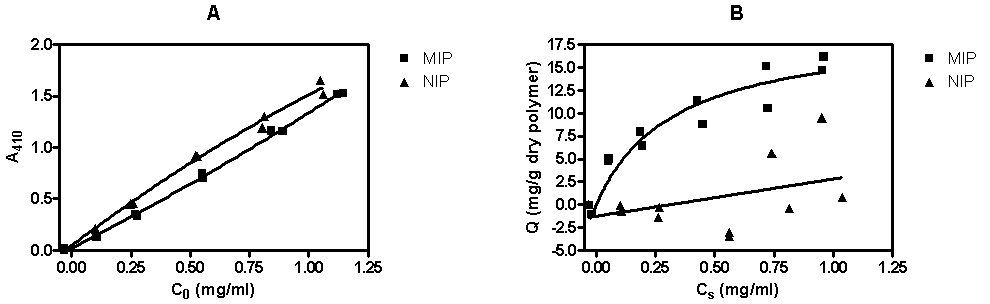

Figure 13. The raw A_{410} data (A) and corresponding Langmuir representation (B) of hemoglobin binding to crush sieved MIP and NIP (n = 2). Hemoglobin was incubated with fixed amount of polymer particles in phosphate buffer (pH 6.8) for 14 h. Particles were pelleted by centrifugation, and the supernatant was filtered (0.2 µm) before determination of the A_{410}. Individual duplicates are shown because the x-coordinate is sample-dependent (in Figure A ,C_0 was determined for each sample immediately after addition of the wet polymer particles, and in Figure B, C_s is an experimental outcome).

Poor reproducibility is also illustrated by another example from our own experiments on surface-imprinting of the bacterial membrane-anchored cell wall precursor lipid II (LII), aiming for bacteria recognizing MIPs. The bacterial cell wall comprises of a biopolymer of alternating amino sugars, *N*-acetylglucosamine (GlcNAc) and *N*-acetylmuramic acid (MurNAc), crosslinked by a pentapeptide (*L*-alanyl-*D*-glutamyl-diaminopimelyl-*D*-alanyl-*D*-alanine). The cell wall is synthesized from LII, which consists of the hydrophilic pentapeptide, GlcNAc and MurNAc, linked to the lipid anchor bactoprenyl-phosphate [83]. LII-surface-imprinted nanoparticles were prepared by the formation of a polymer network inside the aqueous inner compartment of liposomes. LII was immobilized in the liposomal bilayer in order to create surface-imprints of the hydrophilic part of LII directed towards the liposomal interior. The rebinding of surface-imprinted particles to their LII-template was determined by surface plasmon resonance. The hydrodynamic particle size and polydispersity index of the isolated LII-imprinted and non-imprinted particles as determined by dynamic light scattering are shown in table 2.

Table 2. Z-average diameter and polydispersity index (PDI) of LII-imprinted (MIP) and non-imprinted (NIP) polyacrylamide nanoparticles.

	Z-Avg (nm)	*PDI*
MIP	217	0.176
NIP	251	0.205

Figure 14 shows the sensorgrams of LII-imprinted and non-imprinted particles (NIP) flown over the SPR chip on which the LII was immobilized. Upon injection of MIP (at the time point marked by A) a strong increase in signal was observed. The increase in response was dependent on particle concentration; a higher concentration led to a higher association level. Injection of NIP led to much lower association, which was concentration independent. After the injection of particles was finished (time point B), the amount of immobilized material remained constant, i.e. no dissociation of bound particles was observed. The data in Figure 14 suggest that MIP specifically bound to the LII-template and imprinting is therefore successful. Furthermore, the absence of dissociation implies a very strong interaction between template and MIP. Unfortunately, attempts to reproduce these data with a new batch of particles and with a new batch of LII were unsuccessful. The poor reproducibility raises the question whether there are some minor and obviously uncontrollable and unknown experimental details that have an important influence on the successful formation of imprints, or whether the observed effect

were merely a result of experimental errors or artifacts. To say the least, the exact factors that determine whether imprinting is successful are currently poorly understood.

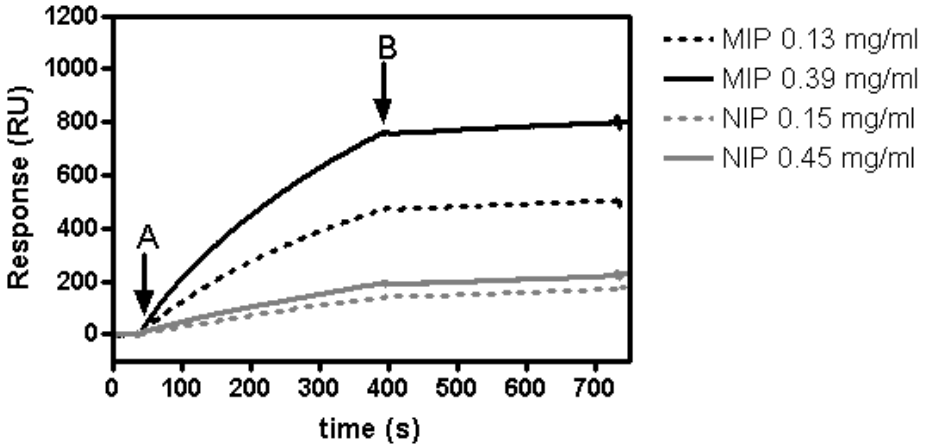

Figure 14. Binding of LII-imprinted particles (MIP) and non-imprinted particles (NIP) to LII immobilized in a DOPC monolayer on a SPR chip. The sensorgrams were corrected for the signal of a reference DOPC surface without LII (flowcell 1).

Conclusions and recommendations

Despite the increase in the number of publications per year, our analysis of data presented by other authors and our own experiments has shown that molecular imprinting of proteins still faces fundamental challenges. A substantial part of the literature contains data that seemingly confirm an imprinting effect, but lack convincing evidence when subjected to a critical analysis. Based on our findings we would like to conclude with some recommendations that in our view will help to avoid the common pitfalls.

Strong electrostatic interactions between monomers and template can lead to very high aspecific binding. The use of charged monomers should therefore be considered carefully. Up till now, it has not been convincingly shown that they lead to better imprinting results. Additionally, factors such as pH and ionic strength seriously complicate the eventual effects. On the other hand, it remains to be seen whether non-charged hydrophilic matrices currently used for imprinting are suitable to form high affinity polymers. In nature, high affinity between for example antibody and antigen or ligand and receptor does not only result from hydrogen bonding. Electrostatic and hydrophobic interactions also play a major role. Interestingly, in a

recent series of papers on peptide (melittin) imprinting in aqueous environment, imprinted polymer particles were prepared from *N*-isopropylacrylamide crosslinked with *N,N'*-methylene-bisacrylamide, supplemented with functional monomers for electrostatic and hydrophobic interactions (AAc and *N*-t-butylacrylamide, respectively) [84-86]. This example illustrates that for imprinting of biomolecules in aqueous media, hydrophobic and electrostatic interactions may substantially contribute to an imprinting effect.

The combination of SDS and AcOH is commonly used for template removal. However, the evidence that this leads to the best results can be seriously doubted. To mention, it has become clear that this combination can also lead to experimental artifacts, and should ideally be avoided. When it is used, MIP and NIP should undergo exactly the same washing protocol and extensive rinsing should ensure complete removal of remainders of AcOH and SDS, which should be checked by pH measurements and addition of KCl, respectively. For validation, destructive analysis of the polymer could be used to rule out minute amounts remaining in the polymer.

Template removal and rebinding should be quantified by validated methods. Proper controls should ensure that changes in concentration are actually the result of binding to the polymer and not due to e.g. protein aggregation/adsorption. The raw data should be presented, either as separate duplicates/triplicates or with error bars, to show convincing differences between MIP and NIP, and reproducibility should be confirmed with different batches. Kinetic measurements should always be employed to determine the time needed to reach binding equilibrium. Rebinding studies should be done with amounts equal to that used for the preparation of MIP to ensure that the measured effects are a plausible result of the formation of specific binding sites.

At present, it can be argued that in numerous publications, the scientific evidence of molecular imprinting of proteins is not convincing. Further studies with improved and solid experimental designs, critical data analysis, and clear presentation and interpretation are needed to make protein imprinting fit for the future.

References

[1] J.P. Schillemans, C.F. van Nostrum, Molecularly imprinted polymer particles: synthetic receptors for future medicine, Nanomed., 1 (2006) 437-447.

[2] M.V. Polyakov, Adsorption properties and structure of silica gel, Zhur. Fiz. Khim., 2 (1931) 799-805.

[3] C. Alexander, H.S. Andersson, L.I. Andersson, R.J. Ansell, N. Kirsch, I.A. Nicholls, J. O'Mahony, M.J. Whitcombe, Molecular imprinting science and technology: a survey of the literature for the years up to and including 2003, J. Mol. Recognit., 19 (2006) 106-180.

[4] C.F. van Nostrum, Molecular imprinting: A new tool for drug innovation, Drug Discov. Today: Technol., 2 (2005) 119-124.

[5] J.Z. Hilt, M.E. Byrne, Configurational biomimesis in drug delivery: molecular imprinting of biologically significant molecules, Adv. Drug Del. Rev., 56 (2004) 1599-1620.

[6] L. Ye, K. Mosbach, The technique of molecular imprinting - Principle, state of the art, and future aspects, J. Incl. Phen. Macrocycl. Chem., 41 (2001) 107-113.

[7] M.E. Byrne, K. Park, N.A. Peppas, Molecular imprinting within hydrogels, Adv. Drug Del. Rev., 54 (2002) 149-161.

[8] K. Flavin, M. Resmini, Imprinted nanomaterials: a new class of synthetic receptors, Anal. Bioanal. Chem., 393 (2009) 437-444.

[9] Y.P. Huang, Z.S. Liu, C. Zheng, R.Y. Gao, Recent developments of molecularly imprinted polymer in CEC, Electrophoresis, 30 (2009) 155-162.

[10] W.C. Lee, C.H. Cheng, H.H. Pan, T.H. Chung, C.C. Hwang, Chromatographic characterization of molecularly imprinted polymers, Anal. Bioanal. Chem., 390 (2008) 1101-1109.

[11] N.M. Maier, W. Lindner, Chiral recognition applications of molecularly imprinted polymers: a critical review, Anal. Bioanal. Chem., 389 (2007) 377-397.

[12] A. Takatsy, A. Vegvari, S. Hjerten, F. Kilar, Universal method for synthesis of artificial gel antibodies by the imprinting approach combined with a unique electrophoresis technique for detection of minute structural differences of proteins viruses and cells, (bacteria). Ib. Gel antibodies against proteins (hemoglobins), Electrophoresis, 28 (2007) 2345-2350.

[13] L.D. Bolisay, J.N. Culver, P. Kofinas, Molecularly imprinted polymers for tobacco mosaic virus recognition, Biomaterials, 27 (2006) 4165-4168.

[14] K. Seidler, P.A. Lieberzeit, F.L. Dickert, Application of yeast imprinting in biotechnology and process control, Analyst, 134 (2009) 361-366.

[15] D.A. Spivak, K.J. Shea, Investigation into the scope and limitations of molecular imprinting with DNA molecules, Anal. Chim. Acta, 435 (2001) 65-74.

[16] M.J. Whitcombe, in.

[17] N.W. Turner, C.W. Jeans, K.R. Brain, C.J. Allender, V. Hlady, D.W. Britt, From 3D to 2D: A review of the molecular imprinting of proteins, Biotechnol. Prog., 22 (2006) 1474-1489.

[18] T. Takeuchi, T. Hishiya, Molecular imprinting of proteins emerging as a tool for protein recognition, Org. Biomol. Chem., 6 (2008) 2459-2467.

[19] A. Valdebenito, P. Espinoza, E.A. Lissi, M.V. Encinas, Bovine serum albumin as chain transfer agent in the acrylamide polymerization. Protein-polymer conjugates, Polymer, 51 (2010) 2503-2507.

[20] E. Breukink, H.E. van Heusden, P.J. Vollmerhaus, E. Swiezewska, L. Brunner, S. Walker, A.J.R. Heck, B. de Kruijff, Lipid II is an intrinsic component of the pore induced by nisin in bacterial membranes, J. Biol. Chem., 278 (2003) 19898-19903.

[21] R.J. Kok, F. Grijpstra, K.H. Nederhoed, F. Moolenaar, D.D. Zeeuw, D.K.F. Meijer, Renal drug delivery with low-molecular-weight proteins: The effect of charge modifications on the body distribution of drug-lysozyme conjugates, Drug Del., 6 (1999) 1-8.

[22] T. Matsunaga, T. Hishiya, T. Takeuchi, Surface plasmon resonance sensor for lysozyme based on molecularly imprinted thin films, Anal. Chim. Acta, 591 (2007) 63-67.

[23] O. Kimhi, H. Bianco-Peled, Study of the Interactions between Protein-Imprinted Hydrogels and Their Templates, Langmuir, 23 (2007) 6329-6335.

[24] O.H. Lowry, N.J. Rosebrough, A.L. Farr, R.J. Randall, Protein measurement with the folin phenol reagent, J. Biol. Chem., 193 (1951) 265-275.
[25] A.C. Dong, L.S. Jones, B.A. Kerwin, S. Krishnan, J.F. Carpenter, Secondary structures of proteins adsorbed onto aluminum hydroxide: Infrared spectroscopic analysis of proteins from low solution concentrations, Anal. Biochem., 351 (2006) 282-289.
[26] S.M. Kelly, T.J. Jess, N.C. Price, How to study proteins by circular dichroism, Biochim. Biophys. Acta - Prot. Proteomics, 1751 (2005) 119-139.
[27] K.D. Hardman, E.H. Eylar, D.K. Ray, L.J. Banaszak, F.R.N. Gurd, Isolation of sperm whale myoglobin by low temperature fractionation with ethanol and metallic Ions, J. Biol. Chem., 241 (1966) 432-&.
[28] D.M. Hawkins, D. Stevenson, S.M. Reddy, Investigation of protein imprinting in hydrogel-based molecularly imprinted polymers (HydroMIPs), Anal. Chim. Acta, 542 (2005) 61-65.
[29] D.S. Janiak, O.B. Ayyub, P. Kofinas, Effects of charge density on the recognition properties of molecularly imprinted polymeric hydrogels, Macromolecules, 42 (2009) 1703-1709.
[30] J.P. Schillemans, F.M. Flesch, W.E. Hennink, C.F. van Nostrum, Synthesis of bilayer-coated nanogels by selective cross-linking of monomers inside liposomes, Macromolecules, 39 (2006) 5885-5890.
[31] G. Rouser, S. Fkeischer, A. Yamamoto, Two dimensional then layer chromatographic separation of polar lipids and determination of phospholipids by phosphorus analysis of spots, Lipids, 5 (1970) 494-496.
[32] S. Hjerten, J.L. Liao, K. Nakazato, Y. Wang, G. Zamaratskaia, H.X. Zhang, Gels mimicking antibodies in their selective recognition of proteins, Chromatographia, 44 (1997) 227-234.
[33] B. Sellergren, The non-covalent approach to molecular imprinting, in: B. Sellergren (Ed.) Molecularly imprinted polymers: man-made mimics of antibodies and theirapplications in analytical chemistry, Elsevier, Amsterdam, 2001, pp. 113-183.
[34] J. Liao, Y. Wang, S. Hjertén, A novel support with artificially created recognition for the selective removal of proteins and for affinity chromatography, Chromatographia, 42 (1996) 259-262.
[35] N. Ghasemzadeh, F. Nyberg, S. Hjerten, Highly selective artificial gel antibodies for detection and quantification of biomarkers in clinical samples. I. Spectrophotometric approach to design the calibration curve for the quantification, J. Sep. Sci., 31 (2008) 3945-3953.
[36] D. Tong, C. Heényi, Z. Bikádi, J. Gao, S. Hjertén, Some studies of the chromatographic properties of gels ('Artificial antibodies/receptors') for selective adsorption of proteins, Chromatographia, 54 (2001) 7-14.
[37] A. Bossi, S.A. Piletsky, E.V. Piletska, P.G. Righetti, A.P. Turner, Surface-grafted molecularly imprinted polymers for protein recognition, Anal. Chem., 73 (2001) 5281-5286.
[38] F. Bonini, S. Piletsky, A.P. Turner, A. Speghini, A. Bossi, Surface imprinted beads for the recognition of human serum albumin, Biosens. Bioelectron., 22 (2007) 2322-2328.
[39] Y. Lu, C.L. Yan, S.Y. Gao, Preparation and recognition of surface molecularly imprinted core-shell microbeads for protein in aqueous solutions, Appl. Surf. Sci., 255 (2009) 6061-6066.
[40] J. Rick, T.-C. Chou, Using protein templates to direct the formation of thin-film polymer surfaces, Biosens. Bioelectron., 22 (2006) 544-549.
[41] S.A. Piletsky, E.V. Piletska, B. Chen, K. Karim, D. Weston, G. Barrett, P. Lowe, A.P.F. Turner, Chemical grafting of molecularly imprinted homopolymers to the surface of microplates. Application of artificial adrenergic receptor in enzyme-linked assay for β-agonists determination, Anal. Chem., 72 (2000) 4381-4385.
[42] N.W. Turner, X. Liu, S.A. Piletsky, V. Hlady, D.W. Britt, Recognition of conformational changes in, beta-lactoglobulin by molecularly imprinted thin films, Biomacromolecules, 8 (2007) 2781-2787.
[43] G.A. Kulikova, I.V. Ryabinina, S.S. Guseynov, E.V. Parfenyuk, Calorimetric study of adsorption of human serum albumin onto silica powders, Thermochim. Acta, 503 (2010) 65-69.
[44] K. Hirayama, Y. Sakai, K. Kameoka, Synthesis of polymer particles with specific lysozyme recognition sites by a molecular imprinting technique, J. Appl. Pol. Sci., 81 (2001) 3378-3387.
[45] A. Uysal, G. Demirel, E. Turan, T. Caykara, Hemoglobin recognition of molecularly imprinted hydrogels prepared at different pHs, Anal. Chim. Acta, 625 (2008) 110-115.
[46] S.H. Ou, M.C. Wu, T.C. Chou, C.C. Liu, Polyacrylamide gels with electrostatic functional groups for the molecular imprinting of lysozyme, Anal. Chim. Acta, 504 (2004) 163-166.

[47] M. Odabasi, R. Say, A. Denizli, Molecular imprinted particles for lysozyme purification, Mater. Sci. Eng. C, 27 (2007) 90-99.
[48] G.Q. Fu, J.C. Zhao, H. Yu, L. Liu, B.L. He, Bovine serum albumin-imprinted polymer gels prepared by graft copolymerization of acrylamide on chitosan, React. Funct. Pol., 67 (2007) 442-450.
[49] D.M. Hawkins, A. Trache, E.A. Ellis, D. Stevenson, A. Holzenburg, G.A. Meininger, S.M. Reddy, Quantification and confocal imaging of protein specific molecularly imprinted polymers, Biomacromolecules, 7 (2006) 2560-2564.
[50] E. Lanz, M. Gregor, J. Slavík, A. Kotyk, Use of FITC as a fluorescent probe for intracellular pH measurement, J. Fluoresc., 7 (1997) 317-319.
[51] L.Y. Ma, H.Y. Wang, H. Xie, L.X. Xu, A long lifetime chemical sensor: study on fluorescence property of fluorescein isothiocyanate and preparation of pH chemical sensor, Spectrochim. Acta. A. Mol. Biomol. Spectrosc., 60 (2004) 1865-1872.
[52] T.Y. Guo, Y.Q. Xia, G.J. Hao, M.D. Song, B.H. Zhang, Adsorptive separation of hemoglobin by molecularly imprinted chitosan beads, Biomaterials, 25 (2004) 5905-5912.
[53] X.S. Pang, G.X. Cheng, Y.H. Zhang, S.L. Lu, Soft-wet polyacrylamide gel beads with the imprinting of bovine serum albumin, React. Funct. Pol., 66 (2006) 1182-1188.
[54] C.J. Tan, Y.W. Tong, The effect of protein structural conformation on nanoparticle molecular imprinting of ribonuclease A using miniemulsion polymerization, Langmuir, 23 (2007) 2722-2730.
[55] Y.Q. Xia, T.Y. Guo, M.D. Song, B.H. Zhang, B.L. Zhang, Hemoglobin recognition by imprinting in semi-interpenetrating polymer network hydrogel based on polyacrylamide and chitosan, Biomacromolecules, 6 (2005) 2601-2606.
[56] G.-Q. Fu, H. Yu, J. Zhu, Imprinting effect of protein-imprinted polymers composed of chitosan and polyacrylamide: A re-examination, Biomaterials, 29 (2008) 2138-2142.
[57] C.J. Tan, M.G. Chua, K.H. Ker, Y.W. Tong, Preparation of bovine serum albumin surface-imprinted submicrometer particles with magnetic susceptibility through core-shell miniemulsion polymerization, Anal. Chem., 80 (2008) 683-692.
[58] C.J. Tan, S. Wangrangsimakul, R. Bai, Y.W. Tong, Defining the interactions between proteins and surfactants for nanoparticle surface imprinting through miniemulsion polymerization, Chem. Mater., 20 (2008) 118-127.
[59] G. Fu, J. Zhu, Y. Jiang, Comment on "Preparation of superparamagnetic ribonuclease a surface-imprinted submicrometer particles for protein recognition in aqueous media", Anal. Chem., 80 (2008) 2634-2635.
[60] C.J. Tan, S. Wangrangsimakul, N. Sankarakumar, Y.W. Tong, Response to comment on "Preparation of superparamagnetic ribonuclease A surface-imprinted submicrometer particles for protein recognition in aqueous media", Anal. Chem., 80 (2008) 9375-9376.
[61] B.R. Young, W.G. Pitt, S.L. Cooper, Protein adsorption on polymeric biomaterials : II. Adsorption kinetics, J. Colloid Interface Sci., 125 (1988) 246-260.
[62] M. Holmberg, X. Hou, Competitive protein adsorption - multilayer adsorption and surface induced protein aggregation, Langmuir, 25 (2009) 2081-2089.
[63] D.S. Janiak, O.B. Ayyub, P. Kofinas, Effects of charge density on the recognition properties of molecularly imprinted polyampholyte hydrogels, Polymer, 51 (2010) 665-670.
[64] O.Y. Tov, S. Luvitch, H. Bianco-Peled, Molecularly imprinted hydrogel displaying reduced non-specific binding and improved protein recognition, J. Sep. Sci., 33 (2010) 1673-1681.
[65] S.L. Lu, G.X. Cheng, X.S. Pang, Protein-imprinted soft-wet gel composite microspheres with magnetic susceptibility. II. Characteristics, J. Appl. Pol. Sci., 99 (2006) 2401-2407.
[66] X.S. Pang, G.X. Cheng, R.S. Li, S.L. Lu, Y.H. Zhang, Bovine serum albumin-imprinted polyacrylamide gel beads prepared via inverse-phase seed suspension polymerization, Anal. Chim. Acta, 550 (2005) 13-17.
[67] X.S. Pang, G.X. Cheng, S.L. Lu, E.J. Tang, Synthesis of polyacrylamide gel beads with electrostatic functional groups for the molecular imprinting of bovine serum albumin, Anal. Bioanal. Chem., 384 (2006) 225-230.
[68] D.V. Nicolau Jr, D.V. Nicolau, Towards a theory of protein adsorption: predicting the adsorption of proteins on surfaced using a piecewise linear model validated using the biomolecular adsorption

database, 2nd Asia-Pacific Bioinformatics Conference; Conferences in Research and Practice in Information Technology, 29 (2004).
[69] H.-Y. Lin, C.-Y. Hsu, J.L. Thomas, S.-E. Wang, H.-C. Chen, T.-C. Chou, The microcontact imprinting of proteins: The effect of cross-linking monomers for lysozyme, ribonuclease A and myoglobin, Biosens. Bioelectron., 22 (2006) 534-543.
[70] N.W. Turner, B.E. Wright, V. Hlady, D.W. Britt, Formation of protein molecular imprints within Langmuir monolayers: A quartz crystal microbalance study, J. Colloid Interface Sci., 308 (2007) 71-80.
[71] O. Hayden, C. Haderspock, S. Krassnig, X.H. Chen, F.L. Dickert, Surface imprinting strategies for the detection of trypsin, Analyst, 131 (2006) 1044-1050.
[72] T.Y. Lin, C.H. Hu, T.C. Chou, Determination of albumin concentration by MIP-QCM sensor, Biosens. Bioelectron., 20 (2004) 75-81.
[73] B. Honore, Protein-binding studies with radiolabeled compounds containing radiochemical impurities - equilibrium dialysis versus dialysis rate determination, Anal. Biochem., 162 (1987) 80-88.
[74] L.E. Limbird, Cell surface receptors: a short course on theory and methods, 3rd ed., Springer, New York, 2005.
[75] Z. Hua, Z. Chen, Y. Li, M. Zhao, Thermosensitive and salt-sensitive molecularly imprinted hydrogel for bovine serum albumin, Langmuir, 24 (2008) 5773-5780.
[76] D. Silvestri, N. Barbani, M.L. Coluccio, C. Pegoraro, P. Giusti, C. Cristallini, G. Ciardelli, Poly(ethylene-co-vinyl alcohol) membranes with specific adsorption properties for potential clinical application, Sep. Sci. Tecnnol., 42 (2007) 2829-2847.
[77] D. Silvestri, N. Barbani, C. Cristallini, P. Giusti, G. Ciardelli, Molecularly imprinted membranes for an improved recognition of biomolecules in aqueous medium, J. Membr. Sci., 282 (2006) 284-295.
[78] T.Y. Guo, Y.Q. Xia, G.J. Hao, B.H. Zhang, G.Q. Fu, Z. Yuan, B.L. He, J.F. Kennedy, Chemically modified chitosan beads as matrices for adsorptive separation of proteins by molecularly imprinted polymer, Carbohydr. Pol., 62 (2005) 214-221.
[79] C.-L. Yan, Y. Yan, S.-Y. Gao, Coating lysozyme molecularly imprinted thin films on the surface of microspheres in aqueous solutions, J. Polym. Sci. A, (2007) 1911-1919.
[80] T. Shiomi, M. Matsui, F. Mizukami, K. Sakaguchi, A method for the molecular imprinting of hemoglobin on silica surfaces using silanes, Biomaterials, 26 (2005) 5564-5571.
[81] E. Gasteiger, C. Hoogland, A. Gattiker, S. Duvaud, M.R. Wilkins, R.D. Appel, A. Bairoch, Protein Identification and Analysis Tools on the ExPASy Server, in: J.M. Walker (Ed.) The Proteomics Protocols Handbook, Humana Press 2005.
[82] NCBI Accession number AJ973635.1, M.D. Bethesda, The NCBI handbook [Internet] Chapter 17, The Reference Sequence (RefSeq) Project, National Library of Medicine (US), National Center for Biotechnology Information, 2002, Available from http://www.ncbi.nlm.nih.gov/entrez/query.fcgi?db=Books, accessed on 23-07-2010
[83] E. Breukink, B. de Kruijff, Lipid II as a target for antibiotics, Nat. Rev. Drug Discov., 5 (2006) 321-332.
[84] Y. Hoshino, T. Kodama, Y. Okahata, K.J. Shea, Peptide imprinted polymer nanoparticles: a plastic antibody, J. Am. Chem. Soc., 130 (2008) 15242-15243.
[85] Y. Hoshino, H. Koide, T. Urakami, H. Kanazawa, T. Kodama, N. Oku, K.J. Shea, Recognition, neutralization, and clearance of target peptides in the bloodstream of living mice by molecularly imprinted polymer nanoparticles: A plastic antibody, J. Am. Chem. Soc., 132 (2010) 6644-6645.
[86] Y. Hoshino, T. Urakami, T. Kodama, H. Koide, N. Oku, Y. Okahata, K. Shea, Design of synthetic polymer nanoparticles that capture and neutralize a toxic peptide, Small, (2009) 1562-1568.

Chapter 5

The effect of network charge on the immobilization and release of proteins from chemically crosslinked dextran hydrogels

Joris P. Schillemans

Wim E. Hennink

Cornelus F. van Nostrum

European journal of pharmaceutics and biopharmaceutics 2010, in press

Abstract

Size is the main protein characteristic that determines its release from non-degrading neutral hydrogels. The effect of network charge on the release of proteins has not been studied systematically so far. Therefore, we investigated the release of proteins from charged hydrogels that were obtained by copolymerization of methacrylated dextran (Dex-MA) with either methacrylic acid (MA) or 2-*N,N*-dimethylaminoethyl methacrylate (DMAEMA). These hydrogels are stable under physiological conditions. The effect of incorporation of the charged monomers on hydrogel charge, equilibrium swelling and release of model proteins was assessed both at low (10 mM HEPES) and physiological ionic strength (HEPES buffered saline, HBS). Model proteins were chosen on the basis of their charge at physiological pH; bovine serum albumin (BSA, negatively charged), myoglobin (neutral), and cytochrome C (positively charged). Interestingly, as opposed to myoglobin, both charged proteins were fully immobilized in the networks with opposite charge by electrostatic interaction at low ionic strength. On the other hand, at physiological ionic strength the percentage of immobilized protein depended on the charge density of the hydrogel. For all proteins, the diffusion coefficient of the mobile fractions was not affected by opposite network charge. However, the release rate of BSA from similarly (negatively) charged networks significantly increased when a relatively high amount of charged monomers was incorporated. We conclude that incorporation of charge in a hydrogel network is suited as a tool for the immobilization of proteins and triggered release by increasing ionic strength.

Introduction

An increasing part of the pharmaceutical compounds introduced to the market consists of peptides and proteins [1]. At present, the therapeutic value of these compounds is compromised by the challenges related to their macromolecular complexity, such as immunogenicity [2-7], bioequivalency [8-11], and formulation [1, 12, 13]. Currently, most proteins are administered parenterally. In order to reduce the administration frequency and burden, research is dedicated to the development of sustained release formulations. Because of their tissue compatibility and possibilities to manipulate protein release, hydrogels are considered as attractive dosage forms for therapeutic proteins. The effect of parameters such as network density, solid content, and polymer degradation kinetics on protein release kinetics are well documented and commonly used to tailor the release of different proteins [14-21]. Provided that the protein is smaller than the mesh size of the network, protein diffusion in hydrogels is described by the free volume theory. According to this theory, diffusion of solutes occurs in the free space between solvent molecules. Inside the hydrogel, the presence of polymer chains decreases the amount of free space. Therefore, the diffusion rate is determined by hydration of the hydrogel and the size of the solute [22, 23]. Size is therefore the most important protein characteristic determining its release from a non-degrading hydrogel with pores bigger than the diameter of the loaded protein. Other protein characteristics such as isoelectric point (*pI*) or hydrophobicity have hardly been exploited to tailor release. It can be expected that modulation of charge interaction between the hydrogel network and protein molecules has an effect on the protein release. In fact, it has been reported that the release rate of myoglobin from polyaspartic acid hydrogels at pH 5 increased with increasing ionic strength [24]. Furthermore, the release of VEGF from ionically crosslinked alginate beads can be modified by the use of different cations [25, 26]. However, to our knowledge, the possibility to tailor the release rate of proteins by adaptation of the absolute charge and the charge density of the hydrogel network at physiological pH has never been explored. Therefore, in this paper we studied the effect of network charge sign and density on the release of proteins from hydrogels.

Proteins can either carry a net positive or negative charge, or be neutral at a certain pH, depending on *pI*. Model proteins were chosen on the basis of their charge at physiological pH; bovine serum albumin (BSA, negatively charged), myoglobin (neutral), and cytochrome C (positively charged). To ensure that protein release from the hydrogels is governed by diffusion only, methacrylated dextran (Dex-MA) hydrogels were used as model gels. Dex-MA hydrogels

are non-degradable at physiological conditions [21], which implies that hydrogel degradation does not play a role in protein release. Charge was introduced to the hydrogels by copolymerization of Dex-MA with various amounts of either methacrylic acid (MA) or 2-*N,N*-dimethylaminoethyl methacrylate (DMAEMA). To ensure equal network density, the total amount of additional monomer was kept constant by supplementing with neutral 2-hydroxyethyl methacrylate (HEMA).

Materials and methods

Materials

Dextran T40 (from *Leuconostoc spp.*), *N,N,N',N'*-tetramethylethylenediamine (TEMED), ammonium peroxodisulfate (APS) and 2-hydroxethyl methacrylate (HEMA) were obtained from Fluka (Buchs, Switzerland). Methacrylic acid (MA), 2-*N,N*-dimethylaminoethyl methacrylate (DMAEMA), bovine serum albumin (BSA, purity > 96%), cytochrome C from bovine heart (purity > 95%), and myoglobin from horse heart (purity > 90%) were purchased from Sigma-Aldrich (Zwijndrecht, the Netherlands). Methacrylated dextran (Dex-MA) with various degrees of substitution (DS) were synthesized according to Van Dijk-Wolthuis *et al.* [27, 28]. The DS was determined using ^{1}H NMR.

Preparation of Dex-MA hydrogels

Solutions of MA, DMAEMA, HEMA and TEMED, respectively, were prepared in 10 mM HEPES or 10 mM HEPES buffered saline (HBS, 10 mM HEPES, 145 mM NaCl), and the pH was adjusted to 7.4 using HCl or NaOH. Dextran hydrogels with an initial Dex-MA content of 15% (w/w) were prepared by free-radical polymerization. Dex-MA (0.15 g/g total weight), varying amounts of additional monomers (MA, DMAEMA, HEMA, total 350 µmol/g gel) and TEMED (67 µmol/g gel) were mixed in the appropriate buffer (HEPES/HBS). For protein loaded hydrogels, 20 µL of a protein stock solution (100 mg/mL) was added (8 mg protein per gram gel). APS in buffer (17 µmol/g gel) was added, and the mixture (final weight 250 mg) was transferred to a 1-mL syringe (radius 0.23 cm, height of the gel 1.5 cm). Polymerization was carried out under nitrogen atmosphere at room temperature for at least 2 h.

Equilibrium swelling

Hydrogels were removed from the syringe, weighed and transferred to vials containing HEPES or HBS. The weight of the gels was measured in time at 37°C until a constant weight was

reached. The swelling ratio is defined as the weight of the gel at equilibrium divided by the initial weight of the gel.

ζ-potential

Gels were washed with water and subsequently fragmented in 2.5 mL 5 mM HEPES pH 7.4 using an ultra-turrax tube drive (IKA® Werke GmbH & Co. KG, Staufen, Germany) for 10 min. The samples were incubated at room temperature for 2 h in order to let the larger particles settle. The ζ-potential of the particles in the supernatant was determined using a Malvern Zetasizer Nano-Z (Malvern Instruments, Malvern, UK) with universal ZEN 1002 'dip' cell and DTS (Nano) software (version 4.20). The system was calibrated with DTS 1050 latex beads (Zeta Potential Transfer Standard, Malvern Instruments, Malvern, UK).

Protein release

Protein loaded hydrogels were placed in vials containing 2 mL buffer (10 mM HEPES or HBS, pH 7.4). The vials were gently rotated at 37°C. Samples (20 µL) were taken periodically and replaced with buffer. The protein concentration in samples was determined by means of a fluorometric assay using fluorescamine as described by Böhlen *et al.* [29], adapted to a 96-well plate format. Subtraction of the background signal measured in the release medium containing blank gels (without protein) was used to correct for possible interference of the gel components with the quantification.

Statistical analysis

First, cumulative release was compared using repeated-measures ANOVA with a post hoc test for linear trend. Subsequently, the total amount released was compared between gel formulations using a one-way ANOVA followed by post hoc analysis with a Bonferroni's multiple comparison test.

The slope of the best fit of the fractional release curves were compared using an *F*-test. Subsequently, the slopes were compared between gel formulations using a one-way ANOVA followed by post hoc analysis with a Bonferroni's multiple comparison test. A p-value < 0.05 was considered significant.

Results and discussion

Hydrogel synthesis and characterization

Positively and negatively charged dextran networks were obtained by free-radical polymerization of Dex-MA with negatively charged MA or positively charged DMAEMA, respectively. To assess whether the charged monomers were incorporated in the polymer network, the electrophoretic mobility of particles obtained by fragmentation of the hydrogels was determined as a function of charged monomer feed (Figure 1). Dex-MA gel particles prepared without charged monomers had a slightly negative ζ-potential, which is in agreement with earlier reports [30], and is likely due to absorption of anions onto the hydrogel particle surface. Input of charged monomers caused a shift of the ζ-potential of hydrogel particles, negative for MA and positive in the case of DMAEMA. Figure 1 also shows that an increase of charged monomer feed led to increased shift of ζ-potential. These findings indicate that the charged monomers copolymerized with Dex-MA to form charged Dex-MA hydrogels, and that an increased charged monomer feed led to increased charge density.

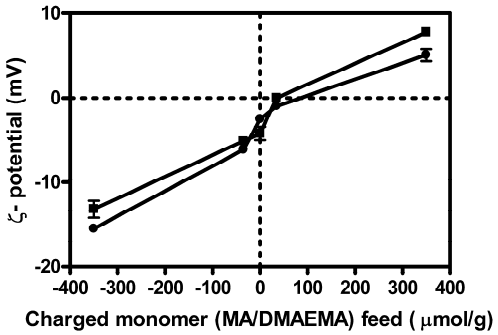

Figure 1. ζ-potential of hydrogel particles. Dex-MA hydrogels (squares = DS 4 and circles = DS 7) with varying concentration of charged monomers were crushed and the ζ-potential was measured at 25°C in 5 mM hepes pH 7.4. Values represent average and range of 2 separately prepared hydrogels.

Hydrogel swelling behavior

Once incubated in buffer, hydrogels reached an equilibrium swelling after 4 h. Figure 2 shows the effect of charged monomers on the equilibrium swelling ratio of Dex-MA hydrogels. Without charged monomers, Dex-MA hydrogels with low DS (4) swell approximately 25% when incubated in buffer, while hydrogels with intermediate DS (7) are dimensionally stable, which is in agreement with earlier findings [22, 27, 31]. In 10 mM HEPES buffer, Dex-MA/DMAEMA or

MA hydrogels (for both DS = 4 and 7) showed an increase in swelling when compared to gels without charged monomers. The degree of swelling increased with increasing charged monomer input. The incorporated charged groups caused a rise of the internal osmotic pressure due to accumulation of counterions (HEPES) in the network [32]. In HBS, a lower equilibrium swelling was observed for all charged Dex-MA hydrogels. Because of the high concentration of ions in this buffer the difference in osmotic pressure between the charged hydrogels and the surrounding buffer is small [32], and therefore the swelling was the same as that of the neutral gels. Similar findings were presented in earlier reports on hydrogels prepared by co-polymerization of Dex-MA and acrylic acid [33, 34].

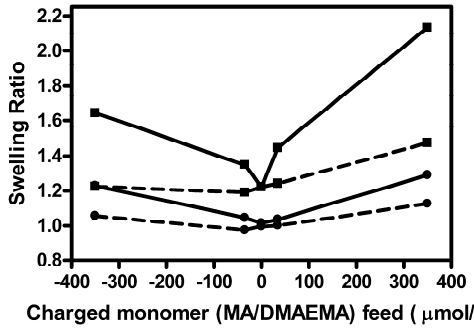

Figure 2. Equilibrium swelling ratio of Dex-MA hydrogels (squares = DS 4 and circles = DS 7) with varying concentrations of charged monomers in hepes (solid lines) and HBS (dashed lines). Values represent average and range of 2 separately prepared hydrogels.

Table 1. Molecular weight, D_o, *pI* and charge at physiological pH of the selected proteins.

	Mw (kD)	*D_o x 10^6 (cm^2/s)*	*pI*	*Overall charge at pH 7.4*
BSA	66	0.59 [41]	4.8	–
Myoglobin	17	1.06 [37]	7.2	± Neutral
Cytochrome C	12	1.30 [39]	10.2	+

Protein release

The release of three model proteins varying in size and *pI* from neutral, positively, and negatively charged dextran networks (obtained from Dex-MA with DS 7) was studied in buffer at low and physiological ionic strength. Table 1 lists the size, the diffusion coefficient in H_2O (D_o), *pI* and overall charge at physiological pH of these model proteins. Figure 3A and B show the release profiles of myoglobin from charged and neutral Dex-MA hydrogels in HEPES and HBS,

respectively. Both at low and at high ionic strength myoglobin was released gradually up to 70 - 90% of the initial load. This indicates that a fraction (10 - 30%) of myoglobin was trapped inside the hydrogel network during polymerization. This fraction was lower for the hydrogels containing 350 µmol/g charged monomer (in HEPES 9.2% ± 3.4 and 10.3% ± 4.0, and in HBS 13.4% ± 0.5 and 13.2% ± 1.4 for MA and DMAEMA, respectively), when compared to neutral hydrogels and hydrogels containing 35 µmol/g charged monomers (in HEPES 24.3% ± 0.6 and 25.8% ± 2.4, and 17.9% ± 3.7 and in HBS 29.1% ± 3.1 and 28.9% ± 0.8 and 28.4% ± 3.2 for 35 µmol MA/g, neutral and 35 µmol DMAEMA/g respectively). This could be due to the higher equilibrium swelling for the hydrogels containing 350 µmol/g charged monomers, resulting in a bigger hydrogel mesh size. With none of the hydrogel compositions, complete release of protein was obtained. This could be due to chemical crosslinking of the protein to the network [35], which leads to permanent entrapment.

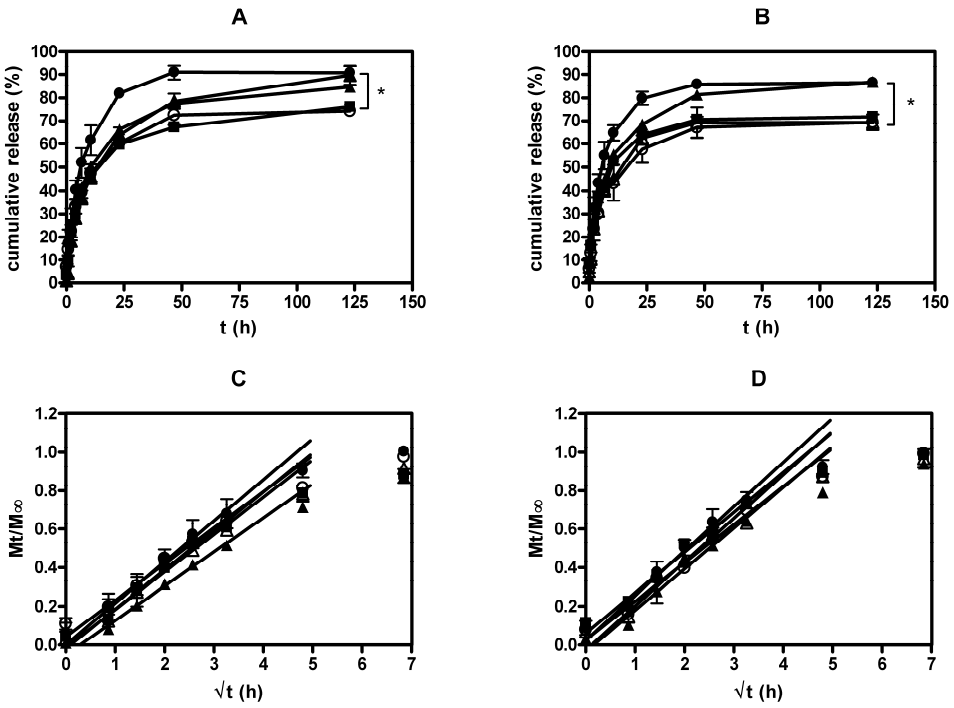

Figure 3. Cumulative release of myoglobin from Dex-MA hydrogels (DS 7) in hepes (A + C) and HBS (B + D). Values represent the average (n = 3, ± s.d.) released from neutral (squares), negatively charged (open circles = 35 µmol, closed circles = 350 µmol MA/g) and positively charged (open triangles = 35 µmol, closed triangles = 350 µmol DMAEMA/g) hydrogels. The symbol * indicates *p*-values < 0.05.

To assess the effect of the hydrogel charge on the diffusion kinetics of myoglobin, the fractional release was plotted as a function of the square root of time (Figure 3C). According to the early-time approximation equation of Fick's second law, diffusion controlled release is linear with the square root of time [36]:

$$\frac{M_t}{M_\infty} = 4\sqrt{\frac{D_m t}{\pi r^2}} \qquad (1)$$

where M_t/M_∞ represents the fractional release of the entrapped protein, D_m is the diffusion coefficient of the solute in the matrix, t is the release time, and r is the radius of the hydrogel cylinder. It should be noted that the dimensions of the cylinder should ideally be such that release through radial diffusion is negligible. For the gels used in this study, the top and bottom plane together make up 15% of the total surface area. Although the D_m calculated using equation 1 is therefore an overestimation, this does not pose a problem since it is used only to compare the diffusion in hydrogels with the same dimensions. Figure 3C shows that the release versus the square root of time of myoglobin was linear up to a fractional release of ~0.6 for all hydrogel formulations, and that the slope was independent of the composition of the hydrogel and the ionic strength of the release medium (p = 0.52 and 0.62 for HEPES and HBS, respectively). From the slope of the release curves the diffusion coefficient of myoglobin in the hydrogel network D_m was calculated using equation 1 (Table 2).

Table 2. The diffusion coefficient of myoglobin in Dex-MA hydrogels (DS 7) with varying charge density in HEPES and HBS calculated using the early-time approximation of Ficks's second law (n = 3). Values between brackets represent the 95% confidence interval.

Charge density (µmol charged monomer/g hydrogel)	*D_m in HEPES x10^7 (cm^2/s)*	*D_m in HBS x10^7 (cm^2/s)*
350 MA	1.3 (0.8 – 1.9)	1.5 (1.1 – 2.0)
35 MA	1.0 (0.8 – 1.3)	1.5 (1.0 – 2.1)
0	1.2 (0.6 – 1.9)	1.2 (0.7 – 1.9)
35 DMAEMA	1.1 (0.5 – 1.9)	1.1 (0.7 – 1.7)
350 DMAEMA	0.9 (0.8 – 1.1)	1.3 (0.9 – 1.8)

The reported D_o of myoglobin is 1.06 x 10^{-6} cm^2/s [37]. The results show that the hydrogel matrix slows down the diffusion of myoglobin by approximately 1 order of magnitude. It becomes clear from table 2 that the diffusion of myoglobin was not affected by the network charge. Since myoglobin is almost neutral at physiological pH, an effect of hydrogel charge on the release of myoglobin was not expected. The higher equilibrium hydrogel swelling at higher

network charge did also not affect protein release kinetics. On the one hand, swelling can lead to a higher release rate due to the increased hydration of the network; on the other hand, the increased diffusional pathlength resulting from the increase in hydrogel volume leads to slower release kinetics. Overall, for these hydrogels, the moderate increase in hydrogel swelling did not affect the release rate of myoglobin.

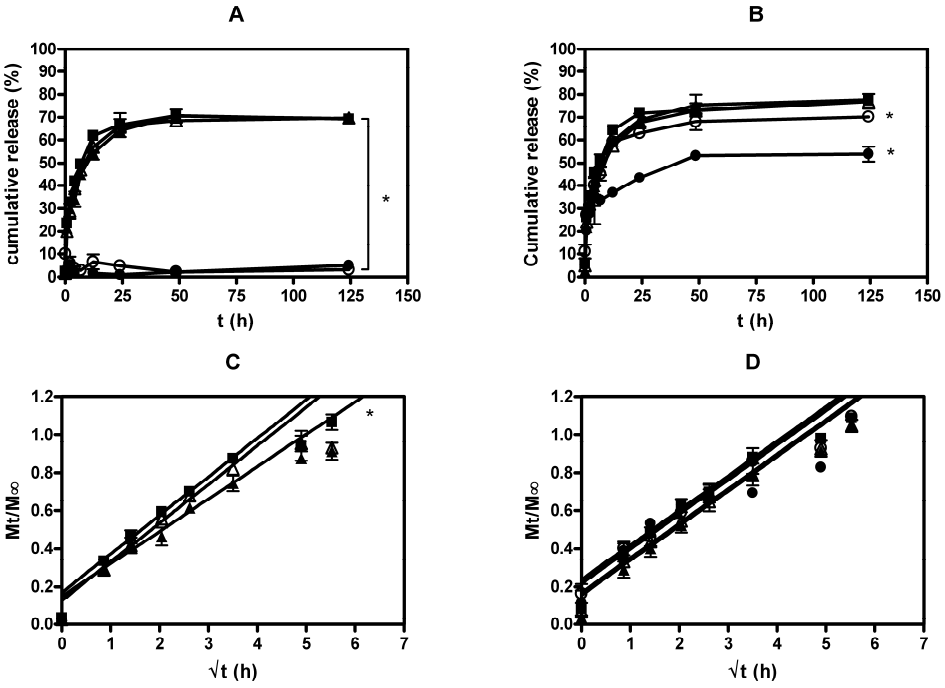

Figure 4. Cumulative release of cytochrome C from Dex-MA hydrogels (DS 7) in hepes (A + C) and HBS (B + D). Values represent the average (n = 3, ± s.d.) released from neutral (squares), negatively charged (open circles = 35 µmol, closed circles = 350 µmol MA/g) and positively charged (open triangles = 35 µmol, closed triangles = 350 µmol DMAEMA/g) hydrogels. The symbol * indicates *p*-values < 0.05.

The release of cytochrome C from neutral, positively, and negatively charged dextran networks is shown in Figure 4. In 10 mM HEPES the release was substantially affected by the charge of the hydrogel network (Figure 4A). The total amount of released cytochrome C was approx. 70% for neutral and positively charged gels (69.2% ± 1.0, 69.7% ± 2.0 and 69.4% ± 1.4 for neutral and 35 and 350 µmol DMAEMA/g gel, respectively). However, no release of this protein from negatively charged dextran networks was observed. At 35 µmol MA/g gel the hydrogel contained an excess of MA when compared to the number of positively charged amino acid residues in

cytochrome C (assuming full co-polymerization of MA; 50 mol MA/mol protein = 2.4 MA/positively charged amino acid residues), which explains that cytochrome C was immobilized quantitatively. Figure 4B shows the release of cytochrome C from neutral, positively and negatively charged gels in HBS. The amount of released cytochrome C from both neutral and positively charged gels in HBS (77.7% ± 0.9, 77.1% ± 3.2 and 77.8% ± 1.5 for neutral and 35 and 350 µmol DMAEMA/g gel, respectively) was similar to the release in HEPES, with similar release kinetics. However, as opposed to what was found in HEPES, cytochrome C was not quantitatively immobilized in negatively charged gels in HBS. The amount of released cytochrome C depended on the charge of the hydrogel, varying from 54% ± 3.2 for 350 µmol MA/g to 70.2% ± 0.39 for 35 µmol MA/g. These results demonstrate that the immobilization in HEPES was reversible and indeed due to electrostatic interactions between the protein and the dextran network. A similar effect of charge and ionic strength was described by Hirota *et al.* who found that the partitioning of myoglobin in negatively charged λ-carrageenan hydrogels at low ionic strength strongly depended on the pH of the medium, but was almost the same for all pH values at 0.5 M KCl [38].

Table 3. The diffusion coefficient of cytochrome C in Dex-MA hydrogels (DS 7) with varying charge density in HEPES and HBS calculated using the early-time approximation of Ficks's second law (n = 3) Values between brackets represent the 95% confidence interval.

Charge density (µmol charged monomer/g hydrogel)	*D_m in HEPES x10^7 (cm^2/s)*	*D_m in HBS x10^7 (cm^2/s)*
350 MA	-	1.3 (0.8 – 2.0)
35 MA	-	1.0 (0.8 – 1.3)
0	1.2 (1.0 – 1.4)	1.4 (1.2 – 1.7)
35 DMAEMA	1.2 (1.0 – 1.4)	1.1 (1.0 – 1.3)
350 DMAEMA	0.8 (0.7 – 1.1)	1.3 (1.1 – 1.6)

Figure 4C and D show that the release of cytochrome C from all hydrogels investigated was linear with the square root of time. The intercept of the linear fit of the release curves (0.1 – 0.2) indicates there was a burst release of cytochrome C. Most likely, this is a result of inhibition of the polymerization by oxygen at outer layer of the hydrogels. The slope of the curves and therefore the diffusion coefficient (Table 3) is comparable to that observed for myoglobin, which is expected considering the similar size. D_o for cytochrome C is 1.30 x 10^{-6} cm^2/s [39], meaning that also in this case diffusion of the protein through the polymer matrix is 1 order of magnitude slower that the diffusion in H_2O. Figure 4C shows that at high charge density, the similarly

charged DMAEMA had a minor effect on the release rate of cytochrome C in HEPES. The slope of the fractional release curve was slightly lower for the release from gels containing 350 µmol DMAEMA/g compared to neutral and 35 µmol DMAEMA/g ($p < 0.001$ for each comparison). This indicates that the diffusion of cytochrome C in the hydrogel was hindered by the repulsive forces at high network charge density.

Strikingly, despite the overall charge on cytochrome C, there were no differences for the release rates from the different hydrogels in HBS ($p = 0.19$). Clearly, the ions in HBS effectively screen the polymer and protein charges, thereby breaking the electrostatic interaction between the hydrogel network and cytochrome C. This is in line with the assumption of Zhang and Amsden that at physiological strength the diffusivity of globular proteins is dominated by steric hindrance and that electrostatic interactions can be neglected [40].

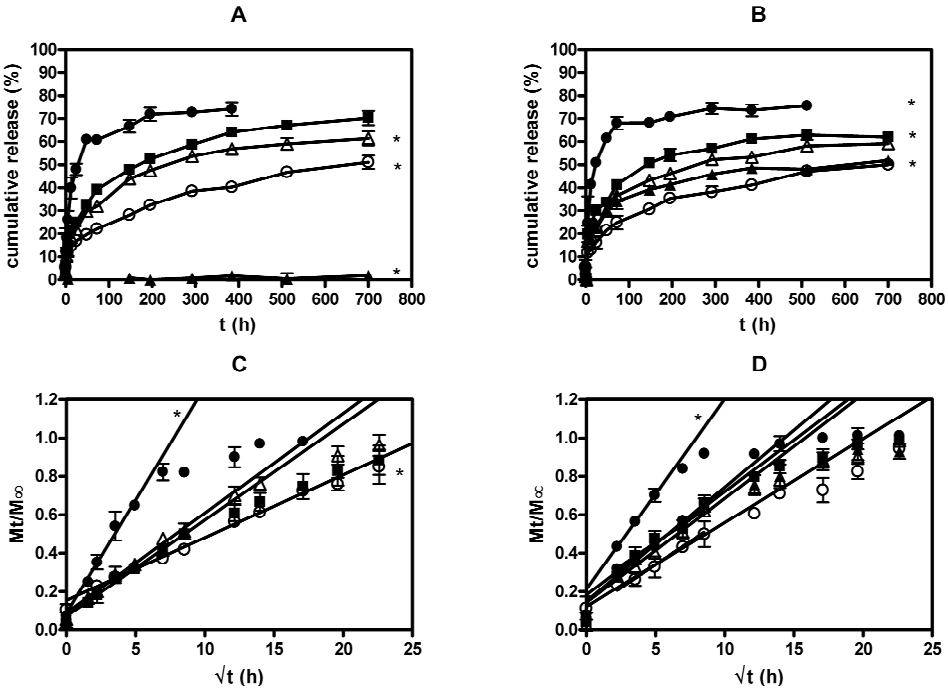

Figure 5. Cumulative release of BSA from Dex-MA hydrogels (DS 7) in hepes (A + C) and HBS (B + D). Values represent the average (n = 3, ± s.d.) released from neutral (squares), negatively charged (open circles = 35 µmol, closed circles = 350 µmol MA/g) and positively charged (open triangles = 35 µmol, closed triangles = 350 µmol DMAEMA/g) hydrogels. The symbol * indicates *p*-values < 0.05.

The release of BSA from neutral, positively and negatively charged dextran networks is shown in Figure 5. The release of BSA from neutral gels was significantly slower than observed for myoglobin and cytochrome C, which is caused by the higher molecular weight of BSA compared to myoglobin and cytochrome C. The calculated diffusion coefficients of BSA are shown in Table 4. As can be seen from the diffusion coefficient in a neutral gel obtained from Dex-MA with DS 7, the hydrogel network decreases the diffusion coefficient by 2 orders of magnitude when compared to the diffusion in H_2O (D_o = 5.90 x 10^{-7} cm^2/s [41]). As expected, decreasing the network density (using Dex-MA with a lower number of methacrylate units, i.e. DS 4) increased the diffusion coefficient (Table 4).

Table 4. The diffusion coefficient of BSA in Dex-MA hydrogels (DS 7 and 4) with varying charge density in HEPES and HBS calculated using the early-time approximation of Ficks's second law (n = 3) Values between brackets represent the 95% confidence interval.

	DS 7		*DS 4*	
Charge density (µmol charged monomer/g hydrogel)	*D_m in HEPES x10^9 (cm^2/s)*	*D_m in HBS x10^9 (cm^2/s)*	*D_m in HEPES x10^9 (cm^2/s)*	*D_m in HBS x10^9 (cm^2/s)*
350 MA	40 (23 – 61)	28 (14 – 46)	22 (19 – 25)	18 (17 – 20)
35 MA	3.1 (2.6 – 3.6)	5.5 (3.3 – 8.3)	10 (8.5 – 12)	11 (9.9 – 12)
0	7.2 (5.8 – 8.8)	8.3 (5.3 – 12)	16 (12 – 21)	15 (13 – 16)
35 DMAEMA	7.8 (6.2 – 9.6)	8.5 (6.9 – 10)	16 (15 – 17)	15 (14 – 16)
350 DMAEMA	-	10 (7.7 – 13)	-	13 (12 – 14)

Figure 5A shows that release of BSA from neutral gels was 70.3% ± 3.1. Co-polymerization of Dex-MA with DMAEMA decreased the total amount of BSA released in HEPES, depending on the input of charged monomer (59.2% ± 2.3 and 1.9% ± 1.6 for 35 and 350 µmol/g, respectively). It becomes clear from Figure 5B that the immobilization of BSA was counteracted in HBS (61.7% ± 1.5 for neutral and 59.2% ± 2.3 and 52% ± 1.7 for 35 and 350 µmol DMAEMA/g, respectively), as was observed with cytochrome C.

The effect of incorporation of MA on the release of negatively charged BSA was twofold. On the one hand, incorporation of 35 µmol MA/g gel surprisingly led to a decrease of the total amount of released BSA (51% ± 2.9, Figure 5A), and a significant decrease of the release rate in HEPES ($p < 0.05$), especially at relatively high network density (Table 4). On the other hand, at higher charge density (350 µmol MA/g gel) the total amount of released BSA was unaffected, while the release rate substantially increased when compared to the neutral gel. This effect was also most pronounced at relatively high network density ($p < 0.001$). The same effect was

observed in HBS (Figure 5B and 5D, Table 4). It is certain that the increased release rate from these gels is not caused by increased equilibrium swelling, since in HBS the equilibrium swelling was not dependent on the network charge density (Figure 2). The observed dualistic effect of the incorporation of MA can be explained by the quaternary structure of BSA and the relative amount of charged moieties in the hydrogel network. Despite the overall negative charge at pH 7.4, BSA has a positively charged surface domain [42]. Probably, during polymerization with a relatively low amount of MA (i.e. 35 µmol/g corresponds to 2.9 mol MA/mol BSA), preferred electrostatic interaction between MA and the positively charged domain of BSA occurred, leading to the formation of pockets in the hydrogel network complementary in charge and shape, a phenomenon often referred to as molecular imprinting [43-45]. Oriented binding of the asymmetric BSA to these pockets may account for the retention of BSA in the hydrogel at low charge density (35 µmol/g gel). At higher charge density however (350 µmol/g gel), the excess of negative charges distributed throughout the network (29 mol MA/mol BSA) renders orientation impossible, resulting in repulsion of the overall negatively charged BSA. The repulsive forces restrict the accessible space for BSA in the hydrogel network, thereby favoring the release from the hydrogel, leading to a higher release rate. In networks with a lower crosslink density (i.e. with DS 4), this effect was also observed, although less pronounced, because in those gels the protein already had a higher release rate (as illustrated by the higher diffusion coefficients in the neutral gels).

As opposed to BSA, the release of cytochrome C from similarly (positively) charged dextran networks was independent of the network charge (Figure 4). First, the surface charge distribution of cytochrome C is more homogenous than that of BSA, and no negatively charged domains are present in this protein [46], which explains the observation that cytochrome C is not retained in similarly charged gels with low charge density. Second, at higher similar charge density, no increase of release rate of cytochrome C when compared to neutral gels was observed. This second difference in behavior of cytochrome C and BSA can be explained by the fact that the diffusion of the considerably larger BSA is influenced by the hydrogel matrix to a much larger extent than the diffusion of cytochrome C. Therefore, it can be anticipated that charge of a relatively dense crosslinked network can have a larger effect on BSA then on cytochrome C. In other words, the effect of a similar network charge is not observed for cytochrome C because the diffusion of the small protein is not inhibited by density of the gel to a sufficiently large extent. This explanation is supported by the release of BSA from hydrogels

with a lower crosslink density (i.e. using Dex-MA of DS 4), where the effect of the similar charge is only just noticeable.

Based on the above results, we propose that incorporation of charged monomers in a hydrogel can be used for the triggered release of proteins. First, electrostatic interaction between a protein and an oppositely charged network can fully immobilize proteins in the hydrogel, while the release is triggered by a change of the ionic strength of the surrounding medium. It is anticipated that a change in pH leading to a change in protonation state of either protein or network could terminate the electrostatic interactions as well.

Conclusions

The results presented in this paper show that charged proteins are immobilized in oppositely charged dextran hydrogels by electrostatic interaction at low ionic strength. At higher ionic strength the amount of immobilized protein depends on the charge density of the hydrogel. The diffusion coefficient of the mobile fraction is determined by the network density and is unaffected by the opposite charge of the network. Therefore, we conclude that incorporation of charge in Dex-MA hydrogels can be used for immobilization and ionic strength triggered release of proteins.

Acknowledgement

This work was financially supported by the Innovational Research Incentives Scheme of the Netherlands Organization for Scientific Research (grant nr 700.53.422).

References

[1] S. Stolnik, K. Shakesheff, Formulations for delivery of therapeutic proteins, Biotechnol. Lett., 31 (2009) 1-11.

[2] G. Antonelli, Reflections on the immunogenicity of therapeutic proteins, Clin. Microbiol. Infect., 14 (2008) 731-733.

[3] A.S. De Groot, L. Moise, Prediction of immunogenicity for therapeutic proteins: state of the art, Curr. Opin. Drug Discov. Devel., 10 (2007) 332-340.

[4] S. Hermeling, D.J. Crommelin, H. Schellekens, W. Jiskoot, Structure-immunogenicity relationships of therapeutic proteins, Pharm. Res., 21 (2004) 897-903.

[5] H. Schellekens, Immunogenicity of therapeutic proteins, Nephrol. Dial. Transplant., 18 (2003) 1257-1259.

[6] H. Schellekens, The immunogenicity of therapeutic proteins and the Fabry antibody standardization initiative, Clin. Ther., 30 Suppl B (2008) S50-51.

[7] E.-M. Jahn, C.K. Schneider, How to systematically evaluate immunogenicity of therapeutic proteins - regulatory considerations, New Biotechnol., 25 (2009) 280-286.

[8] H. Schellekens, Assessing the bioequivalence of biosimilars The Retacrit case, Drug Discov. Today, 14 (2009) 495-499.

[9] F. Sorgel, Biosimilars / Follow-on proteins - a case for clinical pharmacology, Int. J. Clin. Pharmacol. Ther., 47 (2009) 365.

[10] R.G. Wenzel, Biosimilars: illustration of scientific issues in two examples, Am. J. Health Syst. Pharm., 65 (2008) S9-15.

[11] L. Zuniga, B. Calvo, Regulatory aspects of biosimilars in Europe, Trends Biotechnol., 27 (2009) 385-387.

[12] E.H. Moeller, L. Jorgensen, Alternative routes of administration for systemic delivery of protein pharmaceuticals, Drug Disc. Today: Techn., 5 (2008) e89-e94.

[13] Z. Antosova, M. Mackova, V. Kral, T. Macek, Therapeutic application of peptides and proteins: parenteral forever?, Trends Biotechnol., 27 (2009) 628-635.

[14] C. Hiemstra, Z.Y. Zhong, M.J. van Steenbergen, W.E. Hennink, F.J. Jan, Release of model proteins and basic fibroblast growth factor from in situ forming degradable dextran hydrogels, J. Control. Release, 122 (2007) 71-78.

[15] K.D.F. Vlugt-Wensink, T.J.H. Vlugt, W. Jiskoot, D.J.A. Crommelin, R. Verrijk, W.E. Hennink, Modeling the release of proteins from degrading crosslinked dextran microspheres using kinetic Monte Carlo simulations, J. Controlled Release, 111 (2006) 117-127.

[16] W.E. Hennink, S.J. De Jong, G.W. Bos, T.F.J. Veldhuis, C.F. van Nostrum, Biodegradable dextran hydrogels crosslinked by stereocomplex formation for the controlled release of pharmaceutical proteins, Int. J. Pharm., 277 (2004) 99-104.

[17] J.A. Cadee, C.J. de Groot, W. Jiskoot, W. den Otter, W.E. Hennink, Release of recombinant human interleukin-2 from dextran-based hydrogels, J. Control. Release, 78 (2002) 1-13.

[18] T. Meyvis, S. De Smedt, B. Stubbe, W. Hennink, J. Demeester, On the release of proteins from degrading dextran methacrylate hydrogels and the correlation with the rheologic properties of the hydrogels, Pharm. Res., 18 (2001) 1593-1599.

[19] J.A. Cadee, L.A. Brouwer, W. den Otter, W.E. Hennink, M.J.A. van Luyn, A comparative biocompatibility study of micropheres based on crosslinked dextran or poly(lactic-co-glycolic)acid after subcutaneous injection in rats, J. Biomed. Mater. Res., 56 (2001) 600-609.

[20] C.J. De Groot, M.J.A. Van Luyn, W.N.E. Van Dijk-Wolthuis, J.A. Cadee, J.A. Plantinga, W. Den Otter, W.E. Hennink, In vitro biocompatibility of biodegradable dextran-based hydrogels tested with human fibroblasts, Biomaterials, 22 (2001) 1197-1203.

[21] W.N.E. van Dijk-Wolthuis, J.A.M. Hoogeboom, M.J. van Steenbergen, S.K.Y. Tsang, W.E. Hennink, Degradation and release behavior of dextran-based hydrogels, Macromolecules, 30 (1997) 4639-4645.

[22] W.E. Hennink, H. Talsma, J.C.H. Borchert, S.C. DeSmedt, J. Demeester, Controlled release of proteins from dextran hydrogels, J. Control. Release, 39 (1996) 47-55.

[23] B. Amsden, Solute diffusion within hydrogels. Mechanisms and models, Macromolecules, 31 (1998) 8382-8395.
[24] H.L. Jiang, K.J. Zhu, Comparison of poly(aspartic acid) hydrogel and poly(aspartic acid)/gelatin complex for entrapment and pH-sensitive release of protein drugs, J. Appl. Polym. Sci, 99 (2006) 2320-2329.
[25] F. Gu, B. Amsden, R. Neufeld, Sustained delivery of vascular endothelial growth factor with alginate beads, J. Control. Release, 96 (2004) 463-472.
[26] S.M. Jay, W.M. Saltzman, Controlled delivery of VEGF via modulation of alginate microparticle ionic crosslinking, J. Control. Release, 134 (2009) 26-34.
[27] W.N.E. van Dijk-Wolthuis, O. Franssen, H. Talsma, M.J. van Steenbergen, J.J. Kettenes-van den Bosch, W.E. Hennink, Synthesis, characterization, and polymerization of glycidyl methacrylate derivatized dextran, Macromolecules, 28 (1995) 6317-6322.
[28] W.N.E. van Dijk-Wolthuis, J.J. Kettenes-van den Bosch, A. van der Kerk-van Hoof, W.E. Hennink, Reaction of dextran with glycidyl methacrylate: an unexpected transesterification, Macromolecules, 30 (1997) 3411-3413.
[29] P. Böhlen, S. Stein, W. Dairman, S. Udenfriend, Fluorometric assay of proteins in the nanogram range, Arch. Biochem. Biophys., 155 (1973) 213-220.
[30] S.R. Van Tomme, C.F. van Nostrum, M. Dijkstra, S.C. De Smedt, W.E. Hennink, Effect of particle size and charge on the network properties of microsphere-based hydrogels, Eur. J. Pharm. Biopharm., 70 (2008) 522-530.
[31] W.N. van Dijk-Wolthuis, M.J. van Steenbergen, W.J. Underberg, W.E. Hennink, Degradation kinetics of methacrylated dextrans in aqueous solution, J. Pharm. Sci., 86 (1997) 413-417.
[32] A.E. English, T. Tanaka, E.R. Edelman, Polyampholytic hydrogel swelling transitions: limitations of the Debye-Hückel law, Macromolecules, 31 (1998) 1989-1995.
[33] H.C. Chiu, A.T. Wu, Y.F. Lin, Synthesis and characterization of acrylic acid-containing dextran hydrogels, Polymer, 42 (2001) 1471-1479.
[34] H.-C. Chiu, Y.-F. Lin, S.-H. Hung, Equilibrium swelling of copolymerized acrylic acid-methacrylated dextran networks: effects of pH and neutral salt, Macromolecules, 35 (2002) 5235-5242.
[35] A. Valdebenito, P. Espinoza, E.A. Lissi, M.V. Encinas, Bovine serum albumin as chain transfer agent in the acrylamide polymerization. Protein-polymer conjugates, Polymer, 51 (2010) 2503-2507.
[36] P.L. Ritger, N.A. Peppas, A simple equation for description of solute release. II: Fickian and anomalous release from swellable devices, J. Control. Release, 5 (1987) 37-42.
[37] V. Riveros-Moreno, J.B. Wittenberg, The self-diffusion coefficients of myoglobin and hemoglobin in concentrated solutions, J. Biol. Chem., 247 (1972) 895-901.
[38] N. Hirota, Y. Kumaki, T. Narita, J.P. Gong, Y. Osada, Effect of charge on protein diffusion in hydrogels, J. Phys. Chem. B, 104 (2000) 9898-9903.
[39] S.M. Atlas, E. Farber, On the molecular weight of cytochrome c from mammalian heart muscle, J. Biol. Chem., 219 (1956) 31-37.
[40] Y. Zhang, B.G. Amsden, Application of an obstruction-scaling model to diffusion of vitamin B-12 and proteins in semidilute alginate solutions, Macromolecules, 39 (2006) 1073-1078.
[41] E.W. Merrill, K.A. Dennison, C. Sung, Partitioning and diffusion of solutes in hydrogels of poly(ethylene oxide), Biomaterials, 14 (1993) 1117-1126.
[42] E. Seyrek, P.L. Dubin, C. Tribet, E.A. Gamble, Ionic strength dependence of protein-polyelectrolyte interactions, Biomacromolecules, 4 (2003) 273-282.
[43] G. Wulff, D. Oberkobusch, M. Minarik, Enzyme-analogue built polymers, 18 chiral cavities in polymer layers coated on wide-pore silica, React Polym, Ion Exch, Sorbents, 3 (1985) 261-275.
[44] L. Ye, K. Mosbach, The Technique of Molecular Imprinting – Principle, State of the Art, and Future Aspects, J Inclusion Phen Macrocycl Chem, 41 (2001) 107-113.
[45] C. Alexander, H.S. Andersson, L.I. Andersson, R.J. Ansell, N. Kirsch, J. O'Mahony, M.J. Whitcombe, Molecular imprinting science and technology: a survey of the litterature for the years up to and including 2003, J Mol Recognit, 19 (2006) 106-180.
[46] D. Asthagiri, A.M. Lenhoff, Influence of structural details in modeling electrostatically driven protein adsorption, Langmuir, 13 (1997) 6761-6768.

Chapter 6

Anionic and cationic dextran hydrogels for post-loading and release of proteins

Joris P. Schillemans

Ellen Verheyen

Arjan Barendregt

Wim E. Hennink

Cornelus F. van Nostrum

Submitted for publication

Abstract

In this study, post-loading of proteins in and release from chemically crosslinked dextran hydrogels exploiting reversible electrostatic interactions was investigated. Methacrylated dextran (Dex-MA) was co-polymerized with methacrylic acid (MA) or dimethylaminoethyl methacrylate (DMAEMA) to form negatively and positively charged hydrogels, respectively. Incubation of negatively charged hydrogels in a low ionic strength (10 mM HEPES, pH 7.4) solution of cytochrome C (isoelectric point (*pI*) 10.2) led to quantitative absorption of the protein in the hydrogel. BSA (*pI* 4.8) and myoglobin (*pI* 7.2) were post-loaded in positively charged gels at neutral pH and negatively charged gels at pH 5, respectively. Loading efficiency and protein distribution in the gels were dependent on network charge (maximum loading efficiency at 100 – 150 µmol charged monomer/g gel) and crosslink density (higher and more homogenous loading at lower crosslink density) and on the ionic strength during loading (lower but more homogenous loading at higher ionic strength). Diffusion controlled release of the loaded protein was triggered by incubation of the hydrogel in HEPES buffered saline (HBS) pH 7.4. The amount of released cytochrome C in HBS varied from 94% to 70% from gels containing 60 and 150 MA/g, respectively. Importantly, quantitative release was obtained in 1 M NaCl, indicating that post-loading led to neither the formation of insoluble protein aggregates nor irreversible immobilization of the protein in the matrix. ESI-MS analysis of the released cytochrome C revealed that post-loading did not result in oxidation of the protein, as opposed to loading during preparation of the gels.

In conclusion, this paper shows that post-loading of proteins in dextran hydrogels and release exploiting reversible charge interactions can be applied for efficient loading of proteins that are negative, positive or neutral at physiological pH. Importantly, our data demonstrate that using this loading method no chemical modification to the protein occurred.

Introduction

Hydrogels are promising systems for controlled release of pharmaceutically active peptides and proteins, mainly because of their good tissue compatibility and possibilities to tailor the release of solutes [1-4]. Hydrogels consist of hydrophilic polymer networks held together by chemical or physical crosslinks. Chemical crosslinking technologies provide excellent control over the crosslink density and generally lead to mechanically strong hydrogels [4, 5]. A drawback of chemical crosslinking is that when pharmaceuticals are loaded in the hydrogel during hydrogel formation (i.e. conventional loading), exposure to crosslinking agents frequently causes unwanted chemical modification and/or grafting of the therapeutic to the network [2, 6, 7]. Physically crosslinked hydrogels are held together by non-covalent bonds, such as hydrophobic interactions [8, 9], stereocomplex formation [10, 11] or ionic interactions [12] and therefore do not suffer from this drawback. However, generally speaking, due to the non-covalent nature of the crosslinks these systems are mechanically less stable and more complicated in terms of predicting and controlling of release profiles [2].

Unwanted chemical modification of the protein pharmaceutical can be prevented by loading after the hydrogel has been synthesized, i.e. by so-called post-loading. A common post-loading technique is the solvent sorption method, where a dehydrated hydrogel is soaked in a protein solution [2, 3]. The hydrogel then swells by influx of solvent and the protein is loaded along with it. In order to increase protein loading and prevent size exclusion, some recent papers describe post-loading of hydrogels of which the degree of swelling can be controlled by temperature [13-15]. Using a chemically crosslinked thermosensitive hydrogel, a protein is loaded by soaking the hydrogel in a protein solution at a temperature below the lower critical solution temperature (LCST) to give a highly swollen hydrogel. The gels are then taken out from the soaking solution, dried and rehydrated at a temperature above the phase transition, i.e. in the collapsed state. Release then takes place by degradation of the network. The drawback of this method is the low loading efficiency. For example, although Zhang *et al.* reported a relatively high maximum loading of 97 mg BSA/g dry gel [14], this translated into a loading efficiency of maximally 5%. Another more efficient post-loading method was introduced by Gehrke *et al.* [16, 17]. In their approach, proteins were loaded in a dextran hydrogel by preferential partitioning in the aqueous dextran-rich phase in the presence of an external aqueous PEG/salt phase. This way, high partitioning coefficients (concentration in gel/concentration in loading solution) of 4 and 7 were obtained for ovalbumin and α-amylase, respectively. However, a major drawback of this method

is that when the PEG phase is removed, the driving force for protein partitioning in the hydrogels disappears, and washing of the hydrogels, particularly in the form of micro and nanogels, leads to fast extraction of the protein out of the gel.

In a previous paper [18] we reported that conventionally loaded charged proteins can be fully immobilized in oppositely charged hydrogels at low ionic strength and released at physiological ionic strength. We now exploited this phenomenon of reversible electrostatic interactions for post-loading with high efficiency and controlled release of proteins. Chemically crosslinked dextran hydrogels prepared from methacrylated dextran (Dex-MA) were used. These hydrogels are non-degradable under physiological conditions, which ensured that hydrogel degradation did not contribute to protein release. Charge was introduced to the hydrogels by co-polymerization of Dex-MA with either methacrylic acid (MA) or *N, N,*-dimethyl aminoethyl methacrylate (DMAEMA). For post-loading to be successful, the solutes need to be able to diffuse into the hydrogel, and therefore the size of solutes needs to be smaller than the mesh size of the network. The mesh size of a hydrogel in the swollen state is determined by the average distance between two adjacent crosslinks and the polymer volume fraction at equilibrium swelling [19]. Therefore, we used a solid content and crosslink density of the hydrogels that allowed free diffusion of several model proteins (cytochrome C, myoglobin and bovine serum albumin (BSA)) in the hydrogel matrix [18, 20].

Materials and methods

Materials

Dextran T40 (from *Leuconostoc spp.*), *N,N,N',N'*-tetramethylethylenediamine (TEMED), ammonium peroxodisulfate (APS) and 2-hydroxethyl methacrylate (HEMA) were obtained from Fluka (Buchs, Switzerland). Methacrylic acid (MA), 2-*N,N*-dimethylaminoethyl methacrylate (DMAEMA), bovine serum albumin (BSA), cytochrome C from bovine heart, and myoglobin from horse heart were purchased from Sigma-Aldrich (Zwijndrecht, the Netherlands). Methacrylated dextran (Dex-MA) with a degree of substitution (DS) of 7 was synthesized according to Van Dijk-Wolthuis *et al.* [21, 22].

Preparation of Dex-MA hydrogels

Charged Dex-MA hydrogels with an initial Dex-MA content of 15% (w/w) and different charge densities were prepared by co-polymerization of Dex-MA with varying amounts of MA or DMAEMA. The network density was either kept constant by supplementing with HEMA to a constant total amount of added methacrylate monomers, or varied by supplementing with different amounts of HEMA at constant MA content. Solutions of MA, DMAEMA, HEMA, APS and TEMED, respectively, were prepared in 10 mM HEPES and the pH was adjusted to 7.4 using HCl or NaOH. Dex-MA (0.15 g/g total weight), varying amounts of additional monomers (MA, DMAEMA, HEMA) and TEMED (67 µmol/g gel) were mixed in the appropriate buffer (HEPES/HBS). For conventionally loaded hydrogels, 10µL of a protein stock solution (100 mg/mL) was added (8 mg protein per g gel). APS (17 µmol/g gel) was added, and the mixture (final weight 125 mg) was transferred to a 1 mL syringe. Polymerization was carried out under nitrogen atmosphere at room temperature for at least 2 h.

Protein post-loading and release

Cylindrical hydrogels (h = 7.5 mm, r = 2.3 mm) were incubated in 3 mL protein solution (1 mg/mL) of low ionic strength (10 mM HEPES pH 7.4, or 10 mM MES pH 5) at 37°C under gentle rotation. When appropriate, the ionic strength of the loading solution was adjusted by the addition of NaCl. At different time points the amount of protein loaded in the hydrogel was determined by measuring the protein concentration in the loading solution, using a fluorometric fluorescamine assay as described by Böhlen *et al.* [23], adapted to a 96-well plate format. Gels were blotted with a tissue to remove excess of loading solution and transferred to vials containing 3 mL of HEPES buffered saline (HBS, 10 mM HEPES, 150 mM NaCl). The vials were gently rotated at 37°C. The release of protein was followed by periodically taking samples (20 µL) and measuring the protein concentration using fluorescamine. The volume of the release medium was kept constant by replacing the removed amount with HBS.

Mass Spectrometry

Buffer exchange of cytochrome C samples (0.5 mg/mL) to 150 mM ammonium acetate pH 6.8, was performed using ultrafiltration units with a cut-off of 5000 Da (Millipore, Bedford, UK), followed by 10-fold dilution in 50/50 v/v acetonitrile/Milliq + 0.1% formic acid.

MS measurements were performed at room temperature in positive ion mode using an electrospray ionisation time-of-flight (ESI-ToF) instrument (LC-T; Micromass, Manchester, UK)

equipped with a Z-spray nano-electrospray ionisation source. Needles were made from borosilicate glass capillaries (Kwik-Fil, World Precision Instruments, Sarasota, FL) on a P-97 puller (Sutter Instruments, Novato, CA), coated with a thin gold layer by using an Edwards Scancoat (Edwards Laboratories, Milpitas, CA) six Pirani 501 sputter coater. The ions were cooled by increasing the pressure in the first vacuum stages of the mass spectrometer to 7.0-7.3 mbar, and nano-electrospray voltages were optimized for transmission of proteins. The pressure in the interface region was adjusted by reducing the pumping capacity of the rotary pump by closing the speed-valve. The applied voltage on the needle was 1200 V and the sample cone voltage 120V. All spectra were mass calibrated using an aqueous solution of cesium iodide (25 mg/mL).

Results and discussion

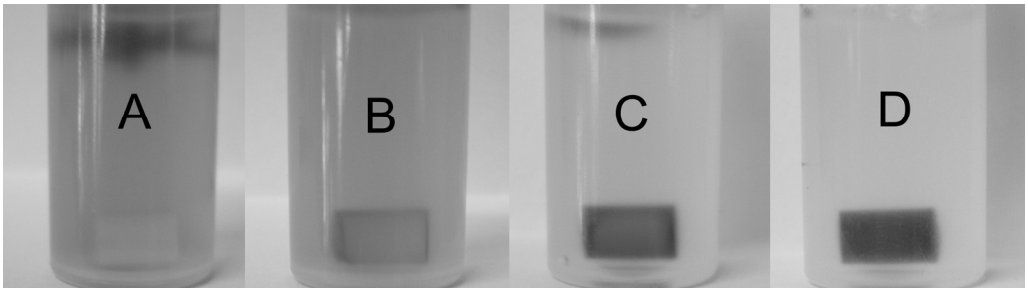

Figure 1. Post-loading of cytochrome C in a negatively charged Dex-MA hydrogel (containing 90 µmol MA/g gel) by incubation in a cytochrome C solution after 0 h (A), 4 h (B), 12 h (C) and 48 h (D) at 37°C.

Post-loading of cytochrome C in negatively charged Dex-MA hydrogels

Negatively charged Dex-MA hydrogels with equal network densities were prepared by copolymerization of Dex-MA with methacrylic acid and HEMA at different feed ratios. The gels were incubated in a cytochrome C solution at 37°C. The isoelectric point of Cytochrome C is 10.2, and therefore it has an overall positive charge at neutral pH. The color of cytochrome C enabled visualization of the loading in the gels, as is shown in Figure 1. At t = 0 cytochrome C resided in the loading solution, visible by the clear red color, and the hydrogel was hardly visible at the bottom of the vial (Figure 1A). After 4 h incubation the hydrogel had taken up some cytochrome C, making it easier to distinguish (Figure 1B). After 24 h the solution was almost colorless, while the hydrogel was dark red (Figure 1C). After 48 h the solution was colorless, and

the hydrogel had become more homogenously colored (Figure 1D). The cytochrome C concentration measured in the supernatant showed that equilibrium was reached within 48 h for all hydrogels.

Figure 2 shows cross-sectional slices of the hydrogels with different charge densities after 72 h of loading. These slices show that cytochrome C was absorbed by the hydrogel rather than adsorbed onto the surface, demonstrating that the pores in the gels are bigger than the size of the loaded protein. Additionally, Figure 2 shows that the penetration of cytochrome C into the hydrogel was dependent on the charge density of the hydrogel. Up to a charge density of 60 µmol MA/g hydrogel, cytochrome C was distributed evenly in the hydrogel. Starting from 90 µmol MA/g hydrogel however, a heterogeneous distribution was observed, with the rim of the hydrogel colored more intensely than the core. At 350 µmol MA/g hydrogel the core of the hydrogel is completely colorless. The distribution of cytochrome C did not change upon incubation of these slices in 10 mM HEPES for 10 days, which demonstrated that equilibrium was obtained. Probably the increasing charge density immobilized the protein more efficiently thereby limiting the diffusion distance.

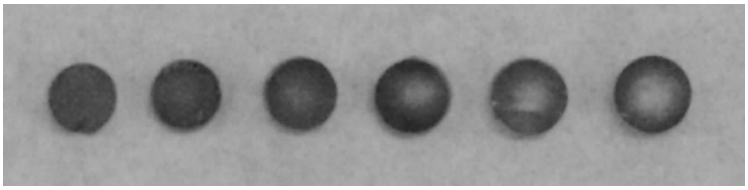

Figure 2. The effect of network charge density on the loading homogeneity of cytochrome C in preformed negatively charged Dex-MA hydrogels. Cross-sectional images show cytochrome C distribution in hydrogel cylinders with charge density of 30, 60, 90, 120, 150 and 350 µmol MA/g hydrogel, respectively. The total amount of added methacrylic monomers was kept constant by addition of HEMA up to 350 µmol/g hydrogel.

Figure 3 shows the effect of varying the charge density of the hydrogel on the cytochrome C loading efficiency. It is evident from Figure 3 that almost quantitative loading was obtained at an optimal charge density of approximately 60 to 90 µmol MA/g gel (loading of 3 mg cytochrome C in a gel of approximately 125 µL). The loading efficiency initially increased linearly with increasing charge density, ranging from < 10% for 0 µmol MA/g gel to ~99% for 60 and 90 µmol MA/g gel. Up to 30 µmol MA/g gel, the molar ratio between positive amino acids in the loaded cytochrome C (22 per molecule including the N-terminal) and MA input was constant (i.e. 0.81 ± 0.08), suggesting very efficient interaction between MA and protein in the hydrogel.

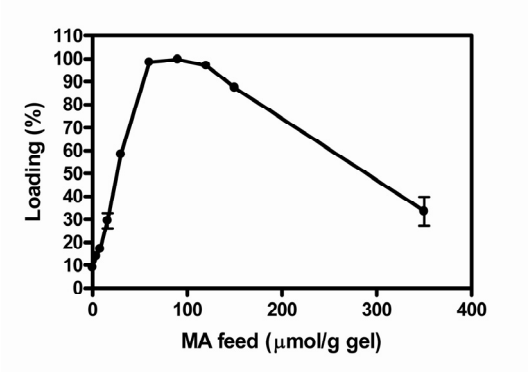

Figure 3. Post-loading efficiency of cytochrome C (3 mg), as a function of hydrogel charge density (μmol MA/g hydrogel, total hydrogel weight 125 mg). The total amount of added methacrylic monomers was kept constant by addition of HEMA up to 350 μmol/g hydrogel (n = 3, error bars represent standard deviation).

At 60 and 90 μmol MA/g gel, the charge ratio decreased (0.59 ± 0.01 and 0.42 ± 0.01, respectively). Considering the loading was almost 100%, this could mean that the amount of offered protein (3 mg) was the limiting factor. At higher charge densities the loading efficiency decreased to 33% for gels containing 350 μmol MA/g, which is likely due to sterical hindrance. To explain; diffusion of cytochrome C into the hydrogel takes place in the hydrogel pores. Strong electrostatic interactions at high charge density led to a high degree of cytochrome C immobilization in the rim of the hydrogel (Figure 2), which apparently limited the available free space for diffusion, thus preventing the loading of additional cytochrome C. This is probably a result of the size of the protein in relation to the mesh size of the hydrogel. It was shown for dextran hydrogels with DS 9 that the mesh size is approximately 11 nm at a polymer volume fraction ($\nu_{2,s}$) of 0.20, and 7 nm at $\nu_{2,s}$ = 0.23 [20]. Based on these data, the mesh size of the post-loaded hydrogels (DS 7, $\nu_{2,s}$ ~ 0.15) should be large enough for diffusion of cytochrome C (~4 nm). However, it is very likely that immobilization of only 1 or 2 cytochrome C molecules in a hydrogel pore reduces the free space below what is needed for additional cytochrome C to diffuse into the network. As a result, strong interaction between network and cytochrome C prevents deep penetration of cytochrome C into the hydrogel.

Figure 4 shows the cytochrome C loading efficiency of negatively charged hydrogels with constant charge density (100 μmol MA/g gel) and decreasing crosslink densities, obtained by varying the amount of HEMA (0 – 200 μmol/g gel, Fig 4A), and the effect of the ionic strength of the loading medium (Fig 4C). Corresponding cross sectional cytochrome C distributions in these gels are shown in Figure 4B and 4D. With decreasing crosslink density (i.e. increasing

amount of HEMA), the loading efficiency and the thickness of the colored rim increased (Fig 4A and B, respectively). Also, increasing the ionic strength of the loading medium led to a more homogeneous distribution (Fig 4D) and a decreasing loading efficiency (Fig 4C). The observed effects of HEMA content and the ionic strength on loading efficiency are in line with the hypothesized sterical hindrance pointed out above. First, an increase of HEMA content widened the polymer network (which was confirmed by increased hydrogel equilibrium swelling, see supporting information, Figure S1), leading to more homogeneous loading. Second, an increase of the ionic strength of the loading buffer decreased the electrostatic interactions between cytochrome C and the network. As a result, cytochrome C was immobilized in the network less densely, which on the one hand decreased the total amount loaded in the hydrogel, but on the other hand also led to less sterical hindrance and to a more homogeneous loading.

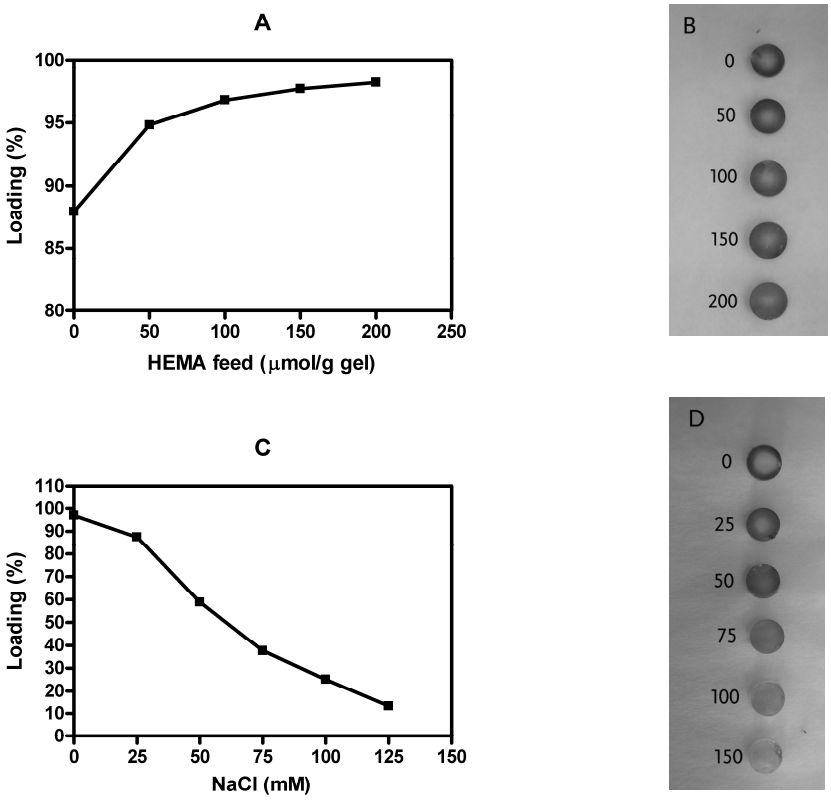

Figure 4. Loading efficiency and distribution homogeneity of Cytochrome C after 5 days of post–loading in negatively charged Dex-MA hydrogels (100 μmol MA/g) as a function of HEMA content (A and B), and ionic strength during loading (C and D).

Release of cytochrome C from post-loaded hydrogels

Figure 5A shows the cumulative release of cytochrome C from post-loaded hydrogels containing 90 and 350 µmol MA/g in HBS at pH 7.4 and at 37°C. It becomes clear that cytochrome C is released in HBS in time dependent manner, reaching a plateau after 24 h at approximately 75% and 55% of loaded amount for 90 and 350 µmol MA/g, respectively. According to the early-time approximation equation of Fick's second law, diffusion controlled release from a cylinder is linear with the square root of time [24]:

$$\frac{M_t}{M_\infty} = 4\sqrt{\frac{D_m t}{\pi r^2}} \qquad (1)$$

where M_t/M_∞ represents the fractional release of the entrapped solute, D_m is the diffusion coefficient of the solute in the matrix, t is the release time and r is the radius of the hydrogel cylinder. It has to be noted that this equation is applicable and can be used to calculate D_m only when the solute is distributed homogenously in the cylinder. Additionally, the dimensions of the cylinder should ideally be such that release through radial diffusion is negligible. For the gels used in this study, the top and bottom plane together make up 23% of the total surface area. Although the D_m calculated using equation 1 is therefore an overestimation, this does not pose a problem since it is used only to compare the diffusion in hydrogels with the same dimensions.

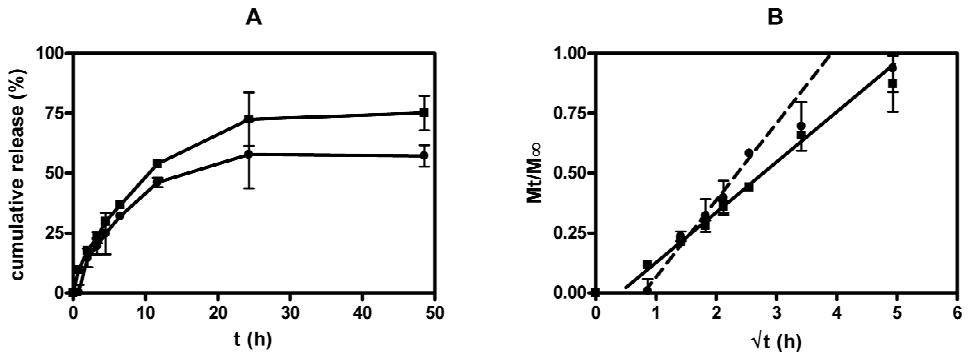

Figure 5. Cumulative release vs. time (A) and fractional release vs. the square root of time (B) of cytochrome C from post-loaded negatively charged hydrogels upon incubation in HBS. Circles: 350 µmol MA/g, squares: 90 µmol MA/g hydrogel (n=3, error bars represent standard deviation). The line in 5B represents the linear fit of the points up to a fractional release of ~0.6.

As shown in Figure 5B the fractional release is linear with the square root of time up to at least 0.6, confirming diffusion controlled release. The intercept of the linear fit with the x-axis shows

that the release has a short lag time of 15 and 35 minutes for 60 and 150 µmol MA/g, respectively, which is attributed to the time needed for the ions (Na^+ and Cl^-) to diffuse into the hydrogel and interfere with the protein/network interactions. The release from gels with 350 µmol MA/g was faster than that from gels containing 90 µmol MA/g. This is attributed to the difference in distribution of the loaded cytochrome C. Since cytochrome was predominantly located in the outer rim of the hydrogel containing 350 µmol MA/g, the diffusional path length was shorter than for the cytochrome in a hydrogel with more homogeneous loading. Assuming homogeneous distribution in the hydrogel containing 90 µmol MA/g, D_m equals 1.3 x 10^{-7} cm^2/s, which is in good agreement with the D_m reported earlier for cytochrome C released from conventionally loaded, MA-containing dextran hydrogels with the same DS and initial water content [18].

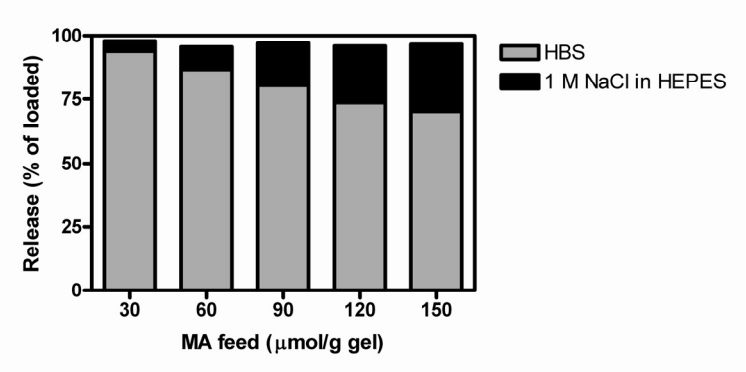

Figure 6. Cumulative release of cytochrome C from post-loaded negatively charged Dex-MA hydrogels with varying charge density after 72 h in HBS, followed by 72 h in and 1 M NaCl (n = 3).

Figure 6 shows the effect of hydrogel charge density on the amount of cytochrome C released from post-loaded negatively charged hydrogels. Release was determined after 72 h in HBS, followed by 72 h of incubation in 10 mM HEPES, pH 7.4 containing 1 M NaCl. For gels with 30 µmol MA/g, 94% of the loaded cytochrome C was released in HBS. Transfer of the hydrogels to 1 M NaCl triggered the release of additional cytochrome C up to 98% of the loaded amount. Increasing the charge density of the gel led to a decrease of the amount of released protein in HBS to 70% for hydrogels with 150 µmol MA/g. Apparently, at increasing charge density more protein molecules are bound to the network so strongly that they remain immobilized at physiological salt concentrations. When the ionic strength was increased (1M NaCl) over 97 % of the loaded cytochrome C was released from all hydrogels. These data show that release of post-loaded cytochrome C is triggered by the ionic strength that counteracts the electrostatic

interaction between cytochrome C and the hydrogel network. More importantly, although quantitative release is not obtained at physiological ionic strength, our data show that the residual protein is neither present in the form of insoluble protein aggregates nor irreversibly immobilized in the polymer network and is still available for release. Therefore it is anticipated that when a degradable hydrogel system is used, for example based on Dex-HEMA [25], quantitative release of post-loaded cytochrome C can be obtained. Because A) the formation of insoluble protein aggregates might be the reason for non-complete release of protein from other controlled release formulations [26] and B) it has been shown that these aggregates are a major cause of immunogenicity of therapeutic proteins [27, 28], quantitative release from post loaded gel presents a major advantage with great importance for clinical application.

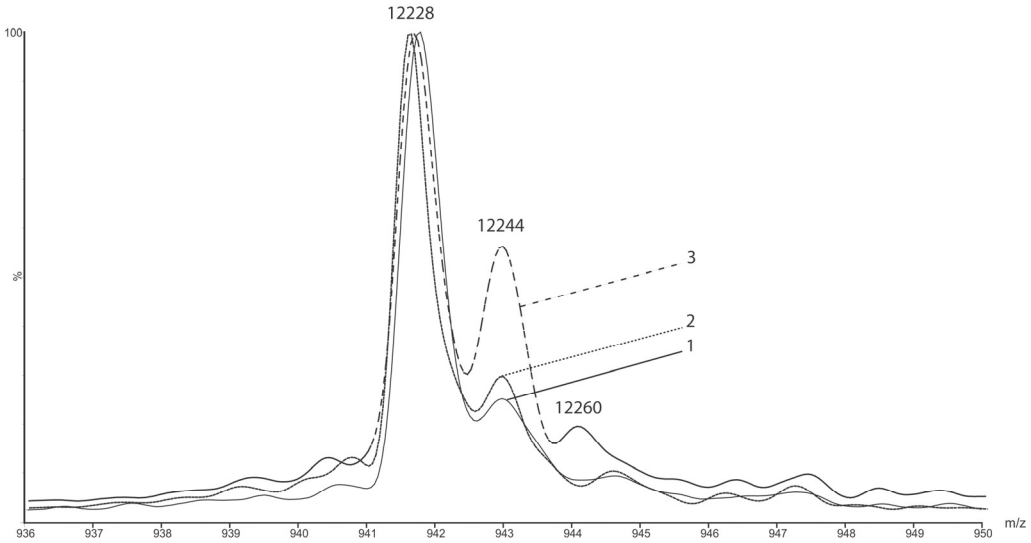

Figure 7. Zoom in (13+ charge state) of ESI-MS spectra of reference cytochrome C (1) and cytochrome C released from post-loaded (2) and conventionally loaded (3) hydrogels. The mass corresponding to the peaks was calculated with Masslynx by determining the mass between sequential m/z-peaks.

Figure 7 shows the ESI-MS spectra of cytochrome C released from hydrogels, both post-loaded and conventionally loaded, and a reference spectrum of native cytochrome C. The reference spectrum showed a main peak corresponding to a mass of 12228 Da. A small peak at a mass of 12244 Da (= M + 16) was also detected, which corresponds to cytochrome C with one oxidized amino acid. Cytochrome C contains 3 methionine residues [29], which is the amino acid most sensitive to oxidation [7, 30]. The spectrum of cytochrome C released from a conventionally

loaded hydrogel (i.e. where the protein was exposed to free radicals during hydrogel formation), the relative intensity of the peak at 12244 Da became considerably larger. Additionally, another peak with a mass of 12260 (= M + 32) appeared, indicating the oxidation of a second methionine. Evidently, significant protein oxidation occurred during the preparation of conventionally loaded hydrogels. This is due to exposure to peroxodisulfate, as was shown earlier for interleukin 2 [7]. Importantly, the mass spectrum of cytochrome C released from a post-loaded gel matched the reference spectrum demonstrating that oxidation of cytochrome C did not occur. These findings show that post-loading is superior to conventional loading with respect to protein integrity.

Post-loading and release of myoglobin and BSA

Myoglobin has a *pI* of 7.2 and is therefore neutral at physiological pH. At pH 7, we could not observe binding of myoglobin in negatively charged gels (see supporting information). Therefore, this protein was post-loaded in negatively charged hydrogels by incubation of the hydrogels in myoglobin solution at pH 5. BSA is negatively charged at physiological pH (*pI* = 4.8) and therefore this protein was post-loaded in positively charged dextran hydrogels (containing various amounts of DMAEMA) by incubation of the hydrogels in BSA solution at pH 7.4.

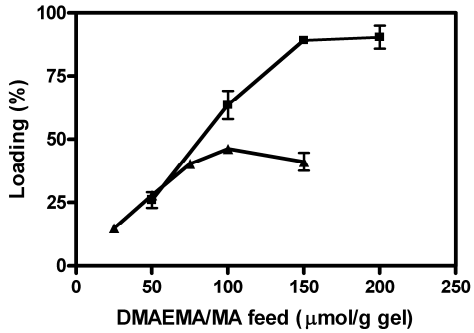

Figure 8. Post-loading efficiency as a function of charged monomer input after 6 days of incubation of 3 mg protein with 125 mg gel (n=3, error bars represent standard deviation). Squares: BSA with positively charged hydrogels (in 10 mM HEPES pH 7.4, co-monomer DMAEMA and HEMA up to 200 μmol/g gel); triangles: myoglobin with negatively charged hydrogels (in 10 mM MES pH 5, co-monomer MA and HEMA up to 150 μmol/g gel).

Figure 8 shows that the loading efficiency of both proteins increased with increasing charge density, reaching 90% for BSA and 48% for myoglobin. For myoglobin, optimum loading efficiency was observed at a charge density of 100 μmol MA/g gel. Up to this charge density, the

ratio between positively charged amino acids in the loaded protein and MA in the network was constant (0.17 ± 0.02). This ratio is lower than what we observed for cytochrome C, suggesting that the interaction between the positively charged residues in myoglobin and the MA moieties in the network is less strong than for cytochrome C. This is probably due to the surface distribution of the positive charges (22 positive charges for both proteins [29, 31]) and the difference in number of negatively charged amino acids in both proteins, i.e. 13 for cytochrome C vs. 22 for myoglobin. For BSA, gels with > 150 µmol DMAEMA/g showed a plateau in loading efficiency rather than an optimum (as observed for cytochrome C and myoglobin), suggesting that saturation of the gel did not occur in the concentration range investigated (3 mg /125 mg gel).

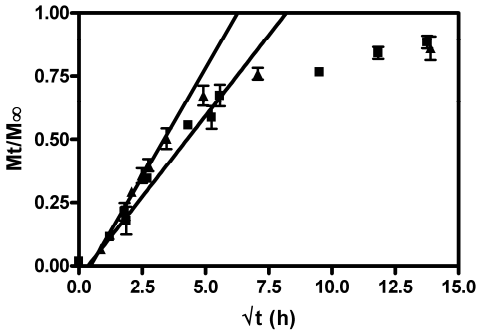

Figure 9. Fractional release of BSA (squares) and myoglobin (triangles) from post-loaded positively charged (150 µmol DMAEMA/g) and negatively charged (100 µmol MA/g) hydrogels, respectively, upon incubation in HBS (n = 3, error bars represent standard deviation).

Upon transfer to HBS pH 7.4, the release of both BSA and myoglobin reached up to 70% of the loaded amount (data not shown). The amount released and release kinetics of BSA and myoglobin from post-loaded hydrogels were independent of charge density. Fractional release curves are shown in Figure 9. Using equation 1, the calculated D_m of myoglobin was 8.5 x 10^{-8} cm^2/s, which is comparable to the D_m reported for myoglobin released from conventionally loaded hydrogels of similar composition [18], suggesting homogeneous distribution of the protein in the gel. Strikingly, Figure 9 shows that the release rate of BSA is similar to that of myoglobin. This is in contrast with earlier observations for the release from conventionally loaded positively charged Dex-MA hydrogels with the same crosslink density and initial water content, where the diffusion coefficient of BSA was found to be 1 order of magnitude lower than that of myoglobin [18]. This could be due to the heterogeneous distribution of BSA in the post-

loaded gel. Indeed, fluorescence images of FITC-labeled BSA showed that the protein was not loaded homogeneously, but mostly located at the surface of the hydrogel (supporting information, Figure S3). As pointed out for cytochrome C, this is probably caused by sterical hindrance as a result of strong electrostatic interaction and immobilization of BSA in the hydrogel pores. Because BSA is bigger than cytochrome C (~7 nm and ~4 nm, respectively) the effect is even more pronounced. As expected, loading at higher ionic strength improved the distribution of the loaded BSA (Figure S3B).

Overall, our results show that by adjusting the gel charge (and pH in the case of myoglobin), post-loading in dextran hydrogels based on charge interactions can be applied for proteins ranging from low to high *pI,* including proteins that have no overall charge at physiological pH.

Conclusions

This paper shows that proteins can be efficiently post-loaded in chemically crosslinked dextran hydrogels exploiting charge interactions at low ionic strength. Loading efficiency and protein distribution in the gel can be tailored by adjusting the gel composition and loading conditions (ionic strength, pH). The method can be applied for loading of proteins that are negative, positive or neutral at physiological pH. Diffusion controlled release of the post-loaded protein is triggered by incubation in a medium of physiological ionic strength. Importantly, it was shown that the post-loaded protein can be released quantitatively, indicating that neither the formation of insoluble protein aggregates nor irreversible immobilization of the protein in the matrix occurred. ESI-MS spectra showed that no additional oxidation occurred to the cytochrome C, confirming that post-loading is more protein-friendly than conventional loading.

Acknowledgement

This work was financially supported by the Innovational Research Incentives Scheme of the Netherlands Organization for Scientific Research (grant nr 700.53.422).

References

[1] N.A. Peppas, Y. Huang, M. Torres-Lugo, J.H. Ward, J. Zhang, Physicochemical, foundations and structural design of hydrogels in medicine and biology, Annu. Rev. Biomed. Eng., 2 (2000) 9-29.

[2] C.-C. Lin, A.T. Metters, Hydrogels in controlled release formulations: Network design and mathematical modeling, Adv. Drug Del. Rev., 58 (2006) 1379-1408.

[3] S.W. Kim, Y.H. Bae, T. Okano, Hydrogels - swelling, drug loading, and release, Pharm. Res., 9 (1992) 283-290.

[4] A.S. Hoffman, Hydrogels for biomedical applications, Adv. Drug Del. Rev., 54 (2002) 3-12.

[5] W.E. Hennink, C.F. van Nostrum, Novel crosslinking methods to design hydrogels, Adv. Drug Del. Rev., 54 (2002) 13-36.

[6] A. Valdebenito, P. Espinoza, E.A. Lissi, M.V. Encinas, Bovine serum albumin as chain transfer agent in the acrylamide polymerization. Protein-polymer conjugates, Polymer, 51 (2010) 2503-2507.

[7] J.A. Cadee, M.J. van Steenbergen, C. Versluis, A.J.R. Heck, W.J.M. Underberg, W. den Otter, W. Jiskoot, W.E. Hennink, Oxidation of recombinant human interleukin-2 by potassium peroxodisulfate, Pharm. Res., 18 (2001) 1461-1467.

[8] B. Jeong, Y.H. Bae, D.S. Lee, S.W. Kim, Biodegradable block copolymers as injectable drug-delivery systems, Nature, 388 (1997) 860-862.

[9] T. Vermonden, N.A.M. Besseling, M.J. van Steenbergen, W.E. Hennink, Rheological studies of thermosensitive triblock copolymer hydrogels, Langmuir, 22 (2006) 10180-10184.

[10] S.J. de Jong, S.C. De Smedt, M.W.C. Wahls, J. Demeester, J.J. Kettenes-van den Bosch, W.E. Hennink, Novel self-assembled hydrogels by stereocomplex formation in aqueous solution of enantiomeric lactic acid oligomers grafted to dextran, Macromolecules, 33 (2000) 3680-3686.

[11] C. Hiemstra, Z.Y. Zhong, L.B. Li, P.J. Dijkstra, J. Feijen, In-situ formation of biodegradable hydrogels by stereocomplexation of PEG-(PLLA)(8) and PEG-(PDLA)(8) star block copolymers, Biomacromolecules, 7 (2006) 2790-2795.

[12] K.Y. Lee, J.A. Rowley, P. Eiselt, E.M. Moy, K.H. Bouhadir, D.J. Mooney, Controlling mechanical and swelling properties of alginate hydrogels independently by cross-linker type and cross-linking density, Macromolecules, 33 (2000) 4291-4294.

[13] M. Gümüsderelioglu, D. Kesgin, Release kinetics of bovine serum albumin from pH-sensitive poly(vinyl ether) based hydrogels, Int. J. Pharm., 288 (2005) 273-279.

[14] Y. Zhang, W. Zhu, B. Wang, J. Ding, A novel microgel and associated post-fabrication encapsulation technique of proteins, J. Control. Release, 105 (2005) 260-268.

[15] Y. Zhang, W. Zhu, B.B. Wang, L. Yu, J.D. Ding, Postfabrication encapsulation of model protein drugs in a negatively thermosensitive hydrogel, J. Pharm. Sci., 94 (2005) 1676-1684.

[16] S.H. Gehrke, L.H. Uhden, J.F. McBride, Enhanced loading and activity retention of bioactive proteins in hydrogel delivery systems, J. Control. Release, 55 (1998) 21-33.

[17] S.H. Gehrke, N.R. Vaid, J.F. McBride, Protein sorption and recovery by hydrogels using principles of aqueous two-phase extraction, Biotechnol. Bioeng., 58 (1998) 416-427.

[18] J.P. Schillemans, W.E. Hennink, C.F. Nostrum, The effect of network charge on the immobilization and release of proteins from chemically crosslinked dextran hydrogels, (submitted).

[19] N.A. Peppas, H.J. Moynihan, L.M. Lucht, The structure of highly crosslinked poly(2-hydroxyethyl methacrylate) hydrogels, J. Biomed. Mater. Res., 19 (1985) 397-411.

[20] W.E. Hennink, H. Talsma, J.C.H. Borchert, S.C. DeSmedt, J. Demeester, Controlled release of proteins from dextran hydrogels, J. Control. Release, 39 (1996) 47-55.

[21] W.N.E. van Dijk-Wolthuis, O. Franssen, H. Talsma, M.J. van Steenbergen, J.J. Kettenes-van den Bosch, W.E. Hennink, Synthesis, characterization, and polymerization of glycidyl methacrylate derivatized dextran, Macromolecules, 28 (1995) 6317-6322.

[22] W.N.E. van Dijk-Wolthuis, J.J. Kettenes-van den Bosch, A. van der Kerk-van Hoof, W.E. Hennink, Reaction of dextran with glycidyl methacrylate: an unexpected transesterification, Macromolecules, 30 (1997) 3411-3413.

[23] P. Böhlen, S. Stein, W. Dairman, S. Udenfriend, Fluorometric assay of proteins in the nanogram range, Arch. Biochem. Biophys., 155 (1973) 213-220.
[24] P.L. Ritger, N.A. Peppas, A simple equation for description of solute release. II: Fickian and anomalous release from swellable devices, J. Control. Release, 5 (1987) 37-42.
[25] W.N. van Dijk-Wolthuis, M.J. van Steenbergen, W.J. Underberg, W.E. Hennink, Degradation kinetics of methacrylated dextrans in aqueous solution, J. Pharm. Sci., 86 (1997) 413-417.
[26] A.H. Ghassemi, M.J. van Steenbergen, H. Talsma, C.F. van Nostrum, W. Jiskoot, D.J.A. Crommelin, W.E. Hennink, Preparation and characterization of protein loaded microspheres based on a hydroxylated aliphatic polyester, poly (lactic-co-hydroxymethyl glycolic acid), J. Control. Release, 138 (2009) 57-63.
[27] S. Hermeling, D.J. Crommelin, H. Schellekens, W. Jiskoot, Structure-immunogenicity relationships of therapeutic proteins, Pharm. Res., 21 (2004) 897-903.
[28] H. Schellekens, Bioequivalence and the immunogenicity of biopharmaceuticals, Nat. Rev. Drug Discov., 1 (2002) 457-462.
[29] NCBI Accession number NP_001039526.1, M.D. Bethesda, The NCBI handbook [Internet] Chapter 17, The Reference Sequence (RefSeq) Project, National Library of Medicine (US), National Center for Biotechnology Information, 2002, Available from http://www.ncbi.nlm.nih.gov/entrez/query.fcgi?db=Books, accessed on 29-06-2010
[30] J.A. Ji, B.Y. Zhang, W. Cheng, Y.J. Wang, Methionine, Tryptophan, and Histidine Oxidation in a Model Protein, PTH: Mechanisms and Stabilization, J. Pharm. Sci., 98 (2009) 4485-4500.
[31] NCBI accession number NP_001157488.1, M.D. Bethesda, The NCBI handbook [Internet] Chapter 17, The Reference Sequence (RefSeq) Project, National Library of Medicine (US), National Center for Biotechnology Information, 2002, Available from http://www.ncbi.nlm.nih.gov/entrez/query.fcgi?db=Books, accessed on 29-06-2010

Supporting information

Equilibrium swelling

After polymerization the hydrogels were weighed and incubated in 3 ml of cytochrome C solution (1 mg/ml) at 37°C for 5 days. Gels were blotted with a tissue to remove excess of loading solution and weighed again. The swelling ratio (Figure S1) is defined as the weight of the gel at equilibrium divided by the initial weight of the gel.

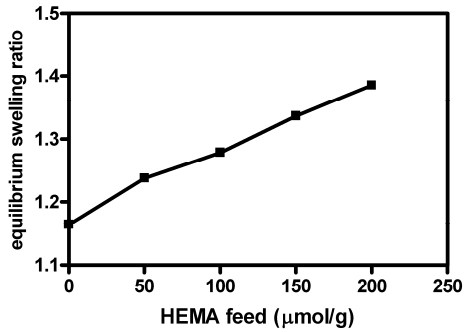

Figure S1. Equilibrium swelling ratio of cytochrome C post-loaded in negatively charged hydrogels (150 μmol MA/g hydrogel) with varying HEMA content.

Post-loading of myoglobin

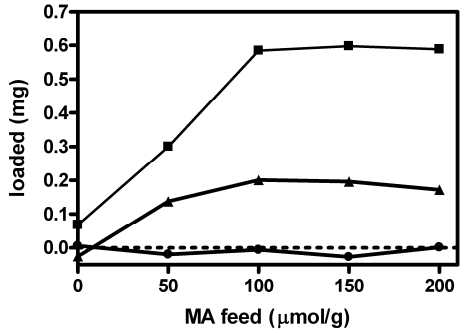

Figure S2. Post loading of myoglobin (3 mg), as a function of hydrogel charge density (μmol MA/g hydrogel, total hydrogel weight 125 mg) after 5 days in 10mM MES pH 7.0 (circles), 6.0 (triangles) and 5.0 (squares). The total amount of added methacrylic monomers was kept constant by addition of HEMA up to 200 μmol/g hydrogel.

Loading homogeneity of post-loaded FITC-labelled BSA

Positively charged Dex-MA hydrogels (100 µmol DMAEMA/g hydrogel) were post loaded with FITC-BSA at pH 7.4 during 37 days. Cross sectional distribution of FITC-BSA was examined using a fluorescent microscope (Nikon Eclipse TE-2000, Nikon, Amstelveen, The Netherlands).

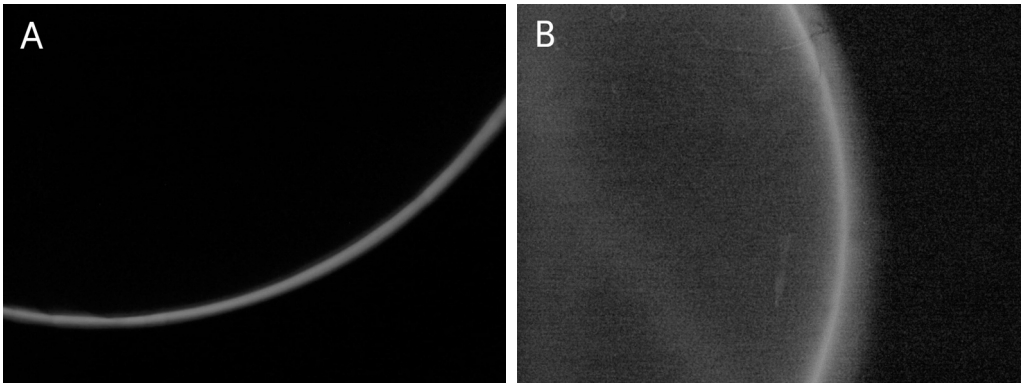

Figure S3. Cross sectional fluorescent image (magnification 4x) of FITC-BSA distribution in a positively charged Dex-MA hydrogel (100 µmol DMAEMA/g hydrogel) post-loaded for 37 days in HEPES containing 0 mM (A) and 100 mM NaCl (B).

Chapter 7

Perspectives

Protein imprinted nanoparticles

As described in the general introduction (chapter 1) the aim of this thesis was to develop a method for the synthesis of protein imprinted nanoparticles (PINAPLES) using a liposomal reactor. The path towards the successful preparation of PINAPLES can be divided into 4 essential steps. First, the template needs to be immobilized in a liposomal membrane with the proper orientation (available in the inner liposomal compartment). Second, hydrogels need to be formed inside the liposomal reactor. Third, the liposomal membrane and template molecule need to be removed to obtain bare nanogels. Fourth, the particles should display high affinity and selectivity towards the template. As described in chapter 3 of this thesis, we have succeeded in 3 out of these 4 steps; proper immobilization of the template, formation of hydrogels, and removal of the bilayer and template. Unfortunately, we did not succeed in obtaining an imprint effect. Due to lack of fundamental knowledge on the parameters controlling the successful formation of protein imprinted polymers, the efforts towards the formation of imprints was mostly driven by trial and error. As described in chapter 4, better understanding of the selection of proper monomers is essential for the creation of high affinity binding sites in aqueous environment. However, if the increase in research efforts seen in the last decade will prevail (see chapter 4), new insights will surely make the preparation of PINAPLES more feasible. In fact, a recent series of papers describes the development of peptide imprinted polymer particles prepared from *N*-isopropylacrylamide crosslinked with *N,N'*-methylene-bisacrylamide, supplemented with functional monomers for electrostatic and hydrophobic interactions (acrylic acid and *N*-t-butylacrylamide, respectively), which successfully bind the toxic peptide melittin in the bloodstream of living mice. As a result, phagocytosis of the melittin-MIP particles by macrophages results in activation of this toxic peptide, and melittin-induced mortality and peripheral toxic symptoms were significantly reduced [1-3]. This example shows that significant progress in the molecular imprinting of biomolecules in aqueous environment is currently being made. In principle, the method used to prepare nanoparticles described in chapter 3 of this thesis provides an elegant method to present a membrane associated protein to interact with the monomers in a pre-polymerization mixture. Therefore, it might be of great value once the imprinting of proteins is better understood. The method of nanoparticle synthesis using a liposomal reactor is not limited to gels consisting of polyacrylamide. It can also be applied for example to synthesize biodegradable nanogels based on Dex-HEMA [4]. Currently, research in our group is aimed to assess whether chemically crosslinked dextran hydrogels form a suitable

matrix for imprinting of proteins. When this appears to be the case, the synthesis of dextran-based PINAPLES using the liposomal reactor would be the next step. Especially for the application as targeted drug carriers (see introduction), such biocompatible and biodegradable PINAPLES would be very interesting.

Protein-polymer charge interactions in controlled release formulations

Chapter 6 describes the exploitation of electrostatic charge interactions between proteins and polymer for post-loading of proteins in preformed hydrogels. The main advantages are that, as opposed to conventional loading, the released protein is chemically unmodified, and the high loading efficiency. However, the macroscopic gels described in chapter 6 are not suited for pharmaceutical applications, because surgery is required for administration, which is expensive and patient unfriendly. Therefore, controlled release devices in the form of micro- or nanospheres are preferred for clinical applications. Microspheres can be injected locally, after which they release their content over a prolonged period of time [5], while nanospheres can be administered systemically, which enables targeting to remote tissues and even intracellular delivery [6]. Charged dextran hydrogels can easily be synthesized in the form of microgels [7] and nanogels [8]. However, when the polymer compositions described in chapter 6 would be applied for micro or nanosphere formulations, the release of post-loaded proteins would be very rapid as a result of the hydrogel dimensions (high surface area, short diffusional path length). To prevent such burst release it would be interesting to investigate the possibility of using the post-loading method based on electrostatic charge interaction in combination with the thermo-sensitive hydrogels with high equilibrium swelling described by Zhang *et al.* [9, 10]. When soaking the hydrogel in a protein solution at a temperature below the lower critical solution temperature (LCST) to give a highly swollen hydrogel, high protein diffusivity would lead to rapid loading. When charged monomers are introduced in this system, electrostatic charge interaction will likely result in high loading efficiency. Increasing the temperature above the phase transition leads to collapse of the hydrogel chains and significant reduction of the protein diffusivity, and as a consequence, lower release rate. In addition, if the hydrogel mesh size in the collapsed state is smaller than the size of the protein, release is controlled and tailorable by degradation of the network.

Alternatively, following post-loading of protein in micro- or nanospheres, a polymer coating could be applied to prevent rapid release. This can for example be done by layer-by-layer (LBL) assembly of oppositely charged linear polyions as introduced by Decher *et al.* [11]. Adsorption of

a polyion to an oppositely charged particle leads to charge reversal of the surface. This way, subsequent layers of oppositely charged polyions can be deposited onto a substrate to form a thin film. The release rate of encapsulated compounds can be regulated by the composition and number of layers [12, 13]. Alternatively, self-rupturing microcapsules of LBL-coated crosslinked Dex-hydroxyethylmethacrylate (Dex-HEMA) can be prepared for pulsed drug delivery [14]. In a preliminary study described below, we investigated the possibility of post-loading of cytochrome C in dextran nanogels, followed by LBL-coating.

Synthesis of Dex-MA nanogels

An appropriate amount of dioleoylphosphatidylcholine (DOPC) (Lipoid GmbH) was dissolved in chloroform in a round-bottom flask. A lipid film was prepared under reduced pressure using a rotary evaporator and dried further under a stream of nitrogen. The lipid film was hydrated with a 15% (w/w) solution of Dex-MA with a degree of substitution (DS) of 12 (DS = number of methacrylate residues introduced per 100 glucopyranose units [15, 16]), also containing 117 mM methacrylic acid (MA) and 0.032% (w/v) Irgacure 2959 (Ciba Specialty Chemicals) in 10 mM HEPES pH 7.4 to a final concentration of 20 mM DOPC. Subsequently, the formed multilamellar liposomes were extruded using a hand extruder (Avanti Polar Lipids) through polycarbonate filters with a pore size of 0.4 µm. Non-encapsulated Dex-MA and MA were removed by ultracentrifugation for 1 hour at 250.000 g, and subsequent removal of the supernatant. The pellet was resuspended in 10 mM HEPES. Photopolymerization of the encapsulated Dex-MA and MA was initiated by illumination for 300 seconds under a N_2 atmosphere using a Bluepoint 4 UVC mercury lamp (150W, λ-range 230-600 nm, Honle UV Technology). Non-charged dex-MA (control) particles were synthesized by the same procedure, except the addition of methacrylic acid.

Bare nanogels were obtained after removal of the DOPC bilayer by addition of TX100 up to 1% (w/v), followed by 4 times ultracentrifugation at 130.000 g for 30 minutes with resuspending of the pellet in 10 mM HEPES. The size and size distribution of the particles were measured by dynamic light scattering (DLS) using a Malvern CGS-3 multiangle goniometer (Malvern Ltd.). The ζ-potential was determined using a Zetasizer Nano-Z (Malvern Instruments) with universal ZEN 1002 'dip' cell in 5 mM HEPES, pH 7.4. The concentration of particles (w/v) was measured by determination of the dry weight after solvent evaporation using a Q50 thermogravimetric analyzer (TA instruments).

The size and ζ-potential of the DOPC coated and bare dextran nanogels are shown in table 1. Removal of DOPC was confirmed by a phosphate determination according to Rouser after destruction with perchloric acid [17]. The ζ-potential of bare MA-containing particles was –13.5 mV compared to –5.2 mV for the control particles, indicating that methacrylic acid was successfully incorporated in the nanogels. The bare particles were larger than the bilayer-coated particles (240 and 425 nm, respectively for MA containing nanogels and 230 and 421 nm, respectively for control nanogels). Likely, this is a result of repeated ultracentrifugation and particle resuspension. An increase in size was observed after every cycle, while more vigorous resuspension led to smaller particles and lower PDI values (data not shown).

Table 1. Z-average, polydispersiy index (PDI) and ζ-potential of bilayer-coated and bare dextran MA-containing and control nanogels. Values represent average ± standard deviation (n = 3).

		Z-Avg (nm)	*PDI*	*ζ-potential (mV)*
MA	Coated	240 ± 21	0.181 ±0.06	-3.6 ± 0.3
	Bare	425 ± 76	0.296 ±0.08	-13.4 ± 0.7
Control	Coated	230 ± 15	0.120 ±0.03	-7.2 ± 5.1
	Bare	421 ±26	0.346 ± 0.07	-3.0 ± 3.9

Post-loading of cytochrome C in Dex-MA nanogels

Varying amounts of Dex-MA nanogels were incubated overnight in a solution of 0.15 mg/mL cytochrome C in HEPES pH 7.4 at room temperature. Samples were filtered using centrifugal filter units with a MWCO of 100 kD (Millipore) to separate cytochrome C loaded in the nanogels from the free protein. The samples of the calibration curve were filtered using the same procedure to correct for loss of protein. The concentration of cytochrome C in the filtrate was determined by means of a fluorometric assay using fluorescamine as described by Böhlen *et al.* [18], adapted to a 96-well plate format.

Figure 1 shows that with increasing amount of negatively charged particles, less cytochrome C was detected in the filtrate. For the control particles this amount was significantly higher. This indicates that the cytochrome C was efficiently loaded to the negatively charged particles. The decrease in concentration translated into a maximum loading of ~0.3 mg cytochrome C/mg particles (dry weight). Assuming full conversion of the MA monomers during synthesis of the nanoparticles, this translates into a ratio of charged residues in cytochrome C (22/molecule) to

charged moieties in the network of 0.73:1, which implies very efficient interaction between MA and cytochrome C in the hydrogel, similar to what was observed for macroscopic hydrogels (0.81:1, chapter 6).

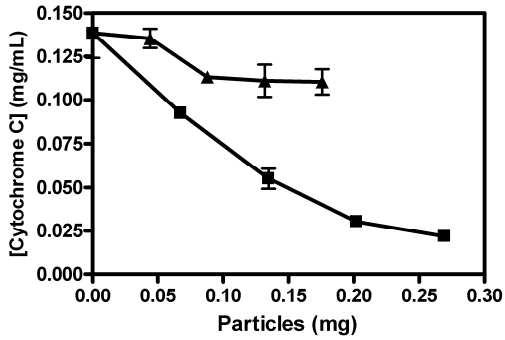

Figure 1. The concentration of free cytochrome C after overnight incubation with varying amounts of MA-containing (squares) and control (triangles) dextran nanogels. Values represent average and standard deviation (n = 3).

Layer-by-layer coating of Dex-MA nanogels

Layer by layer coating was performed using poly-L-arginine (pARG) and poly-L-glutamic acid (pGLU), both bio-polyelectrolytes that have been previously used for LBL coating of dextran microparticles [14]. Particles without loaded cytochrome C (500 µL) were incubated in a solution (2.5 mL, 0.5 mg/mL) of pARG (Mw 15.000-70.000) in 10 mM HEPES pH 7.4 for 10 minutes. Non-bound pARG was removed by ultracentrifugation at 130.000 g for 15 minutes, followed by removal of the supernatant. Particles were resuspended in 10 mM HEPES and the ζ-potential and size were determined. Next, particles were incubated in a solution (2.5 mL, 0.5 mg/mL) of pGLU (Mw 15.000) in 10 mM HEPES pH 7.4 for 10 minutes, followed by removal of the non-bound pGLU by ultracentrifugation. Particle size, PDI and ζ-potential of the particles at different stages of LBL coating are shown in Table 2.

Table 2. ζ-potential and Z-average and polydispersity index (PDI) of unloaded Dex-MA nanogels during the different stages of LBL coating.

	ζ-potential (mV)	*Z-Avg (nm)*	*PDI*
Uncoated	-13	271	0.232
Layer 1 (pARG)	20	295	0.251
Layer 2 (pGLU)	-15	314	0.243

The samples were resuspended vigorously during 5 minutes, which resulted in smaller particles as compared to those reported in Table 1 (271 and 425 nm, respectively). Table 2 shows the reversal of the ζ-potential (negative to positive and back to negative) upon subsequent incubation of the nanogels in pARG and pGLU solutions. The size increased slightly, while the PDI remained low, indicating that particle aggregation did not occur. Although these are preliminary data (n = 1), these results indicate that the Dex-MA nanogels were successfully coated with 2 layers of polyelectrolytes. It is anticipated that using the same protocol, additional layers can be applied to obtain a coating of the desired thickness and (im)permeability.

It was observed that nanogels post-loaded with cytochrome C, which form a bright red pellet after centrifugation, became colorless after incubation with pARG. Since post-loaded cytochrome C is retained in negatively nanogels by electrostatic interactions, polycations that are added to the gels might desorb the bound proteins resulting in their release. In order to prevent this, the polycation used as the first layer of the LBL coating needs to be larger than the mesh size of the hydrogel, so it will not penetrate into the gel and subsequently desorb cytochrome C. Therefore, we tested LBL-coating of post-loaded cytochrome C particles using a polycation with high molecular weight. Poly(diallyldimethylammonium)chloride (pDADMA), a polycation used previously for LBL coating of polymeric particles [19], with a MW 400-500 kD dissolved in water has a radius of over 40 nm [20], which is much larger than the mesh size of Dex-MA hydrogel (5-15 nm) [21]. Cytochrome C loaded particles were separated from free cytochrome C by ultracentrifugation at 130.000 g for 30 minutes. A bright red pellet was obtained (not present after centrifugation of a cytochrome C solution without particles). Resuspended particles were sonicated in a bath sonicator (UR 198, Retsch) for 5 minutes. Particles (500 µL) were incubated in a solution (2.5 mL, 0.5 mg/mL) of pDADMA in 10 mM HEPES pH 7.4 for 10 minutes. Non-bound pDADMA was removed by ultracentrifugation, followed by removal of the supernatant.

Table 3. ζ-potential and Z-average and polydispersity index (PDI) of cytochrome C loaded Dex-MA nanogels before and after coating with pDADMA.

	ζ-potential (mV)	*Z-Avg (nm)*	*PDI*
Coated	n.d.	209	0.159
Uncoated	n.d.	324	0.299
Uncoated sonicated	-11	185	0.131
Layer 1 (pDADMA)	33	203	0.145

n.d.: not determined

Interestingly, Table 3 shows that sonication resulted in smaller particles with a lower PDI compared to resuspended particles. The size of the sonicated particles was slightly smaller compared to the bilayer coated particles, which can be explained by removal of the bilayer. This effect of sonication was confirmed in several experiments, and therefore sonication should be included in the protocol in the future.

The ζ-potential of cytochrome C loaded particles remained negative (–11 mV) but less negative than unloaded particles (–13 mV, Table 1). Probably, the charge density in cytochrome C is not high enough to result in a reversal of the ζ-potential. Coating with pDADMA did lead to charge reversal to a ζ-potential of +33 mV. The effect of pDADMA on cytochrome C loading was evaluated by SDS-PAGE analysis (Figure 2). It becomes clear that post-loaded Dex-MA nanogels still contained cytochrome C after coating with pDADMA.

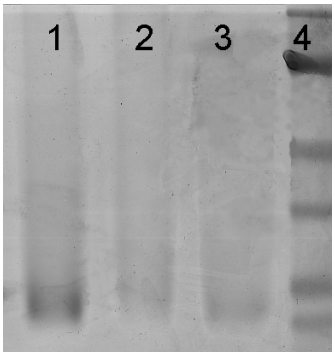

Figure 2. SDS-PAGE (12.5% polyacrylamide) analysis with silver staining of cytochrome C content of post-loaded nanoparticles before (lane 1) and after (lane 2) coating with pDADMA. Reference cytochrome C (lane 3, 0.01 mg/mL) and a molecular weight ladder (lane 4) are also shown.

Future perspectives

The data presented in chapter 6 in combination with our preliminary data presented above are very encouraging. Chapter 6 shows that post-loading of proteins in crosslinked dextran hydrogels is a very efficient and versatile method. The preliminary data presented in this chapter indicate that it can be applied for the post-loading of cytochrome C in nanogels with subsequent LBL-coating. However, further research is needed aiming to optimize and quantify the post-loading of cytochrome C in these nanogels. Furthermore, it needs to be shown that the protein can be mobilized by increasing the ionic strength, and the effect of the LBL-coating on the release rate of cytochrome C needs to be studied. Also, when release is accomplished, the integrity of the released protein needs to be assessed.

Currently, nanogels are under intensive investigation as devices for controlled drug delivery [6, 22-26], because their nanoscale dimensions allow intravenous injection of nanogels, which facilitates targeted delivery to specific tissues or even intracellular compartments. Post-loaded nanogels could prove to be very useful vehicles for therapeutic proteins. As pointed out, the high loading efficiency is one of the main advantages. Furthermore, the use of a liposomal reactor results in straightforward control of particle size and size-distribution, while the LBL coating enables control over surface charge. As was shown by Gratton *et al*, both size and surface charge are important factors that influence the cellular uptake mechanism and thereby the intracellular fate of nanoparticles [27]. Furthermore, it has been shown that size and surface modification determine the biodistribution of nanogels after iv administration [6, 23]. Future research will have to show the real value of post-loaded nanogels for pharmaceutical applications.

References

[1] Y. Hoshino, T. Kodama, Y. Okahata, K.J. Shea, Peptide imprinted polymer nanoparticles: A plastic antibody, J. Am. Chem. Soc., 130 (2008) 15242-15243.

[2] Y. Hoshino, H. Koide, T. Urakami, H. Kanazawa, T. Kodama, N. Oku, K.J. Shea, Recognition, neutralization, and clearance of target peptides in the bloodstream of living mice by molecularly imprinted polymer nanoparticles: A plastic antibody, J. Am. Chem. Soc., 132 (2010) 6644-6645.

[3] Y. Hoshino, T. Urakami, T. Kodama, H. Koide, N. Oku, Y. Okahata, K.J. Shea, Design of synthetic polymer nanoparticles that capture and neutralize a toxic peptide, Small, 5 (2009) 1562-1568.

[4] T.G. Van Thienen, B. Lucas, F.M. Flesch, C.F. Van Nostrum, J. Demeester, S.C. De Smedt, On the synthesis and characterization of biodegradable dextran nanogels with tunable degradation properties, Macromolecules, 38 (2005) 8503-8511.

[5] V.R. Sinha, A. Trehan, Biodegradable microspheres for protein delivery, J. Control. Release, 90 (2003) 261-280.

[6] K. Raemdonck, J. Demeester, S. De Smedt, Advanced nanogel engineering for drug delivery, Soft Matter, 5 (2009) 707-715.

[7] S.R. Van Tomme, M.J. van Steenbergen, S.C. De Smedt, C.F. van Nostrum, W.E. Hennink, Self-gelling hydrogels based on oppositely charged dextran microspheres, Biomaterials, 26 (2005) 2129-2135.

[8] K. Raemdonck, B. Naeye, K. Buyens, R.E. Vandenbroucke, A. Hogset, J. Demeester, S.C. De Smedt, Biodegradable Dextran Nanogels for RNA Interference: Focusing on Endosomal Escape and Intracellular siRNA Delivery, Advanced Functional Materials, 19 (2009) 1406-1415.

[9] Y. Zhang, W. Zhu, B. Wang, J. Ding, A novel microgel and associated post-fabrication encapsulation technique of proteins, J. Control. Release, 105 (2005) 260-268.

[10] Y. Zhang, W. Zhu, B.B. Wang, L. Yu, J.D. Ding, Postfabrication encapsulation of model protein drugs in a negatively thermosensitive hydrogel, J. Pharm. Sci., 94 (2005) 1676-1684.

[11] G. Decher, Fuzzy nanoassemblies: Toward layered polymeric multicomposites, Science, 277 (1997) 1232-1237.

[12] A.A. Antipov, G.B. Sukhorukov, Polyelectrolyte multilayer capsules as vehicles with tunable permeability, Adv. Colloid Interface Sci., 111 (2004) 49-61.

[13] J.P.K. Tan, Q. Wang, K.C. Tam, Control of burst release from nanogels via layer by layer assembly, J. Control. Release, 128 (2008) 248-254.

[14] B.G. De Geest, C. Dejugnat, M. Prevot, G.B. Sukhorukov, J. Demeester, S.C. De Smedt, Self-rupturing and hollow microcapsules prepared from bio-polyelectrolyte-coated microgels, Adv. Funct. Mater., 17 (2007) 531-537.

[15] W.N.E. van Dijk-Wolthuis, O. Franssen, H. Talsma, M.J. van Steenbergen, J.J. Kettenes-van den Bosch, W.E. Hennink, Synthesis, characterization, and polymerization of glycidyl methacrylate derivatized dextran, Macromolecules, 28 (1995) 6317-6322.

[16] W.N.E. van Dijk-Wolthuis, J.J. Kettenes-van den Bosch, A. van der Kerk-van Hoof, W.E. Hennink, Reaction of dextran with glycidyl methacrylate: an unexpected transesterification, Macromolecules, 30 (1997) 3411-3413.

[17] G. Rouser, S. Fkeischer, A. Yamamoto, Two dimensional then layer chromatographic separation of polar lipids and determination of phospholipids by phosphorus analysis of spots, Lipids, 5 (1970) 494-496.

[18] P. Böhlen, S. Stein, W. Dairman, S. Udenfriend, Fluorometric assay of proteins in the nanogram range, Arch. Biochem. Biophys., 155 (1973) 213-220.

[19] L.J. De Cock, S. De Koker, B.G. De Geest, J. Grooten, C. Vervaet, J.P. Remon, G.B. Sukhorukov, M.N. Antipina, Polymeric Multilayer Capsules in Drug Delivery, Angew. Chem. Int. Ed. Engl.

[20] H. Dautzenberg, E. Görnitz, W. Jaeger, Synthesis and characterization of poly(diallyldimethylammonium chloride) in a broad range of molecular weight, Macromol. Chem. Phys., 199 (1998) 1561-1571.

[21] R.J.H. Stenekes, S.C. De Smedt, J. Demeester, G.Z. Sun, Z.B. Zhang, W.E. Hennink, Pore sizes in hydrated dextran microspheres, Biomacromolecules, 1 (2000) 696-703.
[22] M. Hamidi, A. Azadi, P. Rafiei, Hydrogel nanoparticles in drug delivery, Adv. Drug Del. Rev., 60 (2008) 1638-1649.
[23] A.V. Kabanov, S.V. Vinogradov, Nanogels as pharmaceutical carriers: finite networks of infinite capabilities, Angew. Chem. Int. Ed. Engl., 48 (2009) 5418-5429.
[24] N. Morimoto, S.I.M. Nomura, N. Miyazawa, K. Akiyoshi, Nanogel engineered designs for polymeric drug delivery, in: S. Svenson (Ed.) Polymeric drug delivery II: polymeric matrices and drug particle engineering, American Chemical Society, Washington, 2006, pp. 88-101.
[25] J.K. Oh, R. Drumright, D.J. Siegwart, K. Matyjaszewski, The development of microgels/nanogels for drug delivery applications, Progress in Polymer Science, 33 (2008) 448-477.
[26] S.V. Vinogradov, Nanogels in the race for drug delivery, Nanomed., 5 (2010) 165-168.
[27] S.E.A. Gratton, P.A. Ropp, P.D. Pohlhaus, J.C. Luft, V.J. Madden, M.E. Napier, J.M. DeSimone, The effect of particle design on cellular internalization pathways, Proc. Natl. Acad. Sci. U. S. A., 105 (2008) 11613-11618.

Chapter 8

Summary

A hydrogel consists of a hydrophilic crosslinked polymer network with high water content. **Chapter 1** provides a general introduction of the use of hydrogels in the fields of protein drug delivery and protein imprinting. Furthermore, it introduces the concept of the synthesis of protein imprinted nanoparticles (PINAPLES). Additionally, the outline of this thesis is presented.

In **chapter 2** the different methods currently used to prepare molecular imprinted micro- and nanoparticles are discussed. Traditionally, molecular imprinted polymers are prepared by bulk polymerization, followed by crushing and sieving to obtain polymer beads. However, several methods can be used to directly synthesize polymer micro- and nanoparticles, such as dispersion, precipitation, suspension and (mini-)emulsion polymerization. Compared to the traditional bulk (monolith) polymerization, direct synthesis of molecularly imprinted particles has proven to be more convenient because the time and labor consuming process of crushing and sieving is avoided. More importantly, it leads to production of regularly shaped imprinted particles with controlled particle size and a large surface area, resulting in improved rate of mass transfer and better MIP performance (binding capacity and affinity/selectivity).

A novel method for the preparation of nanoparticles intended for the preparation of PINAPLES is described in **chapter 3**. Polyacrylamide nanoparticles were prepared inside the internal aqueous compartment of liposomes. This method offers straightforward control over the size of the particles. Importantly, the liposomal bilayer offers the possibility to incorporate membrane proteins, which can then be used as templates for surface imprinting. Liposomes were formed in acrylamide (AAm)/methylene-bisacrylamide (MBA)-solutions from mixed micelles of lipid/Triton X-100 (TX100) by adsorption of TX100 onto Bio-Beads SM2 by which unilaminar liposomes are formed. The hydrodynamic diameter of the liposomes was approximately 100 nm with low polydispersity. Free-radical polymerization of the monomers entrapped in the liposomes was initiated by illumination, in the presence of a photoinitiator (Irgacure). Macroscopic hydrogel formation due to polymerization of the monomers outside the liposomes was prevented by inhibition of free-radical polymerization of non-encapsulated monomers by addition of ascorbic acid, which does not cross the liposomal bilayer, before photopolymerization. Bare nanogel particles were obtained by removal of the lipid bilayer. This convenient and versatile method of nanogel synthesis allows the use of monomers that readily pass the lipid membrane. Moreover, using the detergent removal method enables functional reconstitution of membrane proteins in the bilayer which is essential for the development of

PINAPLES. In the **appendix of chapter 3** it is shown that using this method, SN/GpA, a membrane protein construct containing the transmembrane region of glycophorin A fused to the C-terminus of staphylococcal nuclease, is successfully incorporated in the liposomal bilayer. Moreover, biotinylation with the membrane impermeable biotin-sulfo-NHS showed that hydrophilic domain of SN/GpA was oriented towards the internal compartment of the liposome, and therefore would be available for the formation of imprints.

Despite many attempts towards the synthesis of PINAPLES, a proof of concept was not obtained. This is partially due to the current state of the art of protein imprinting. As discussed in **chapter 4**, protein imprinting is still a relatively new scientific field. Although the number of research papers that describe protein imprinting is increasing, the actual scientific proof of the feasibility of selective recognition of proteins by MIPs in aqueous environment is not convincing. Proper monomer selection, template removal, and assessment of template rebinding are identified as major issues, which is illustrated with examples from literature and our own experimental data. Use of charged monomers can lead to strong electrostatic interactions between monomers and template but also to undesired high aspecific binding. Up till now, it has not been convincingly shown that electrostatic interactions are beneficial for protein imprinting. The combination of a detergent (SDS) and acetic acid, commonly used for template removal, can lead to experimental artifacts, and should therefore be avoided. In many cases template rebinding is unreliably quantified, results are not reviewed critically or lack statistical analysis. Therefore, it can be argued that presently, in numerous publications the scientific evidence of molecular imprinting of proteins is not convincing.

In **chapter 5** the effect of electrostatic charge interaction between a protein and hydrogel network on protein release was investigated. Charged hydrogels that are stable under physiological conditions were obtained by copolymerization of methacrylated dextran (Dex-MA) with either methacrylic acid (MA) or 2-N,N-dimethylaminoethyl methacrylate (DMAEMA). The effect of incorporation of the charged monomers on hydrogel charge, equilibrium swelling and release of model proteins was assessed both at low (10 mM HEPES) and physiological ionic strength (HEPES buffered saline, HBS). Model proteins were chosen on the basis of their charge at physiological pH; bovine serum albumin (BSA, negatively charged), myoglobin (neutral), and cytochrome C (positively charged). Interestingly, as opposed to myoglobin, both charged proteins were fully immobilized in networks with opposite charge by electrostatic interaction at low ionic strength. On the other hand, at physiological ionic strength the

percentage of immobilized protein depended on the charge density of the hydrogel. The diffusion coefficient of the mobile proteins was the same in oppositely charged and non-charged gels. However, the release rate of BSA from similarly (negatively) charged networks significantly increased when a relatively high amount of charged monomers was incorporated. It was concluded that incorporation of charge in a hydrogel network is suited as a tool for the immobilization of proteins and triggered release by increasing ionic strength.

In **chapter 6** the reversible electrostatic interactions described in **chapter 5** were exploited for post-loading with high efficiency and controlled release of proteins. Dex-MA was co-polymerized with MA or DMAEMA to form negatively and positively charged hydrogels, respectively. Incubation of negatively charged hydrogels in a low ionic strength (10 mM HEPES, pH 7.4) solution of cytochrome C (*pI* 10.2) led to quantitative absorption of the protein in the hydrogel. BSA (*pI* 4.8) and myoglobin (*pI* 7.2) were post-loaded into positively charged gels at neutral pH and negatively charged gels at pH 5, respectively. Loading efficiency and protein distribution in the gels were dependent on network charge, crosslink density and on the ionic strength during loading. Diffusion controlled release of the loaded protein was triggered by incubation of the hydrogel in HBS pH 7.4. The amount of released cytochrome C in HBS varied from 94% to 70% from gels containing 60 and 150 MA/g, respectively. Importantly, quantitative release was obtained in 1 M NaCl, indicating that post-loading led to neither the formation of insoluble protein aggregates nor irreversible immobilization of the protein in the matrix. ESI-MS analysis of the released cytochrome C revealed that post-loading did not result in oxidation of the protein, as opposed to loading during preparation of the gels. These data showed that post-loading of proteins in dextran hydrogels and release exploiting reversible charge interactions can be applied for efficient loading of proteins that are negative, positive or neutral at physiological pH. Importantly, no chemical modification to the protein occurred using this loading method.

Chapter 7 discusses the future perspectives of the work presented in this thesis. It is argued that in principle, the method used to prepare nanoparticles described in chapter 3 of this thesis provides an elegant method to present a membrane associated protein to interact with the monomers in a pre-polymerization mixture. If the increase in research efforts seen in the last decade will prevail, new insights will surely make the preparation of PINAPLES more feasible. With respect to the post-loading of proteins it is pointed out that macroscopic hydrogels are not the preferred systems for clinical applications, because surgery is required for the

administration. Post-loading in injectable micro- or nanogels is preferred. Nanogels are particularly interesting because they open up the possibility of reaching remote tissues and intracellular delivery of biopharmaceuticals. As a result of the large surface area and short diffusion distance, post-loading in and release kinetics of proteins from nanogels would be very fast. Therefore, layer-by layer coating is proposed as a possible method to prevent burst release of post-loaded proteins from nanogels. The release rate is then determined by the diffusion rate of the protein through the layers, and/or degradation kinetics of the coating. Preliminary data are presented showing that cytochrome C can be efficiently loaded in negatively charged dextran nanogels at low ionic strength. Additionally, the applicability of LBL-coating to dextran nanogels is shown.

Appendices

Inleiding

Therapeutische eiwitten

Een eiwit (of proteïne) is een macromolecuul dat bestaat uit een of meerdere ketens van aan elkaar geregen aminozuren. De functionele eigenschappen van een eiwit worden niet alleen bepaald door de volgorde van aminozuren in de keten, maar ook door de manier waarop deze keten(s) driedimensionaal gevouwen zijn. Eiwitten vormen een grote en diverse groep biologische macromoleculen, die essentiële functies verrichten in levende organismen. Ze kunnen o.a. dienen als bouwstenen (bv. van haar, nagels, het cytoskelet en de extracellulaire matrix), katalysatoren die chemische reacties mogelijk maken of versnellen (enzymen), antistoffen (van het immuunsysteem), transportsystemen (bv. over het membraan van een cel), en cellulaire communicatiemiddelen (bv. receptoren).

Door hun directe betrokkenheid bij ontelbare processen in het lichaam ligt het voor de hand eiwitten te gebruiken als geneesmiddelen. De productie op grote schaal van deze zeer complexe en kwetsbare moleculen was echter lange tijd de moeilijkheid. De ontdekking van DNA en de daar uit voortvloeiende ontwikkelingen in de biotechnologie in de 2^{e} helft van de 20^{e} eeuw hebben productie van grote hoeveelheden zuiver eiwit mogelijk gemaakt. Inmiddels is er dan ook een behoorlijk aantal eiwitten in gebruik als geneesmiddel. Er kan hierbij worden gedacht aan behandeling van ziekten die worden veroorzaakt door een verminderde functie of ontbreken van bepaalde eiwitten, zoals bij bloedarmoede veroorzaakt door een gebrek aan erythropoietine (beter bekend als EPO), hemofilie door een gebrek aan stollingsfactor VIII, of het syndroom van Hunter (stofwisselingsziekte). Ook kunnen eiwitten worden ingezet ter voorkoming van ongewenste processen, zoals auto-immuunreacties (bv. bij multiple sclerose), of het afstoten van organen na transplantatie. Het enorme potentieel van de toepassing van eiwitten voor therapeutische doeleinden wordt geïllustreerd door het gegeven dat 30 tot 40% van alle recentelijk tot de markt toegelaten geneesmiddelen in deze categorie valt.

Orale toediening van farmaceutische eiwitten is niet mogelijk, omdat deze over het algemeen niet bestand zijn tegen de condities in het maag-darmkanaal, en niet intact door het lichaam kunnen worden opgenomen. Het merendeel van de therapeutische eiwitten wordt daarom toegediend via injectie. Om de belasting van de patiënt te verminderen, wordt er veel aandacht besteed aan het ontwikkelen van formuleringen die na eenmalige toediening het eiwit gedurende een langere tijd afgeven (een soort depot). Zoals eerder vermeld zijn eiwitten

complexe en zeer kwetsbare macromoleculaire structuren die met grote voorzichtigheid behandeld moeten worden. Het is daarom van groot belang dat het materiaal gebruikt voor eiwitformuleringen een omgeving vormt die niet schadelijk is voor het eiwit. Een groep van materialen die aan deze voorwaarde voldoet en daarom veel wordt toegepast in eiwitformuleringen wordt gevormd door hydrogelen.

Hydrogelen

Een hydrogel bestaat uit een driedimensionaal polymeernetwerk. Polymeren zijn lange ketens van moleculen bestaande uit aan elkaar gekoppelde, repeterende eenheden (monomeren). Het polymeernetwerk van een hydrogel kenmerkt zich doordat het grote hoeveelheden water kan vasthouden, zonder zijn structuur te verliezen. Mede door dit hoge watergehalte worden hydrogelen over het algemeen goed verdragen door biologische weefsels, waardoor ze uitermate geschikt zijn voor medische en farmaceutische toepassingen. De structuur van een hydrogel blijft behouden door de aanwezigheid van dwarsverbindingen ('crosslinks') tussen de polymeerketens. Deze dwarsverbindingen kunnen zowel chemisch als fysisch van aard zijn. Een chemische dwarsverbinding komt tot stand door een chemische reactie tussen de moleculen (samen 1 molecuul vormend), terwijl fysische verbindingen bestaan door interactie tussen de moleculen. Hierbij kan bijvoorbeeld worden gedacht aan elektrostatische interactie (tussen positieve en negatieve lading). Beide type dwarsverbindingen hebben hun voor- en nadelen. Zo zorgen chemische dwarsverbindingen in het algemeen voor zeer stevige hydrogelen, waarbij een uitstekende controle over het aantal dwarsverbindingen tussen de polymeerketens mogelijk is (bepalend voor de grootte van de mazen van het netwerk, zie verderop). Fysische dwarsverbindingen leiden tot veel minder stevige hydrogelen. Aan de andere kant zijn fysische dwarsverbindingen vaak omkeerbaar, bijvoorbeeld door verandering van temperatuur of mechanische krachten. Dit maakt het mogelijk dat het netwerk tijdelijk wordt verbroken, zodat de hydrogel per injectie kan worden toegediend en na injectie weer een hydrogel vormt (in tegenstelling tot implanteren d.m.v. een chirurgische ingreep). Daarnaast komen fysische dwarsverbindingen tot stand onder milde omstandigheden, terwijl het vormen van chemische dwarsverbindingen vaak onder hardvochtige reactiecondities plaatsvindt, of schadelijke reagentia vereist. Dit laatste kan zeker in het geval van eiwitten leiden tot schade aan of zelfs het ongewenst mee-reageren van het therapeuticum..

Gereguleerde afgifte van eiwitten uit hydrogelen kan op drie verschillende manieren (of een combinatie daarvan) plaatsvinden: gecontroleerd door diffusie, zwelling, of degradatie. Diffusie

is het proces van verplaatsing door spontane, willekeurige beweging van een deeltje. Indien de mazen van het hydrogelnetwerk groter zijn dan het eiwit, kan het eiwit vrij door het netwerk diffunderen (verplaatsen). De snelheid waarmee dit gebeurt, en dus de snelheid waarmee het eiwit uit de hydrogel vrijkomt, is o.a. afhankelijk van de grootte van de mazen in verhouding tot het eiwit (hoe groter de mazen, hoe sneller het eiwit kan bewegen). De tijd waarover een eiwit wordt afgegeven kan dus worden beïnvloed door de maaswijdte te veranderen.

Bij zowel zwelling- als degradatie-gereguleerde afgifte is de initiële maaswijdte kleiner dan de grootte van het eiwit, met het gevolg dat het eiwit niet door het netwerk kan bewegen. Bij zwelling-gereguleerde afgiftesystemen neemt de maaswijdte in verloop van tijd toe als gevolg van zwelling door de opname van water, terwijl dit bij degradatie een gevolg is van afbraak van het polymeer/dwarsverbindingen. In beide gevallen leidt de toename van de maaswijdte tot een toename van de bewegelijkheid en dus tot afgifte van het eiwit.

In dit proefschrift wordt de eiwitafgifte bestudeerd uit hydrogelen op basis van dextraan. Dextraan is een natuurlijk, hydrofiel (waterminnend), bacterieel polymeer, opgebouwd uit repeterende suiker-eenheden (D-glucopyranose). Dextraan wordt al meer dan 60 jaar toegepast (als 'plasma expander' en anti-trombolytisch middel), en de ervaring leert dat dit polymeer veilig is voor menselijk gebruik. Door chemische modificatie kunnen groepen in de polymeerketen worden geïntroduceerd die het vormen van een hydrogel met chemische dwarsverbindingen mogelijk maken. De dextraan-variant gemodificeerd met methacryl-groepen (Dex-MA genoemd) vormt niet-degradeerbare hydrogelen, en vertoont diffusie-gecontroleerde eiwitafgifte Het introduceren van hydroxyethyl methacrylaat (HEMA) groepen gevolgd door chemische dwarsverbinding leidt tot DEX-HEMA hydrogelen, welke biodegradeerbaar zijn, zowel in het laboratorium (*in vitro)* als in proefdieren (*in vivo)*.

Hydrogelen voor het maken van eiwitafdrukken

Naast het gebruik als formulering voor gereguleerde afgifte van eiwitten, worden hydrogelen toegepast voor het maken van moleculaire afdrukken (een techniek die "molecular imprinting" wordt genoemd) van eiwitten. Het maken van dergelijke afdrukken werkt zoals weergegeven in figuur 1, en is te vergelijken met het maken van een mal of gietvorm. Het af te drukken molecuul ("template") wordt gemengd met monomeren. Afhankelijk van de mogelijke moleculaire interacties rangschikken de monomeren zich om het template (A). Vervolgens worden de monomeren d.m.v. dwarsverbindingen gefixeerd (B). Tenslotte wordt het template verwijderd, en blijft er een complementaire holte achter (C). Omdat het template precies in deze

holte past, is deze holte in staat het template te “herkennen” en te herbinden (sleutel-slot principe).

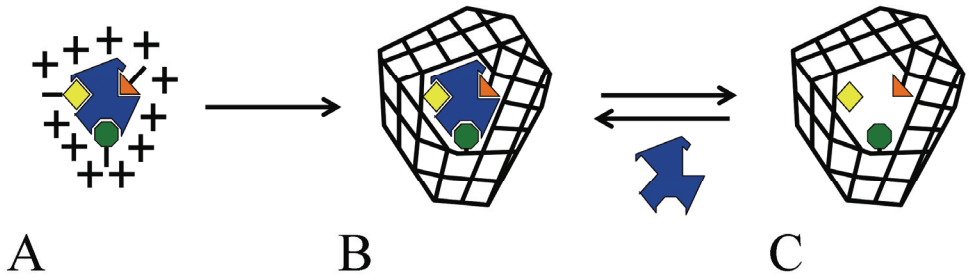

Figuur 1. (A) Monomeren (geel, oranje en groen) rangschikken zich rond het template (weergegeven in blauw). (B) De rangschikking van de monomeren rond het template wordt gefixeerd door formatie van een netwerk d.m.v. polymerisatie waarbij dwarsverbindingen worden gevormd (C) Het template wordt verwijderd waardoor een complementaire holte achterblijft.

Polymeren met moleculaire afdrukken hebben verschillende toepassingen. Ze kunnen bijvoorbeeld worden gebruikt voor het isoleren van het afgedrukte molecuul uit complexe mengsels voor analyse (de juiste sleutels uit een grote berg), of als hulpmiddelen bij het ontwikkelen van nieuwe geneesmiddelen (het vinden van nieuwe sleutels). Tot op heden is het maken van moleculaire afdrukken vooral succesvol gebleken met kleine (eenvoudige) moleculen. De kwetsbaarheid, de grootte en de beperkte keuze aan oplosmiddelen anders dan water zijn belangrijke factoren die mogelijkheden voor het afdrukken van eiwitten beperken. Desondanks zijn er verschillende voorbeelden van eiwitafdrukken beschikbaar in de wetenschappelijke literatuur. De meest gebruikte materialen om deze afdrukken in te maken zijn hydrogelen.

In dit proefschrift wordt een innovatieve manier geïntroduceerd om eiwitafdrukken te maken op het oppervlak van minuscule hydrogel balletjes (‘protein imprinted nanoparticles’ of PINAPLES). Het gaat hierbij om afdrukken van zogenaamde membraaneiwitten. Het celmembraan vormt de scheiding van een cel en zijn omgeving, en bestaat uit een dubbellaag van vetmoleculen (lipiden). Celmembranen bevatten tal van eiwitten, die o.a. communicatie tussen cel en omgeving en transport van stoffen over het membraan mogelijk maken. Het concept van het maken van PINAPLES is weergegeven in figuur 2. Allereerst wordt het membraaneiwit in het membraan van een lipiden-blaasje (liposoom) ingebouwd. Dit blaasje is gevuld met water en wateroplosbare monomeren en dwarsverbinders. Ook een deel van het

eiwit steekt naar de binnenkant van het blaasje (Figuur 2A). Vervolgens wordt binnenin het blaasje een hydrogelnetwerk gevormd door polymerisatie (Figuur 2B). Tenslotte wordt het oppervlak van het hydrogeldeeltje vrijgemaakt door verwijderen van de lipidenlaag en eiwit.

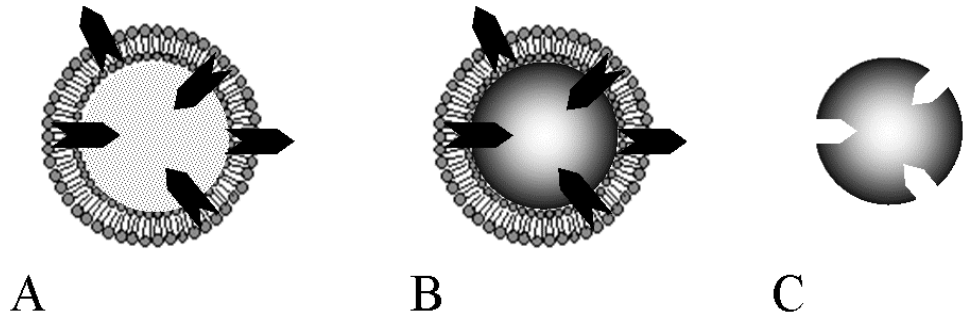

Figuur 2. Concept van het maken van PINAPLES. Een membraaneiwit (weergeven in het zwart) wordt ingebouwd in een liposoom. De binnenkant van het liposoom is gevuld met water, monomeren, dwarsverbinder en een deel van het eiwit. (A). Polymerisatie leidt tot het vormen van een hydrogelnetwerk binnenin het liposoom (B). De PINAPLE (C) wordt vrijgemaakt door het verwijderen van lipidenlaag en eiwit.

De voorgestelde methode heeft als voordeel dat de afdrukken van het eiwit exclusief op het oppervlak van het hydrogel-deeltje voorkomen. Daarnaast vormt de lipidenlaag de natuurlijke omgeving van het membraaneiwit, wat leidt tot een afdruk van het eiwit in zijn oorspronkelijke vorm.

De ontwikkeling van PINAPLES kan in vier kritische stappen worden onderverdeeld:

1. Het eiwit moet op de juiste manier, d.w.z. met een deel naar binnen gericht, in het blaasje worden ingebouwd.
2. Het hydrogelnetwerk moet binnen in het blaasje worden gevormd. Formatie van een netwerk buiten het blaasje (waardoor het blaasje zelf in het netwerk wordt gevangen) moet worden voorkomen.
3. De lipidenlaag en het eiwit moeten worden verwijderd.
4. De PINAPLES moeten het membraaneiwit kunnen herkennen en herbinden.

De beoogde toepassing van PINAPLES is als dragermateriaal voor geneesmiddelen. Door de aanwezigheid van de afdruk op het oppervlak kunnen deze deeltjes cellen die het afgedrukte eiwit op het oppervlak hebben herkennen en er aan blijven plakken. Verschillende soorten

cellen hebben verschillende soorten eiwitten op hun oppervlak. Hierdoor kan een geneesmiddel specifiek naar bepaalde cellen (bv. tumorcellen) worden toegestuurd. Het is eveneens mogelijk dat de PINAPLE zelf als geneesmiddel werkt doordat het door te binden de natuurlijke functie bv. van het eiwit verhindert. De verwachte voordelen van de synthetische PINAPLES boven reeds bestaande manieren om geneesmiddelen te sturen, zoals bv. wordt gedaan m.b.v. natuurlijke antilichamen, zijn verminderde afweerreacties door het lichaam en hoge stabiliteit.

Samenvatting

In hoofdstuk 2 worden de verschillende methoden besproken die momenteel in gebruik zijn voor het bereiden van micro-(tienduizend keer kleiner dan een cm) en nano- (tien miljoen keer kleiner dan een cm) deeltjes met moleculaire afdrukken. Oorspronkelijk worden polymeren met moleculaire afdrukken bereid door polymerisatie van een groot volume (bulk polymerisatie), gevolgd door breken en zeven van het polymeer om kleinere deeltjes te verkrijgen. Er zijn echter verschillende methoden voorhanden om direct polymeren micro- en nanodeeltjes te synthetiseren, zoals dispersie-, neerslag-, suspensie-, en (mini-) emulsiepolymerisatie. Het is gebleken dat deze directe synthese van deeltjes met moleculaire afdrukken veel gemakkelijker is omdat het tijd- en arbeidrovende proces van breken en zeven wordt vermeden. Nog belangrijker, het leidt tot de productie van regelmatig gevormde deeltjes met uniforme deeltjesgrootte en een groot oppervlak, wat resulteert in verbeterde snelheid van massaoverdracht en betere prestaties (bindend vermogen en affiniteit/selectiviteit).

Hoofdstuk 3 beschrijft vervolgens een nieuwe methode voor het maken van nanodeeltjes, die gebruikt kan worden voor de bereiding van PINAPLES. Polyacrylamide nanodeeltjes werden bereid binnenin het interne waterhoudende compartiment van liposomen. Deze methode biedt eenvoudige controle over de grootte van de deeltjes. Belangrijk is dat de liposomale lipidenlaag de mogelijkheid biedt om membraaneiwitten in te bouwen, die vervolgens moleculair kunnen worden afgedrukt. In een waterige oplossing van acrylamide (AAM, monomeer) en methyleen bisacrylamide (MBA, dwarsverbinder) werden liposomen gevormd uit gemengde micellen van lipiden en Triton X-100 (TX100) door adsorptie van TX100 aan Bio-Beads SM2. De diameter van de liposomen bedroeg ongeveer 100 nm met een kleine spreiding in deeltjesgrootte. Polymerisatie van de monomeren m.b.v. vrije radicalen binnenin de liposomen werd gestart door belichting in de aanwezigheid van een foto-initiator (Irgacure). Macroscopische hydrogel-vorming als gevolg van de polymerisatie van de monomeren buiten de liposomen werd voorkomen door remming van de polymerisatie van niet-ingekapselde

monomeren door toevoeging van ascorbinezuur, dat niet door de liposomale lipidenlaag heen kan. Kale nanogeldeeltjes werden verkregen door de verwijdering van de lipidenlaag. Deze handige en veelzijdige methode voor nanogelsynthese maakt het mogelijk monomeren te gebruiken die door de lipidenlaag heen kunnen dringen. Bovendien is deze methode geschikt voor het inbouwen van membraaneiwitten in de lipidenlaag, wat essentieel is voor de ontwikkeling van PINAPLES. In de bijlage van hoofdstuk 3 wordt aangetoond dat deze methode inderdaad kan worden gebruikt voor het inbouwen van het membraaneiwit SN/GpA. Bovendien bleek dat een deel van het wateroplosbare domein van SN/GpA naar de binnenkant van het liposoom was gericht, en dus beschikbaar was voor de vorming van de afdrukken. Helaas, ondanks vele pogingen is het niet gelukt PINAPLES te maken die herbinding aan het template vertoonden. Dit is deels te wijten aan de huidige stand van de kennis met betrekking tot het moleculair afdrukken van eiwitten. **Zoals besproken in hoofdstuk 4, is het moleculair afdrukken van eiwitten nog een betrekkelijk nieuw wetenschappelijk terrein. Hoewel het aantal wetenschappelijke publicaties op dit gebied de laatste jaren is toegenomen, is het wetenschappelijke bewijs van de haalbaarheid van een selectieve herkenning van eiwitten door polymeren in waterig milieu niet overtuigend.** Keuze van geschikte monomeren, verwijderen van het template, en de beoordeling van het herbinden van het template zijn enkele belangrijke uitdagingen. Dit wordt geïllustreerd met voorbeelden uit de literatuur en onze eigen experimentele gegevens. Gebruik van geladen monomeren kan leiden tot de gewenste sterke (elektrostatische) interacties tussen de monomeren en het template, maar ook tot ongewenste hoge aspecifieke binding van andere moleculen met vergelijkbare lading. Tot nu toe is het niet overtuigend aangetoond dat elektrostatische interacties een gunstige bijdrage leveren aan afdrukken van eiwitten. De combinatie van een detergent (SDS) en azijnzuur, gewoonlijk gebruikt voor verwijderen van het template, kan leiden tot experimentele artefacten, en moet daarom worden vermeden. In veel gevallen is template-herbinding op een onbetrouwbare manier gekwantificeerd, zijn de resultaten niet kritisch bezien of ontbreekt het aan statistische analyse. Daarom kan worden gesteld dat in talloze publicaties het wetenschappelijk bewijs van het moleculair afdrukken van eiwitten niet overtuigend is.

In hoofdstuk 5 worden de effecten van elektrostatische ladingsinteractie tussen een eiwit en hydrogel-netwerk op de afgifte van het eiwit onderzocht. Elektrostatisch geladen hydrogelen die stabiel zijn onder fysiologische omstandigheden werden verkregen door copolymerisatie van gemethacryleerd dextraan (Dex-MA) met ofwel een negatief geladen

monomeer (methacrylzuur, MA) of een positief geladen monomeer (2-N,N-dimethyl-amino-ethylmethacrylaat, DMAEMA). Het effect van gebruik van de monomeren op de lading en zwellinggraad van de hydrogel in de evenwichtsituatie en de afgifte van modeleiwitten uit de hydrogel werd onderzocht zowel bij lage (10 mM HEPES) als bij fysiologische ionsterkte (HEPES buffered saline, HBS). Modeleiwitten werden gekozen op basis van hun lading bij fysiologische pH; runderserum albumine (BSA, negatief geladen), myoglobine (neutraal) en cytochroom C (positief geladen). Zoals verwacht had de lading van het netwerk geen effect op de afgifte van myoglobine. Aan de andere kant waren zowel BSA als cytochroom C volledig immobiel in hydrogelnetwerken met een *tegengestelde* lading bij lage ionsterkte. Bij fysiologische ionsterkte hing het percentage van het eiwit dat was geïmmobiliseerd af van de hoeveelheid lading in de hydrogel. De ladingsinteractie had echter geen effect op de snelheid waarmee de eiwitten door de gel bewogen (diffusiecoëfficiënt). Daarentegen, de afgiftesnelheid van BSA uit netwerken met een relatief grote hoeveelheid *gelijk*e ladingen (negatief) was aanzienlijk hoger. Deze bevindingen leidden tot de conclusie dat elektrostatische interacties tussen eiwit en hydrogel kunnen worden gebruikt voor eiwitimmobilisatie en prikkel-afhankelijke eiwitafgifte (door verhoging van ionsterkte).

In hoofdstuk 6 worden de eerder beschreven omkeerbare elektrostatische interacties gebruikt voor efficiënte hydrogelbelading en gereguleerde afgifte van eiwitten. In tegenstelling tot de gebruikelijke manier van beladen, waarbij het eiwit wordt toegevoegd voordat de monomeren tot een hydrogel worden gepolymeriseerd, vindt bij deze methode de belading met eiwit plaats *na* het vervaardigen van de hydrogel (na-beladen). Het voordeel hiervan is dat het eiwit niet wordt blootgesteld aan de polymerisatiecondities. Negatief en positief geladen hydrogelen werden vervaardigd door copolymerisatie van Dex-MA met respectievelijk MA of DMAEMA. Incubatie van negatief geladen hydrogelen in een oplossing van cytochroom C (positief geladen) bij een lage ionsterkte (10 mM HEPES, pH 7,4) leidde tot kwantitatieve opname van het eiwit in de hydrogel. Positief geladen hydrogelen konden worden na-beladen met BSA (negatief geladen) bij een neutrale pH, en negatief geladen gelen met myoglobine (positief geladen bij pH < 7) bij een pH van 5. De efficiëntie van het na-beladen en de verdeling van het eiwit in de gelen waren afhankelijk van hoeveelheid lading in het netwerk, netwerkdichtheid en de ionsterkte tijdens het beladen. Diffusie-gereguleerde eiwitafgifte werd geïnduceerd door incubatie van de hydrogelen in HBS pH 7,4. De hoeveelheid vrijgegeven cytochroom C in HBS varieerde van 94% tot 70% uit gelen met respectievelijk 60 en 150 MA/g

hydrogel. Belangrijk is dat bij hoge ionsterkte (1 M NaCl) volledige afgifte werd verkregen, wat aangeeft dat de na-belading niet leidde tot de vorming van onoplosbare eiwitaggregaten, of onomkeerbare immobilisatie van het eiwit in de matrix. Massaspectrometrie aan het vrijgegeven cytochroom C toonde aan dat na-beladen geen oxidatie van het eiwit veroorzaakte. Dit in tegenstelling tot het conventionele beladen tijdens de bereiding van de gelen. Deze gegevens laten zien dat, op basis van omkeerbare elektrostatische interacties, dextraan hydrogelen efficiënt kunnen worden beladen met negatieve, positieve of neutrale eiwitten. Het is hierbij vooral van belang dat deze beladingmethode geen chemische modificatie van het eiwit tot gevolg heeft.

Hoofdstuk 7 bespreekt de toekomstperspectieven van het werk gepresenteerd in dit proefschrift. Er wordt betoogd dat de methode om nanodeeltjes te bereiden (beschreven in hoofdstuk 3) in principe een elegante manier is om een membraaneiwit interacties aan te laten gaan met monomeren in het pre-polymerisatie mengsel. Drie van de vier kritische stappen die nodig zijn voor het bereiden van PINAPLES (inbouwen van het eiwit in liposoom, maken van hydrogelen binnenin het liposoom en het verwijderen van de lipidenlaag) zijn genomen. Door een gebrek aan basale kennis op het gebied van het maken afdrukken van eiwitten is het maken van PINAPLES echter niet gelukt. Als de toename van de onderzoeksinspanningen op dit gebied van de afgelopen jaren zal doorzetten, zal dit ongetwijfeld tot nieuwe inzichten leiden die de bereiding van PINAPLES waarschijnlijker maken. Met betrekking tot het na-beladen van eiwitten wordt erop gewezen dat macroscopische hydrogelen niet de voorkeur hebben voor klinische toepassing, omdat een operatie nodig is voor de toediening. Na-beladen van injecteerbare micro- of nanogelen heeft de voorkeur. Nanogelen zijn bijzonder interessant omdat deze het bereiken van diep gelegen weefsels en het intracellulaire afleveren van biofarmaceutica mogelijk maken. Als gevolg van het grote oppervlak en korte diffusieafstand, zou het na-beladen en de afgifte van eiwitten uit nanogelen een zeer snel proces zijn. Een te snelle eiwitafgifte zou echter ongewenst zijn, omdat het deeltje tijd nodig heeft om zijn doel te bereiken. Om onmiddellijke eiwitafgifte te voorkomen wordt daarom laag-op-laag-coating voorgesteld. De afgifte uit een deeltje met een dergelijke coating wordt bepaald door de diffusiesnelheid van het eiwit door de lagen en/of door de snelheid waarmee de coating wordt afgebroken. Eerste resultaten worden gepresenteerd waaruit blijkt dat negatief geladen dextraan nanogelen bij lage ionsterkte efficiënt kunnen worden beladen met cytochroom C. Daarnaast wordt de toepasbaarheid van laag-op-laag-coating van dextraan nanogelen aangetoond.

Dankwoord

Nu ik aan de laatste woorden van mijn proefschrift toe ben, kan ik het niet laten mijn gedachten eens te laten gaan over de zin en onzin van dankbaarheid. Volgens Joseph Stalin is het een ziekte waar honden aan lijden. Gelukkig verschillen meneer Stalin en ik wel op meer punten van inzicht. Ik kan me dan ook meer vinden in uitspraken als: “Aan stille dankbaarheid heeft niemand iets” (G. Stein), “Dankbaarheid is een kenmerk van een nobele ziel” (Aesop), “Dankbaarheid is wel een plicht die men moet betrachten, maar niet een recht dat men kan eisen” (P. de Vledder), en “We hopen dat wanneer de insecten de wereld overnemen, zij zich dankbaar zullen herinneren dat zij op al onze picknicks waren” (B. Vaughan). Om al deze redenen wil ik hier graag de mensen bedanken die mijn tijd als aio en het tot stand komen van dit proefschrift hebben gemaakt tot wat het was: een zeer leerzame, waardevolle en plezierige ervaring.

Wim, dank voor je begeleiding. Ik heb de deur nooit bij je platgelopen, maar de wetenschap dat ik altijd bij je binnen kon stappen en je tijd had als het nodig was betekende veel voor me. Jouw nuchtere kijk en recht voor z’n raap mentaliteit heb ik altijd zeer prettig gevonden, en ik heb grote bewondering voor de betrokken wijze waarop je leiding geeft aan zo’n grote en diverse groep.

Rene, bedankt voor je vertrouwen, je ideeën en de mogelijkheden die je mij hebt geboden mijn proefschrift met succes af te ronden. Ondanks dat de grote doorbraak uitbleef, ben jij er altijd in blijven geloven. Molecular imprinting is een harde noot om te kraken gebleken, maar moge de aanhouder winnen.

Natuurlijk gaat mijn dank uit naar de overige MIPers; Frits, Ellen, Adrienne, Najim en Lise. Het team veranderde nog al eens van samenstelling, maar de samenwerking was altijd uitstekend. Ook verschillende studenten hebben zich ingezet voor het PINAPLE-project en verdienen het te worden vermeld. Maarten, Sergio, Markus, Hassan en Ou, bedankt voor jullie bijdrage. Ik hoop dat jullie tijd onder mijn hoede voor jullie net zo leerzaam is geweest als voor mij. Ten slotte ben ik Mies, Martin en Roel dank verschuldigd voor hun onbaatzuchtige en onmisbare hulp bij experimenteel werk, en de Riesenkindjes Stef en Afra voor het zo fraai verpakken van het eindresultaat.

Toen ik in 2004 mijn lange weg als aio begon, voelde ik me in een enthousiaste, kritische, betrokken maar ook gezellige groep mensen meteen op mijn plek. Marieke, Marjan, Maryam, Myrra, Cris, Sabrina, Manuela, Natasa, Suzanne, Sophie, Marion, Barbara, Lidija, Cor, Martin Albert, Marc, Jordi, Mark, Maarten, Aissa, Xulin, Wim J., Enrico, Ray, Mies, Herre, Gert en Daan, allen bedankt voor jullie geheel eigen bijdrage hieraan. Sindsdien heb ik met veel genoegen zelf vele nieuwe collega's mogen verwelkomen. Het gaat me te ver om ook die lijst proberen volledig te krijgen, dus ik zou willen volstaan met allen te danken voor de geweldige sfeer, het in stand houden van de vele tradities en de prettige samenwerking. Een aantal van deze collega's verdient nog een speciale vermelding, omdat ik hun gezelschap bijzonder op prijs stel: Gassy, Rodolfo en Blondie/Captain.

Z505, er lijkt een vloek op te rusten. Desondanks niets dan goede herinneringen. In het begin met labgenoten Birgit, Marcel, Louis, Holger, Adrienne, Ellen, en Inge, en ook in de nieuwere versie met Maria, Bart, Afrouz, Grzegorz, en Naushad.

Voor spijkers met koppen moet je toch in N501 zijn. Biofarmacie met Ethlinn gaat nergens zo voorspoedig als daar. Etje, het was me een waar genoegen jouw paranimf te mogen zijn. Ik bewonder je om je verantwoordelijkheid, gedrevenheid en je grondige manier van werken, maar ik geniet er het meest van als je dat allemaal even laat varen.

En dan zijn er natuurlijk nog mijn paranimfen, Ellen en Frits. Ellen, door de samenhang van onze projecten en het verloop ervan waren we op elkaar aangewezen. De ware verbondenheid zit echter veel dieper dan dat. Ik ben dan ook ontzettend blij dat jij België een paar jaartjes hebt kunnen missen, en het leven in Utrecht kleur hebt gegeven. Frits, ik houd jou mede verantwoordelijk voor het feit dat ik aan het PINAPLE project ben begonnen. Je schat aan ervaring, inzicht en onnavolgbaar snelle redenering vind ik fantastisch, maar het is je sociale kant die je bijzonder maakt. Je hebt in het begin eens gezegd dat ik waarschijnlijk tegen de tijd van mijn promotie wel schoon genoeg van je zou hebben. Gelukkig zit jij er ook wel eens naast.

Papa, mama, Michiel, Rita, Dorien, Barbera, Roderik, en Hagit, alles wat ik ben heb ik aan jullie te danken. Ik hoop dat jullie trots op jezelf zijn.

Curriculum Vitae

Joris Schillemans was born on the 2nd of April 1978 in Enschede, the Netherlands. In 1996 he graduated from secondary school at the Kandinsky College in Nijmegen, and started studying Pharmacy at Utrecht University. During his undergraduate research project at the Laboratory of Membrane and Liposome research of the Hebrew University of Jerusalem under the supervision of prof. Y. Barenholz, he studied the incorporation of lipophilic drugs in liposomal membranes. After graduating as a pharmacist in February 2004 he worked as a public pharmacist for a few months. In November 2004 he joined the Department of Pharmaceutics of Utrecht University to start his Ph.D. project, the results of which are described in this thesis.

List of publications

Schillemans JP, Flesch FM, Hennink WE, Van Nostrum CF. Synthesis of bilayer-coated nanogels by selective cross-linking of monomers inside liposomes. *Macromolecules* 2006. 39: 5885-5890

Schillemans JP, Van Nostrum CF. Molecularly imprinted polymer particles: synthetic receptors for future medicine. *Nanomedicine* 2006. 1: 437-447

Schillemans JP, Hennink WE, Van Nostrum CF. The effect of protein-network charge interaction on the release of proteins from crosslinked dextran hydrogels. *European journal of pharmaceutics and biopharmaceutics, in press*

Schillemans JP, Verheyen E, Barendregt A, Hennink WE, Van Nostrum CF. Post loading and release of proteins from chemically crosslinked dextran hydrogels. *Submitted*

Schillemans JP, Verheyen E, Van Wijk M, Demeniex M-A, Hennink WE, Van Nostrum CF. Molecular imprinting of proteins: Fit for the future. *In preparation*

Eliyahu H, Joseph A, **Schillemans JP**, Azzam T, Domb AJ, Barenholz Y. Characterization and in vivo performance of dextran-spermine polyplexes and DOTAP/cholesterol lipoplexes administered locally and systemically. *Biomaterials* 2007. 28: 2339-2349

Khazanov E, Priev A, **Schillemans JP**, Barenholz Y. Physicochemical and biological characterization of ceramide-containing liposomes: Paving the way to ceramide therapeutic application. *Langmuir* 2008. 24: 6965-6980

Hultberg A, Temperton NJ, Rosseels V, Koenders M, Gonzalez-Pajuelo M, Schepens B, Itatí Ibañez L, Vanlandschoot P, **Schillemans JP**, Weiss RA, Saelens X, Melero JA, Verrips CT, Van Gucht S, De Haard HJ. Llama-derived single domain antibodies to build multivalent superpotent and broadened neutralizing anti-viral molecules. *In preparation*

Crielaard BJ, Yousefi A, **Schillemans JP**, Vermehren C, Buyens K, Braeckmans K, Lammers T, Storm G. Anticipating the in vivo circulation time of liposomes by measuring their interactions with proteins using surface plasmon resonance. *In preparation*

Affiliations of contributing authors

Arjan Barendregt

Biomolecular Mass Spectrometry and Proteomics Group, Bijvoet Center for Biomolecular Research and Utrecht Institute for Pharmaceutical Sciences (UIPS), Utrecht University, Utrecht, The Netherlands, and The Netherlands Proteomics Centre, Utrecht, The Netherlands

Marie-Astrid Demeniex

Department of Pharmaceutics, Utrecht Institute for Pharmaceutical Sciences (UIPS), Utrecht University, Utrecht, The Netherlands

Frits M. Flesch

Department of Pharmaceutics, Utrecht Institute for Pharmaceutical Sciences (UIPS), Utrecht University, Utrecht, The Netherlands

Wim E. Hennink

Department of Pharmaceutics, Utrecht Institute for Pharmaceutical Sciences (UIPS), Utrecht University, Utrecht, The Netherlands

Cornelus F. van Nostrum

Department of Pharmaceutics, Utrecht Institute for Pharmaceutical Sciences (UIPS), Utrecht University, Utrecht, The Netherlands

Ellen Verheyen

Department of Pharmaceutics, Utrecht Institute for Pharmaceutical Sciences (UIPS), Utrecht University, Utrecht, The Netherlands

Martin van Wijk

Department of Pharmaceutics, Utrecht Institute for Pharmaceutical Sciences (UIPS), Utrecht University, Utrecht, The Netherlands